PNNL-10918

Glass Optimization for Vitrification of Hanford Site Low-Level Tank Waste

X. Feng
P. R. Hrma
J. H. Westsik, Jr.
N. R. Brown
M. J. Schweiger
H. Li
J. D. Vienna
G. Chen
G. F. Piepel
D. E. Smith
B. P. McGrail
S. E. Palmer
D. Kim
Y. Peng
W. K. Hahn
A. J. Bakel
W. L. Ebert
D. K. Peeler
C. Chang

March 1996

Prepared for the U.S. Department of Energy
under Contract DE-AC06-76RLO 1830

Pacific Northwest National Laboratory
Operated for the U.S. Department of Energy
by Battelle Memorial Institute

Battelle

PNNL-10918

DISCLAIMER

PACIFIC NORTHWEST NATIONAL LABORATORY
operated by
BATTELLE
for the
UNITED STATES DEPARTMENT OF ENERGY
under Contract DE-AC06-76RLO 1830

Printed in the United States of America

Available to DOE and DOE contractors from the Office of Scientific and Technical Information, P.O. Box 62, Oak Ridge, TN 37831; prices available from (615) 576-8401.

Available to the public from the National Technical Information Service, U.S. Department of Commerce, 5285 Port Royal Rd., Springfield, VA 22161


The document was printed on recycled paper.

PNNL-10918
UC-510

Glass Optimization for Vitrification of Hanford Site Low-Level Tank Waste

X. Feng
P. R. Hrma
N. R. Brown
M. J. Schweiger
H. Li
J. D. Vienna
G. Chen
G. F. Piepel
D. K. Peeler
D. E. Smith
B. P. McGrail
S. E. Palmer
D. Kim
Y. Peng
W. K. Hahn
A. J. Bakel
W. L. Ebert
C. Chang

March 1996

Prepared for
the U.S. Department of Energy
under Contract DE-AC06-76RLO 1830

Pacific Northwest National Laboratory
Richland, Washington 99352

Summary

Immobilization of Hanford low-level waste (LLW), which is characterized by a high content of Na_2O, necessitates the development of durable high-sodium glasses. Simulated LLW glasses containing 20 wt% Na_2O, 6 to 12 wt% B_2O_3, 6 to 12 wt% CaO, 6 to 15 wt% Al_2O_3, and 48 to 72 t% SiO_2 were tested at 90°C by 7-day Product Consistency Test (PCT), vapor-hydration tests, and single-pass flow-through (SPFT) tests at Pacific Northwest National Laboratory (PNNL). Glass dissolution extent decreased as Al_2O_3 concentration increased, replacing SiO_2. Replacing SiO_2 by B_2O_3 in glasses with 9-16 wt% Al_2O_3 improved PCT durability up to the level of 6-9 wt% B_2O_3. When CaO was used instead of B_2O_3, only a mild improvement resulted at < 6 wt% CaO. Generally, Na_2O-B_2O_3-Al_2O_3-SiO_2 glasses showed better leach resistance in both PCT and vapor-hydration tests than did the Na_2O-CaO-Al_2O_3-SiO_2 glasses. However, the durability order ranked by a SPFT at pH 12 is opposite to that of the vapor-hydration test and PCT.

The dependency of solubilities of minor components S, P, Cl, and F on temperature is negligible, but is significant on glass compositions. Volatilities of molten glass with the addition of F, Cl, S, and P can be significant once the minor components are in excess of their solubilities, which were in the order: $Cl > SO_3 \geq F$. Higher B_2O_3 content in glass further increases the volatilities.

A vendor glass formulation study was carried out at PNNL and was built upon the LLW glass optimization effort, supporting the Phase I and Phase II melter vendor testing activities for Westinghouse Hanford Company. For Phase I vendor melter testing, six glass formulations were developed at PNNL and additional glasses were developed by Phase I vendors. All the glasses were characterized in terms of viscosity and chemical durability by the 7-day PCT.

Twelve Phase II glass formulations were developed to accommodate 2.5 wt% P_2O_5 and 1.0 wt% SO_3 without significant processing problems. These levels of P_2O_5 and SO_3 are expected to be the highest possible concentrations from Hanford Site LLW streams, at 25 wt% waste loading in glass. The Phase II compositions formulated were 6 to 23 times more durable than the Defense Waste Processing Facility (DWPF) environmental assessment (EA) glass. They melt within the temperature range of 1160° to 1410°C to suit different melting technologies. The composition types included boron-free glasses for volatilization-sensitive melters; boron-containing glasses for cold-cap melters; Zr-containing glasses for enhanced long-term durability; and Fe-containing glasses for reducing melting temperature and melt volatility while maintaining chemical durability.

Glasses made from simulated waste slurries were more prone to foaming and phase segregation than were glasses prepared from dry chemicals, especially those with high sulfur and phosphorus content. Surprisingly, glasses prepared from slurries were more oxidized, i.e., had lower Fe(II)/(total Fe) ratios, and had higher solubilities of sulfur. The glasses made from dry chemicals and slurries had similar chemical durabilities, viscosities, and phosphorus solubilities. The Phase II formulations were also demonstrated to be capable of incorporating a total 3 wt% of Cu, Zn, Pb, Sn, Cr, Mn, Ni, Mo, Sb, As, Bi, and Cd, although these metal-containing glasses were slightly less durable.

Contents

Figures

Tables

1.0 Introduction

1.1 Background

The radioactive defense wastes stored in 177 underground single-shell tanks (SST) and double-shell tanks (DST) at the Hanford Site will be separated into low-level and high-level fractions. The Tri-Party Agreement (TPA) between the State of Washington Department of Ecology, the U.S. Department of Energy, and the U.S. Environmental Protection Agency specifies vitrification as the immobilization method for Hanford Site low-level waste (LLW) (TPA 1993). A program is underway at Westinghouse Hanford Company (WHC) to implement this TPA strategy through the LLW Disposal Program element of the Tank Waste Remediation System (TWRS) Program. The Pacific Northwest National Laboratory (PNNL) is providing technology support to the LLW Disposal Program through the PNNL Vitrification Technology Development (PVTD) Program.

One technology activity underway at PNNL is the development of glass formulations for the immobilization of the low-level tank wastes. A glass formulation strategy has been developed that describes development approaches to optimize glass compositions prior to the projected LLW vitrification facility start-up in 2005 (Kim et al. 1995). The Glass Formulation Strategy addresses the near-term needs driven by TPA milestones (M-60-02) to select a reference melter technology and reference glass formulation by June 1996. Shade and Kelly[(a)] prepared a path forward strategy to outline the process and logic sequence for defining a LLW reference glass formulation region as stated in the TPA milestone. The Glass Formulation Strategy also addresses the longer term needs to develop and verify glass formulations based on evolving waste characterization information, vitrification system design, and disposal system requirements. Initial glass formulations for the high-sodium LLW are being developed from the alumino-silicate glass family. The glasses will be characterized and selected based on their long-term chemical durability and their processing behavior. The Strategy also includes verification of the glass formulations through 1) testing in small- and pilot-scale melter systems to confirm processability and to support design and 2) radioactive testing with actual wastes and formulations to validate simulants and models. Glass property models will be developed/adapted to aid the formulation effort and as process control tools.

Implementation of this strategy requires testing of glass formulations spanning a number of waste loadings, compositions, and additives over the range of expected waste compositions. The resulting glasses will then be characterized and compared to processing and performance specifications yet to be developed.

A multi-phase melter-systems technology demonstration, testing, and evaluation program is underway to identify the best overall melter-system technology available for vitrification of Hanford Site LLW to meet the TPA milestones (Wilson 1995). Phase I is a "proof of principle" test to demonstrate that a melter system can process a simulated highly alkaline, high nitrate/nitrite content aqueous LLW feed and produce a glass product of consistent quality. Seven melter vendors were selected for the Phase I evaluation, as follows: Joule-heated melters from GTS Duratek, Incorporated (GDI); Envitco, Incorporated (EVI); Penberthy Electromelt, Incorporated (PEI); and Vectra Technologies, Incorporated (VTI); gas-fired cyclone burner from

---

(a) Internal Memo 74610-95-016, DJ Washenfelder, WHC, to RJ Murkowski, Transmittal of Letter Report "Path Forward Strategy; Low-Level Waste Reference Glass Formulation Development" Milestone Control No. T3B-95-234, July 21, 1995.

Babcock & Wilcox (BCW); plasma torch-fired, cupola furnace from Westinghouse Science and Technology Center (WSTC); and electric arc furnace with top-entering vertical carbon electrodes from U.S. Bureau of Mines (UBM).

Phase II evaluations will allow for more comprehensive testing of equipment and procedures for selected promising technologies. Melter capability for handling wastes with high contents of F, Cl, P, and S will be tested. Melter systems with the greatest flexibility to process feeds with these components will be identified. Requirements Analysis will indicate concentration limits for these components that can be realistically processed by vitrification. At the end of Phase II, a preferred and a backup technology will be selected by Westinghouse Hanford Company (WHC).

Pacific Northwest National Laboratory is providing glass formulation support for this melter technology evaluation program (Feng et al. 1995). Melter vendors could select the glasses from the formulations provided by PNNL or they were free to develop their own glass compositions, provided the glass meet the two aforementioned criteria. Glasses adopted by vendors were also tested at PNNL to verify the required properties. Testing included durability evaluation through PCT, viscosity measurements, and composition analysis.

This report documents the glass formulation work conducted at PNL in fiscal years 1994 and 1995 including glass formulation optimization, minor component impacts evaluation, Phase I and Phase II melter vendor glass development, liquidus temperature and crystallization kinetics determination. This report also summarizes relevant work at PNNL on high-iron glasses for Hanford tank wastes conducted through the Mixed Waste Integrated Program and work at Savannah River Technology Center to optimize glass formulations using a Plackett-Burnam experimental design.

1.2 Objectives

The overall objectives of the glass formulation effort are to develop optimized glass compositions containing the maximum fraction of waste while maintaining satisfactory long-term durability, acceptable processing characteristics, and adequate flexibility to handle waste variations, and to develop a methodology to respond to waste variations. The purpose of optimizing glass compositions through waste loading maximization is to achieve reduction of final glass product volume and processing cost without adversely affecting durability and requiring more elaborate disposal systems, and thus to minimize the overall vitrification and disposal costs. Specific activities conducted in FY 1994 and FY 1995 to support these objectives include the following:

- develop optimized glass compositions for vitrification of high-sodium tank waste;
- provide proper formulations for Phase I and Phase II melter testing;
- determine the solubility limits of F, Cl, P, S, and Cr in LLW glasses and develop optimized composition to increase solubility of these minor components, while maintaining the required processability and chemical durability; and
- evaluate glasses generated by vendors through durability testing, viscosity measurement, and composition analysis.

1.3 Approach

1.3.1 Considerations

The most important considerations for acceptable LLW waste glass compositions are the capability to incorporate high sodium content from LLW; satisfactory long-term durability; and proper processability, such as the capability of achieving the desired viscosity at melting temperature.

1.3.2 Chemical Durability

Long-term durability requirements and the link between short-term laboratory tests and long-term durability have not been established (McGrail 1992). However, a three-stage corrosion mechanism of typical silicate glasses in aqueous media is generally accepted (Cunnane 1994). The initial stage under solution-dominated condition (dilute solution) is characterized by a forward-reaction rate; that is, the maximum rate achievable depends only on glass composition, temperature, and solution pH. In the intermediate stage, the glass reaction rate continuously decreases as the concentration of elements released from the glass in the solution increases. The final stage of enhanced glass corrosion begins when secondary mineral phases precipitate from the concentrated or "saturated/over-saturated" solution. The precipitation of mineral phases causes the solution to become less concentrated and the glass reaction affinity increases.

Glass development demands testing many glasses in a short time; it is not practical to perform long-term durability tests on every glass. The current chemical durability approach focuses on a suite of short-term laboratory tests, such as dynamic flow-through tests (McGrail 1992), static PCT (Jantzen 1992), and vapor hydration tests (Bates 1982).

The static PCTs will provide information about the second stage of glass reaction, which includes the lowest rate attainable before secondary phase formation. These tests couple solution chemistry and glass corrosion. Static PCT includes tests under standard test conditions (at 2000/m and 90°C for 7 days) and under extended conditions, such as 20,000/m and longer test durations. The LLW glass optimization program uses PCTs under both types of conditions. Only the results from the standard conditions are discussed here. The results from extended test conditions will be discussed in a future report.

The dynamic flow-through test provides the glass forward-reaction rate, the maximum corrosion rate of a glass composition at a given temperature, and solution pH. This is a single-path flow-through (SPFT) test under controlled chemical conditions, including pH and temperature. Constant chemical conditions are attained by flowing buffer solution through the system at high flow-rates. Controlled environmental test conditions allow for the determination of key parameters (such as the intrinsic rate constant and power law coefficients) required for modeling the dissolution kinetics of silicate glasses or minerals. In traditional static leach tests, these parameters cannot be determined because the chemical affinity term (1-Q/K) and pH change over the course of the test. The conditions of the flow-through test are meant to keep the leachant undersaturated to eliminate precipitation effects and to maintain a constant pH. The results of this test (obtained from leachant samples taken as a function of time) should provide supplementary performance assessment information to model the kinetics of dissolution of various waste forms adequately.

Vapor hydration and product consistency tests under extended test conditions provide information regarding the final stage of glass reaction. The final stage/or long-term glass reaction may be best described by the dissolution rates in the presence of secondary phases formed from the glass/water reactions

(Bates 1994). The long-term glass corrosion rate could be either close to the minimum rate of the intermediate stage or similar to the forward-reaction rate, depending on the secondary phases formed. Vapor hydration tests expose glass samples to saturated vapor conditions at elevated temperatures. This environment greatly accelerates the progression of glass corrosion into the final stage.

1.3.3 Melter Technology

Until recently, nuclear waste vitrification developers focused on low-temperature melters ($\leq 1150°C$). Glasses for such melters are mainly borosilicates. However, various glass-melting technologies available in the commercial glass industry have been further developed for waste vitrification. The high-temperature melters ($\geq 1250°C$) attempt to match commercial glass melters in their capabilities of processing glass at a high melting rate and reducing waste-form volume by allowing the waste loading to increase above that of low-temperature glasses.

The large variety of melting temperatures precludes development of any single glass composition that could be used for all melter vendors. The Phase I vendor glasses research focused on high-temperature glasses with melting temperatures (at viscosity = 10 Pa.S) between 1290-1380°C. The Phase II glasses were tested at both low and high temperatures (1150 to 1420°C).

1.3.4 Waste Loading and Compositions

Reasonable chemical durability can be obtained with aluminosilicate glasses at 20 wt% sodium content (Kim 1994). Such sodium-loading gives a practical and reasonable 25 wt% dry-solid loading of Hanford Site LLW. The glass development effort has been focusing on compositions at 20 wt% Na_2O. This waste-loading can be adjusted in the future, depending on future decisions concerning glass performance and waste volume reduction requirements.

Two waste simulants were provided for the Phase I vendor test. The first waste simulant was based on the analysis of six tanks of double-shelled slurry feed (DSSF) waste and on the projected composition of the wastes exiting the pretreatment operation (Shade 1994). The second LLW stream simulant, referred to as the remaining inventory (RI), included wastes not included in the DSSF tanks and the projected LLW fraction of single-shell tank wastes (Shade 1994). Only the DSSF waste simulant was used in the Phase I vendor testing. The waste compositions are shown in Table 1.1.

Two compositions of LLW simulants, modified DSSF (M-DSSF) and modified RI (M-RI), were provided for use in Phase II melter vendor tests (Shade 1995). The modified DSSF simulants were spiked with Cl and F at levels which would result in concentrations at their solubility limit in normal silicate glasses, based on a 25 wt% waste oxide-loading in the glass. The simulant contained concentrations of F and Cl at four times their solubility in glasses. Similarly, the modified RI contained four times the solubility of P_2O_5 and SO_3. The compositions used in the Phase II vendor glass formulations were shown in Table 1.1.

Table 1.1. Compositions of LLW Waste Simulants (wt%)

	NLLW	DSSF	M-DSSF	M-RI
SiO_2	0.03			
Na_2O	84.42	76.05	74.02	78.93
CaO	0.01	0.01	0.01	0.01
Al_2O_3	6.19	12.20	11.69	3.46
Others	9.35	11.74	14.28	17.59
Others Components				
Bi_2O_3	0.06			
Cr_2O_3	0.15	0.15	0.15	0.14
Cs_2O		0.56*	0.53*	0.60*
Fe_2O_3	0.02	0.01	0.01	0.01
K_2O	1.38	5.54	5.31	0.12
MgO		0.01	0.01	
MnO	0.03	0.01	0.01	0.04
MoO_3		0.57*	0.54*	0.61*
Nd_2O_3	0.05			
SrO		0.40*	0.38*	0.44*
ZrO_2	0.02			
P_2O_5	5.01	0.72	0.69	9.95
SO_3	1.35	0.82	0.78	3.98
Cl	0.39	1.33	2.38	0.14
F	0.90	1.12	3.02	1.04
I		0.50*	0.47*	0.54*

* These elements were spiked to increase the concentration so that mass balance across the melter during melter evaluation tests can be determined.

The nominal LLW composition shown in Table 1.1 represents the average composition of all tank wastes except those included in the DSSF. The simulated nominal LLW composition (NLLW) was used in glass formulation activities except Phase I and Phase II vendor glass studies.

1.3.5 Glass Systems

The following aluminosilicate systems are being considered for the development of vendor glasses:

Na_2O-Al_2O_3-B_2O_3-SiO_2
Na_2O-Al_2O_3-CaO-SiO_2
Na_2O-Al_2O_3-CaO-B_2O_3-SiO_2
Na_2O-Al_2O_3-Fe_2O_3-SiO_2
Na_2O-Al_2O_3-B_2O_3-ZrO_2-SiO_2
Na_2O-Al_2O_3-B_2O_3-Fe_2O_3-SiO_2
Na_2O-Al_2O_3-CaO-ZrO_2-SiO_2
Na_2O-Al_2O_3-CaO-Fe_2O_3-SiO_2
Na_2O-Al_2O_3-CaO-B_2O_3-ZrO_2-Fe_2O_3-SiO_2

These glass systems are assessed by chemical durability, processibility (viscosity and devitrification behavior), and the capability to incorporate troublesome components (Cl, F, S, P, and Cr). The study focused on glasses with 20 wt% Na_2O; the range of Na_2O was expanded to 15-35 wt%. A comprehensive study of the solubilities of troublesome components was carried out on the Na_2O-Al_2O_3-CaO-B_2O_3-SiO_2 glass system.

2.0 Experimental Considerations

2.1 Waste Simulants

Waste simulants used in this study included nominal low-level waste (NLLW), double-shelled slurry feed (DSSF), modified DSSF (M-DSSF), and modified remaining inventory (M-RI), as shown in Table 1.1. For purposes of this composition study, these waste simulants were added as solid reagent-grade chemicals. To assess the effect on glass properties from actual slurry wastes, a few glasses were made from both reagent-grade solid chemicals and from simulated slurry wastes. Lokken (1995) described the detailed procedures for makeup of these slurry simulants.

2.2 Glass Melting

The glasses were batched and melted according to PNL Procedure PSL-417-GBM ("Procedure for Glass Batching and Melting, Rev. 0"). For each glass, the major glass components to be varied were batched separately as oxides and carbonates. The remaining components were batched together in constant proportions and treated as a single component, "Others." Glasses with different Others compositions were shown in Table 1.1. Using an Angstrom grinding machine, each batch was then mixed in a grinding cell for 5 min to achieve homogeneous mixture.

About 500 g of each glass was melted in a platinum crucible under a lid (to reduce volatilization) using an electrically heated resistance furnace (Deltech DT-31). Furnace temperature was controlled by a Honeywell controller/programmer and monitored by one S-type thermocouple on the controller and a second independent S-type thermocouple. These thermocouples were located in the middle of furnace hot zone. Variation in temperature readout from the two thermocouples was $\pm$ 1.0°C with respect to the preset melting temperatures. For better homogeneity, the glass was removed from the furnace after one hour of melting, cooled, crushed in a tungsten-carbide disc mill, and remelted under a lid for another hour. Molten glass was poured into bars and annealed for 2 h at 520°C for MCC-1 test, glass solid characterization, and archive purposes. The remaining glass was poured onto a steel plate and air-quenched.

Samples (4-5 g) of selected glasses were sent for elemental analysis for comparison to the as-batched compositions.

2.3 Viscosity Measurements

Viscosity was measured by a rotating-spindle technique and evaluated using standard viscosity-measurement procedures GDL-VSC ("Viscosity Spindle Calibration, Rev. 0") and GDL-VIS ("Standard Viscosity Measurement, Rev. 0"). Each glass sample was heated to its approximate melting temperature in a platinum crucible and was maintained until thermal equilibrium was reached (approximately 30 minutes). A measurement was then taken at the melting temperature and subsequent measurements were taken about 50°C apart. The viscosity measurements within the temperature range were taken twice, first at decreasing and then at increasing temperature, to check that viscosity was independent of time. Two replicate viscosity measurements were made at the same nominal temperature as that of the initial measurement during the cycle of increasing and decreasing

melt temperatures, i.e., the viscosity was measured three times at this temperature. Usually eleven measurements were made for each glass (i.e., three measurements at initial melting temperature and eight duplicate measurements at four temperatures near the melting temperature). The melt viscosity was expected to be affected by volatilization at higher temperatures and by crystallization at low temperatures. Examination of the viscosity changes at the initial melting temperature provides information about how prone this melt is to volatilization and crystallization.

Temperatures at viscosity = 10 Pa.S were obtained by fitting the raw viscosity at temperature data for each glass to the Arrhenius equation:

$$\text{Ln } V = A + B/T \quad (1)$$

where A and B = the Arrhenius equation coefficients,
T = temperature (K), and
V = viscosity in Pa.S.

Accuracy of viscosity was controlled by using National Institute of Standards and Technology (NIST) lead-silicate glass (NBS-711) for equipment calibration. Previous experience has demonstrated that viscosity measurements of the same glass by different laboratories typically have good agreement. Also, overcheck measurements of viscosity were made by Corning, Inc. on glass samples provided by this laboratory.

2.4 Durability Testing

The chemical durability of the glasses was determined by three types of tests: PCT, single-pass flow-through, and vapor hydration. The rationale for using these tests is discussed in Section 1.3.2.

2.4.1 Product Consistency Test

The product consistency test (PCT) was based on previous research (Jantzen 1992) and adapted as PNL Procedure MCC-TP-19 ("Leaching Test Using PCT Test Method, Rev. 0"). The test was conducted using deionized water in Teflon™ containers at 90°C. The new containers were baked at 200°C for one week to drive off fluorine and washed thoroughly according to the PCT procedure. The glass was ground in a tungsten-carbide grinding chamber and then sieved through 100- and 200-mesh stainless-steel sieves to obtain particle sizes between 75 and 150 μm. The large particles remaining on the top of the 100-mesh sieve were crushed repeatedly until all glass particles could pass through it. Using an ultrasonic cleaner, the crushed glass was cleaned by washing it in deionized water and ethanol. It was then dried, weighed, and 4 g of glass was added to a 60-mL Teflon container filled with 40 mL of deionized water. The ratio of the surface area of glass to solution volume was taken as 200/m. The Teflon container and its contents were placed for seven days in an oven that had been preheated to 90°C. Aliquots of the leachate were filtered through a 0.45-μm filter, after the test was terminated, and submitted for chemical elemental analysis. The PCT is performed in duplicate.

Results are reported as normalized elemental-mass releases according to:

$$NL_i = \frac{C_i}{f_i \cdot \frac{S}{V}} \qquad (2)$$

where NL_i = the normalized mass release based on element i (g/m^2),
C_i = the analyzed concentration of element i in leachate (g/m^3),
f_i = mass fraction of element i in the glass (unitless), and
S/V = the ratio of glass surface are to solution volume (1/m), which is 2000/m here.

Nominal compositions were used for most of the normalized mass release calculations except where the analyzed glass compositions were very different from the nominal compositions.

2.4.2 Single-Pass Flow-Through Test

In this test, monolithic or powdered samples were exposed to controlled environmental conditions, including pH and temperature. A general schematic of the single-pass flow-through test equipment (see Figure 2.1) and process description are described here. The test equipment uses 13 holding reservoirs for evaluating the effect of pH on dissolution kinetics of various waste form compositions. Twelve of the 13 holding reservoirs were 2000-mL vessels into which a range of pH buffer solutions could be placed, allowing the evaluation of the effect of pH on a single waste-form composition. The single large holding reservoir (25-L carboy) held a constant pH solution that was supplied to 12 independent cells/lines, from which the dissolution kinetics of 12 varying waste form compositions were evaluated at a constant pH. The system also could have been set up to evaluate 24 varying compositions as a function of a constant pH (i.e., a single buffer solution placed in the 12 2000-mL vessels as well as the 25-L carboy). Nitrogen was used continuously as a cover gas for the buffer-solution reservoirs.

Once the test conditions (buffers, flow rates, temperature, etc.) were defined and verified through pretest procedures, a predetermined quantity of glass (powder or monolith) was added to the solution in each preheated, 2-port sample vessel. The 2-port vessels were then sealed and flow of the buffer solution was initiated by activating the pump(s) and the cover-gas source. The buffer composition chosen should minimize compositional overlap between the buffer solution and the glass component. Nitrogen flowed into the 3-port vessels and aided in the transfer of buffer solution to and through the 2-port sample vessels into the sample collection vessels. Flow rates varied depending on the durability of the sample, pH of the buffer solution, and test temperature. The test conditions were controlled to keep the leachant undersaturated with respect to precipitation of secondary phases, but above elemental detection limits of the analytical equipment used.

Corrosion rates in the single-pass flow-through experiments were calculated for each pH value from the steady-state concentrations of component (i) measured in the effluent. The measured concentrations were converted to corrosion rate by:

$$R_{i,j} = \frac{Q_i C_{i,j}}{S_j f_i} \qquad (3)$$

where
- $R_{i,j}$ = corrosion rate for component i at time period j ($g/m^2/d$),
- Ci,j = blank corrected steady-state concentration of Si (g/m^3),
- Q_i = flow rate at time period j (m^3/d),
- f_i = mass fraction of component i in the sample, and
- S_j = average total glass surface area over time period j-1 to j (m^2).

The test conditions for the LLW glasses were as follows:

- Test temperature: 90°C
- Sample size: approximately 1 g
- Sample type: powder between 75 and 150 μm
- Flow Rate: approximately 100 mL/d
- Buffer solution: 0.0107 m LiOH
- pH @ 20°C: 11.95 (measured)
- pH @ 90°C: 10.56 (calculated).

2.4.3 Vapor Hydration Test

The vapor hydration test (Bates 1982; Ebert 1991) was used as an accelerated corrosion test to measure the long-term durability of the glasses. This test was performed in saturated water vapor at various temperatures. Durability was measured as a function of the rate and amount of secondary alteration phase-formation on the surface of the glass and the thickness of the altered surface layers surrounding the samples, as measured in cross-section. This information provided insight into the long-term durability of the glasses.

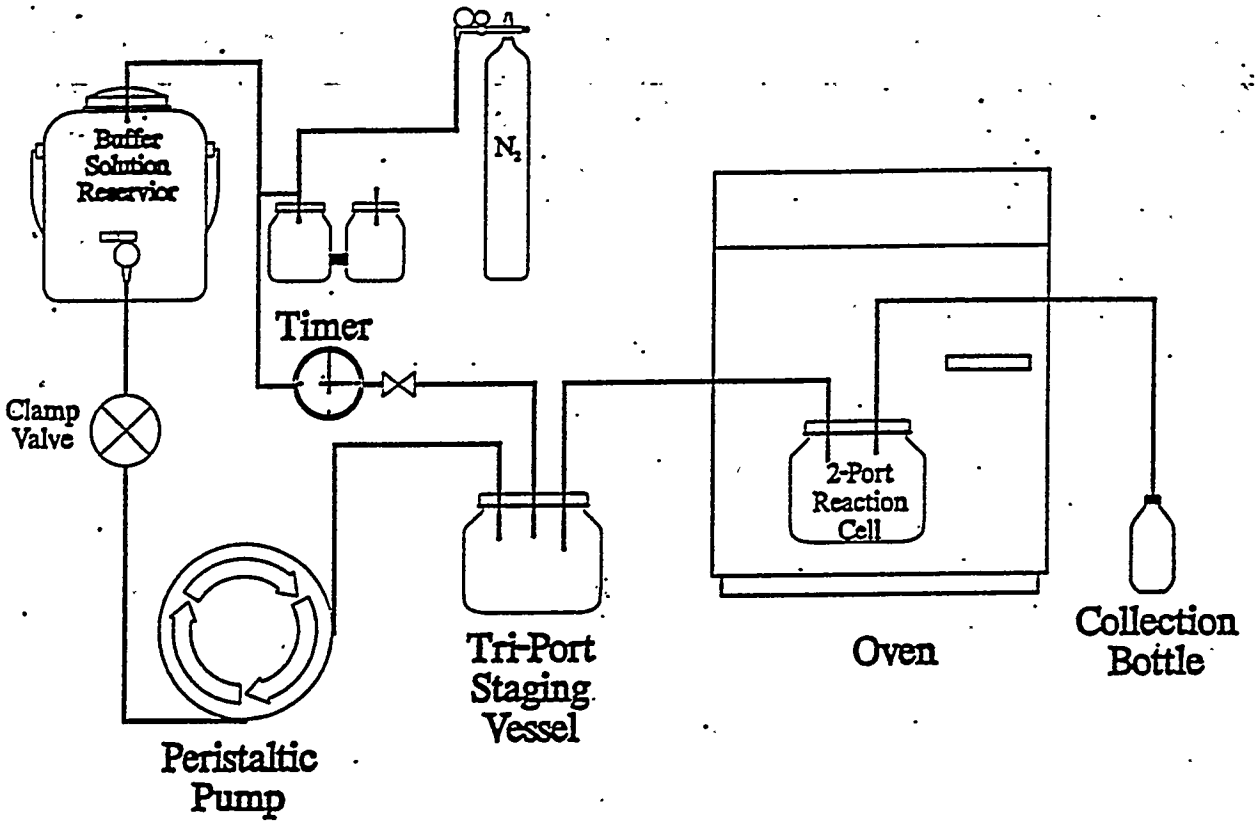

Figure 2.1. Schematic of Single-Pass Flow-Through Apparatus

Monoliths were used in the vapor hydration tests. The sample preparation procedure involved cutting 10-mm-diameter cylinders from solidified glass casts. These cylinders were sectioned into 1-mm-thick circular disks which were then notched in two locations on opposite ends of the sample to provide locations to attach the support threads to the samples. Surfaces of the glass samples were next polished to a 600-grit finish and the samples were cleaned ultrasonically in a methanol bath. All samples were examined by optical microscopy before vapor hydration testing began.

Tests were begun by suspending the sample disks from Teflon threads which were then attached, in pairs, to a stainless-steel support rod. The entire sample support-rod assembly was placed in a stainless-steel reaction vessel. A predetermined volume of water (0.25 mL for 200°C test) was added to each vessel; this amount was sufficient to saturate the vessel atmosphere with water vapor after heating to the appropriate experimental temperature, but was not sufficient to result in water refluxing between the samples and the fluid in the bottom of the vessel.

After adding the water, the vessels were hermetically sealed and inserted into a preheated oven that was controlled to $\pm$ 2°C. The elevated temperatures were chosen to accelerate reactions between the condensed fluid and the samples.

Upon completion of the prescribed test interval, the sample vessels were removed from the oven, cooled in an ice bath, and opened. All sample disks were first examined by optical microscopy

and representative samples were then chosen for detailed scanning electron microscopy/energy-dispersive X-ray analysis (SEM/EDS). Surfaces of the altered samples were characterized with respect to the extent of alteration phase development.

2.4.4 Solution Analyses

Cations and radionuclides were analyzed with inductively coupled plasma atomic emission spectrometry (ICP/AES) with an accuracy of $\pm$ 10% for major elements and $\pm$ 50% for radionuclides and minor elements. Anions were analyzed with ion chromatography with an accuracy of about 50%. The pH was analyzed with a combination electrode with an accuracy of $\pm$ 0.1 pH unit.

3.0 Results and Discussion

3.1 Glass Optimization Investigation

The glass optimization investigation consisted of the 44 glasses shown in Table 3.1.

L7-series glasses were borosilicate glasses with calcium at the sodium contents of 15 to 35 wt%. The rest of the glasses had the same sodium content of 20 wt%. Glass L0-0 is made of SiO_2 plus 25 wt% waste (which results in 20 wt% Na_2O in the glass) and belongs to alkali-silicate glass. L1-series are glasses made from wastes plus silica and alumina, and belong to aluminosilicate glasses. L4-series glasses are borosilicate glasses without calcium. L5-series glasses are soda-lime-aluminosilicate glasses. L6-series glasses are borosilicate glasses with calcium. L8-series glasses are glasses designed to evaluate the effects on glass properties by replacing B_2O_3 or CaO using Fe_2O_3 or ZrO_2. Glass L8-8 was designed to determine the effect of replacing CaO with MgO. The nominal compositions of these glasses are shown in Table 3.1. The detailed composition and the available analyzed compositions are shown in Appendix A.

3.1.1 Product Consistency Test Results

The product consistency test (PCT) results in terms of the normalized element releases (g/m^2) of major elements of Si, Al, B, Ca, and Na and leachate pHs are tabulated in Table 3.1. The releases of all the elements are listed in Appendix B.

In Alkali Silicate Glass System - L0

The PCT results for glass L0-0 suggests that no durable glass can be made at 25 wt% waste-loading of nominal Hanford waste by addition of just silica into the waste, since this alkali silicate glass was completely dissolved within 7 days under PCT conditions.

In Alkali Aluminosilicate Glass System - L1

Figure 3.1 shows that replacing silica with alumina resulted in more durable glasses. This improvement in durability is almost linear with the alumina content in the glass. Glass L1-6 with 6 wt% alumina is still not durable enough to withstand the 7-day PCT, since so much glass content was dissolved and the solution became gel. However, this glass is obviously more durable than L0-0 since L1-6 was not completely dissolved. This improvement of glass durability by the addition of alumina is due to the capability of alumina to convert the nonbridging oxygen (NBO) bonds created by alkalis into bridging oxygen (BO) bonds (Alexander 1986; Dickenson 1981, 1986).

In Borosilicate Glass System Without Calcium - L4

The PCT results for this glass system are shown in Figures 3.2 and 3.3. Figure 3.2a shows that the addition of 6 wt% B_2O_3 (at the expense of SiO_2) to a glass with 9% Al_2O_3 improved the durability in terms of sodium release by 12 times. The same 6 wt% B_2O_3 addition to glasses with 12 and 15 wt% Al_2O_3 resulted in respective improvement of 10 and 4 times. Boron oxide also improves glass durability by replacing the NBO bonds in the glass with BO bonds (Dell 1983). In the glasses with higher Al_2O_3 contents, there were fewer

Table 3.1. Glass Composition and PCT Results of Glasses for Optimization Investigation

Glass	Composition (mass fraction)									7-day PCT at 90°C Normalized Release (g/m2)					Final
	SiO2	B2O3	Na2O	CaO	Al2O3	MgO	Fe2O3	ZrO2	Others	Si	Al	B	Ca	Na	pH
L0-0	0.763		0.2		0.01				0.022	Almost completely dissolved					
L1-6	0.718		0.2		0.06				0.022	Gel formed					
L1-9	0.688		0.2		0.09				0.022	0.68	0.65			5.99	12.72
										0.70	0.66			6.18	12.75
L1-12	0.658		0.2		0.12				0.022	0.40	0.39			2.65	12.33
										0.40	0.39			2.64	12.35
L1-15	0.628		0.2		0.15				0.022	0.21	0.22			0.86	11.63
										0.21	0.22			0.86	11.63
L4-69	0.628	0.06	0.2		0.09				0.022	0.22	0.11	0.47		0.53	10.88
										0.22	0.11	0.47		0.53	10.88
L4-612	0.598	0.06	0.2		0.12				0.022	0.13	0.13	0.15		0.27	10.71
										0.13	0.13	0.16		0.27	10.70
L4-615	0.568	0.06	0.2		0.15				0.022	0.13	0.13	0.15		0.24	10.62
										0.13	0.13	0.14		0.23	10.61
L4-96	0.628	0.09	0.2		0.06				0.022	0.78	0.01	2.95		2.28	10.60
										0.79	0.01	3.00		2.30	10.64
L4-99	0.598	0.09	0.2		0.09				0.022	0.21	0.06	0.78		0.60	10.43
										0.21	0.06	0.77		0.59	10.59
L4-912	0.568	0.09	0.2		0.12				0.022	0.13	0.13	0.28		0.30	10.52
										0.13	0.13	0.28		0.30	10.54
L4-915	0.538	0.09	0.2		0.15				0.022	0.12	0.12	0.20		0.22	10.41
										0.12	0.12	0.20		0.23	10.26
L4-129	0.568	0.12	0.2		0.09				0.022	0.24	0.04	1.61		1.10	10.36
										0.25	0.03	1.69		1.16	10.41
L4-1212	0.538	0.12	0.2		0.12				0.022	0.13	0.12	1.02		0.64	10.37
										0.13	0.13	1.14		0.75	10.41
L4-1215	0.508	0.12	0.2		0.15				0.022	0.11	0.11	0.60		0.39	10.11
										0.12	0.12	0.68		0.43	10.04
										0.12	0.12	0.66		0.41	10.08

Table 3.1. Glass Composition and PCT Results of Glasses for Optimization Investigation (continued)

Glass	Composition (mass fraction)									7-day PCT at 90°C Normalized Release (g/m2)					Final
	SiO2	B2O3	Na2O	CaO	Al2O3	MgO	Fe2O3	ZrO2	Others	Si	Al	B	Ca	Na	pH
L5-69	0.628		0.2	0.06	0.09				0.022	0.34	0.31		0.01	1.87	12.18
										0.36	0.31		0.02	1.94	12.15
L5-612	0.598		0.2	0.06	0.12				0.022	0.15	0.14		0.05	1.00	11.95
										0.16	0.15		0.05	1.02	11.93
L5-615	0.568		0.2	0.06	0.15				0.022	0.12	0.11		0.05	0.54	11.64
										0.12	0.11		0.05	0.54	11.63
L5-96	0.628		0.2	0.09	0.06				0.022	0.50	0.33		0.01	2.18	12.22
										0.50	0.33		0.01	2.29	12.22
L5-99	0.598		0.2	0.09	0.09				0.022	0.35	0.28		0.01	1.70	12.09
										0.32	0.27		0.01	1.65	12.24
L5-912	0.568		0.2	0.09	0.12				0.022	0.17	0.16		0.02	0.93	12.01
										0.19	0.17		0.02	0.96	11.90
L5-915	0.538		0.2	0.09	0.15				0.022	0.11	0.12		0.07	0.61	11.86
										0.11	0.11		0.06	0.67	11.74
L5-129	0.568		0.2	0.12	0.09				0.022	0.29	0.23		0.01	1.34	12.17
										0.29	0.26		0.01	1.48	12.03
										0.29	0.23		0.01	1.39	12.07
L5-1212	0.538		0.2	0.12	0.12				0.022	0.21	0.19		0.01	1.04	11.97
										0.21	0.19		0.02	1.06	11.97
L5-1215	0.508		0.2	0.12	0.15				0.022	0.10	0.09		0.06	0.59	11.84
										0.10	0.09		0.06	0.61	11.75

Table 3.1. Glass Composition and PCT Results of Glasses for Optimization Investigation (continued)

Glass	Composition (mass fraction)									7-day PCT at 90°C					
										Normalized Release (g/m2)					Final
	SiO2	B2O3	Na2O	CaO	Al2O3	MgO	Fe2O3	ZrO2	Others	Si	Al	B	Ca	Na	pH
L6-546	0.628	0.05	0.20	0.04	0.06				0.022	0.22	0.18	0.23	0.04	0.91	11.89
										0.22	0.19	0.24	0.04	0.97	11.91
L6-549	0.598	0.05	0.20	0.04	0.09				0.022	0.16	0.14	0.17	0.03	0.58	11.64
										0.16	0.15	0.17	0.03	0.61	11.66
L6-5412	0.568	0.05	0.20	0.04	0.12				0.022	0.12	0.11	0.13	0.02	0.39	11.39
										0.12	0.12	0.13	0.02	0.40	11.41
L6-5415	0.538	0.05	0.20	0.04	0.15				0.022	0.10	0.10	0.11	0.02	0.31	11.22
										0.10	0.10	0.11	0.02	0.30	11.26
L6-3312	0.598	0.03	0.20	0.03	0.12				0.022	0.15	0.15	0.16	0.02	0.56	11.63
										0.16	0.15	0.17	0.02	0.59	11.64
L6-6612	0.538	0.06	0.20	0.06	0.12				0.022	0.11	0.10	0.12	0.04	0.39	11.47
										0.10	0.10	0.11	0.04	0.37	11.46
L6-669	0.568	0.06	0.20	0.06	0.09				0.022	0.13	0.12	0.14	0.05	0.49	11.36
										0.13	0.12	0.14	0.05	0.49	11.37
L7-15	0.612	0.05	0.15	0.04	0.12				0.017	0.06	0.06	0.07	0.03	0.15	10.39
										0.06	0.06	0.07	0.03	0.15	10.41
L7-25	0.524	0.05	0.25	0.04	0.12				0.028	0.37	0.34	0.38	0.02	1.50	12.22
										0.37	0.35	0.40	0.02	1.51	12.22
L7-30	0.480	0.04	0.30	0.03	0.11				0.033	0.97	0.97	1.28	0.01	6.38	12.88
										0.94	0.91	1.10	0.01	5.66	12.90
L7-35	0.436	0.04	0.35	0.03	0.11				0.039	13.60	0.10	36.10	0.00	29.10	13.38
										19.60	0.30	52.50	0.00	41.90	13.33

Table 3.1. Glass Composition and PCT Results of Glasses for Optimization Investigation (continued)

Glass	Composition (mass fraction)									7-day PCT at 90°C					
										Normalized Release (g/m2)					Final
	SiO2	B2O3	Na2O	CaO	Al2O3	MgO	Fe2O3	ZrO2	Others	Si	Al	B	Ca	Na	pH
L8-1	0.568	0.06	0.20		0.09			0.06	0.022	0.12	0.12	0.17		0.34	11.01
										0.12	0.13	0.17		0.35	10.99
L8-2	0.568		0.20	0.06	0.09			0.06	0.022	0.19	0.14		0.00	0.95	11.86
										0.18	0.19		0.00	1.11	11.87
L8-3	0.568	0.03	0.20	0.03	0.09			0.06	0.022	0.16	0.14	0.24	0.00	0.69	11.57
										0.15	0.12	0.24	0.00	0.65	11.59
L8-4	0.568	0.06	0.20		0.09		0.06		0.022	0.44	0.00	1.28		1.00	10.70
										0.43	0.00	1.30		1.03	10.71
L8-5	0.568		0.20	0.06	0.09		0.06		0.022	0.21	0.22		0.01	1.17	11.93
										0.22	0.20		0.01	1.15	11.94
L8-6	0.568	0.03	0.20	0.03	0.09		0.06		0.022	0.19	0.17	0.24	0.02	0.62	11.46

Table 3.2. The Durability Ranking by PCT Results

Glass	PCT-Si	Glass	PCT-Na
L7-15	0.06	L7-15	0.15
L5-1215	0.1	L4-915	0.225
L6-5415	0.1	L4-615	0.235
L6-6612	0.105	L4-612	0.27
L5-915	0.11	L4-912	0.3
L4-1215	0.12	L6-5415	0.305
L4-915	0.12	L8-1	0.345
L5-615	0.12	L8-7	0.35
L6-5412	0.12	L6-6612	0.38
L8-1	0.12	L6-5412	0.395
L4-1212	0.13	L4-1215	0.41
L4-612	0.13	L6-669	0.49
L4-615	0.13	L4-69	0.53
L4-912	0.13	L5-615	0.54
L6-669	0.13	L6-3312	0.575
L8-7	0.14	L4-99	0.595
L5-612	0.155	L6-549	0.595
L6-3312	0.155	L5-1215	0.6
L8-3	0.155	L8-6	0.615
L6-549	0.16	L5-915	0.64
L5-912	0.18	L8-3	0.67
L8-2	0.185	L4-1212	0.695
L8-6	0.19	L1-15	0.86
L1-15	0.21	L6-546	0.93
L4-99	0.21	L5-912	0.945
L5-1212	0.21	L5-612	1.01
L8-5	0.215	L8-4	1.015
L4-69	0.22	L8-2	1.03
L6-546	0.22	L5-1212	1.05
L4-129	0.245	L4-129	1.13
L5-129	0.29	L8-5	1.16
L5-99	0.335	L8-8	1.285
L5-69	0.35	L5-129	1.37
L7-25	0.37	L7-25	1.505
L1-12	0.4	L5-99	1.675
L8-8	0.4	L5-69	1.905
L8-4	0.435	L5-96	2.235
L5-96	0.5	L4-96	2.29
L1-9	0.69	L1-12	2.645
L4-96	0.785	L7-30	6.02
L7-30	0.955	L1-9	6.085
L7-35	16.6	L7-35	35.5

NBO bonds available for such replacement; therefore, the durability improvement decreased as the alumina content increased at fixed alkali content. It should be emphasized that the reaction of boron oxide, in trigonal configuration with alkali to form the BO bond of tetrahedral boron, is usually far from complete (Dell 1983). The additional 3 wt% boron oxide beyond 6 wt% made no improvement in durability; the addition of B_2O_3 beyond 9 wt% made the glass less durable. This is consistent with findings that maximum tetrahedral boron can only be formed at certain ratios of alkali-to-boron and silica-to-boron (Dell 1983). Figure 3.2b presents the same boron effects on glass durability in terms of silicon releases in PCTs. However, the addition of B_2O_3 (at the expense of SiO_2) to a glass consistently reduced leachate pH, as shown in Figure 3.2c. Figure 3.3 presents the same data as Figure 3.2, but in terms of replacing SiO_2 with Al_2O_3. This figure shows that the addition of Al_2O_3 into glasses with different levels of B_2O_3 always improves glass durability. The extent of improvement was also similar among the glasses investigated, because alumina always reacted with alkalis to form tetrahedral aluminum, even though the alkalis were bound to boron; i.e., alkalis always satisfied the charge-balance needs of alumina before boron. The alumna addition also reduced leachate pH due to its capability to bind alkalis, which made the alkalis less available for ion-exchange reactions.

In Soda-Lime-Aluminosilicate Glass System - L5

The effects on chemical durability by replacement of SiO_2 with CaO in aluminosilicate glasses are shown in Figures 3.4 and 3.5. The CaO addition clearly showed improvement in glass durability, up to 12 wt% in glasses with 9 wt% Al_2O_3, but only up to 9 wt% in glasses with 12 wt% Al_2O_3. Slight improvement in glass durability was observed in up to 6 wt% CaO addition in glasses with 15 wt% Al_2O_3. The durability improvement when CaO replaced SiO_2 was probably due to sharing NBO bonds with alkalis and making the NBO bonds into hybrid bonds of NBO and BO bonds; i.e., the hybrid bonds were more durable than pure NBO bonds, but less durable than pure BO bonds. Therefore, the improvement of durability by alkaline earths depended on the availability of NBO bonds, and the durability improvement was less than formation of BO from NBO bonds. This conversion reaction of NBO bonds into hybrid bonds seemed also far from completion, because the addition of CaO (at the expense of SiO_2) no longer improved glass durability in L5-915, L5-1215, and L5-1212, although these glasses have NBO bonds. The effects of CaO on leachate pH were consistent with its effect on chemical durability, as seen in Figure 3.4c; i.e., it reduced leachate pH if it improved glass durability and it increased leachate pH if it reduced glass durability. Figure 3.5 shows that the addition of alumina at the expense of silica to soda-lime-silicate glasses always improved glass durability, regardless of the levels of CaO in the glasses. This effect was similar to the addition of alumina into the alkali-borosilicate glass system discussed above, because alumina bound to alkalis preferentially over B_2O_3 and CaO and the alumina-alkali reaction usually goes to completion. The addition of alumina into calcium-containing glasses lowered the solution pH more than that in boron-containing glasses (compare Figure 3.5 with Figure 3.3). The addition of alumina in calcium-containing glasses brought greater durability improvement than the same in the boron-glass system, where there were more BO bonds than in the calcium-glass system.

In Borosilicate Glass System With Calcium - L6

The addition of a mixture of CaO and B_2O_3 (at the expense of SiO_2) into alkali-aluminosilicate glasses improved durability until the total addition reached 9 wt%, as shown in Figure 3.6. Beyond 9 wt%, the addition showed no appreciable improvement in terms of sodium release (Fig. 3.6a) and slight improvement in silica release (Figure 3.6b). The addition of B_2O_3 + CaO also caused the leachate pH to lower until the addition reached 9 wt% and increased leachate pH when beyond 9 wt%, as shown in Figure 3.6c. The addition of alumina into soda-lime-borosilicate glasses always improved glass durability, as shown in Figure 3.7. The alumina addition was expected to lower the solution pH, as shown in Figure 3.7c. There is one

anomalous point in Figure 3.7c where the pH values of the glass with 12 wt% Al_2O_3 at 6 wt%B_2O_3 and 6 wt% CaO are higher than the pH in the glass with 9 wt% Al_2O_3 at 6 wt% B_2O_3 and 6 wt% CaO. The validity of these pH values is being reevaluated.

Figure 3.8 compares the effectiveness in improving glass durability by addition of alumina at the expense of silica to the three glass systems, L4, L5, and L6. The general trend was that addition of alumina to all three glass systems always improved glass durability. However, the extent of improvement was larger in the alkali-soda-silicate glass system (L5) than in the alkali-borosilicate glass systems (L4 and L6). This was probably due to the fact that CaO is much less effective in stabilizing NBO bonds, in comparison with B_2O_3, and the CaO-glasses (L5) were less durable than L4 and L6 glasses where boron oxides were added, as shown in Figure 3.8. The addition of the same amounts of Al_2O_3 into L5 glasses will be more effective in improving the overall glass durability in comparison with the addition to L4 and L6, where the glasses were already more durable than L5 glasses, although similar numbers of BO bonds were formed by the addition of Al_2O_3 among the three glass systems. Figure 3.8c clearly shows that the solution pH was lowered in all three glass systems (L4, L5, and L6) by replacing silica with alumina, but the pH level was determined by boron and calcium concentrations. L4 glasses with the highest amount of B_2O_3 and, without CaO, had the lowest leachate pH. L5 glasses with the highest amount of CaO and without B_2O_3 had the highest leachate pH. L6 glasses with both CaO and B_2O_3 had the intermediate pH.

In Borosilicate Glass System with CaO and Variant Sodium Levels - L7

The L7 series glasses were based on glass L6-5412 by addition of Na_2O to dilute other components to produce L7-25, L7-30, and L7-35 with sodium contents of 25, 30, and 35 wt%, respectively, and by subtracting Na_2O to concentrate other components to create L7-15 with 15 wt% Na_2O. The 7-day PCT releases of these glasses are shown in Figure 3.9. The data showed that the glasses with less than 25 wt% Na_2O, based on L6-5412, were relatively durable. L7-30 with 30 wt% Na_2O had a similar chemical durability as did the high-level EA glass; the glass with 35 wt% Na_2O was much less durable than EA glass. Decreasing 5 wt% Na_2O from L6-5412 to L7-15 improved the durability by 2.6 times. Increasing 5 wt% Na_2O from L6-5412 to L7-25, from L7-25 to L7-30, and from L7-30 to L7-35, decreased the durabilities by a factor of 3.8, 4.0, and 5.9, respectively. The pH increase was almost linear with the sodium content increase, as shown in Figure 3.9c.

In L8 Glass System

The L8-series glasses evaluated the effects on glass properties by replacing B_2O_3 or CaO using Fe_2O_3 or ZrO_2. Glass L8-8 was designed to determine the effect of replacing CaO with MgO. Figures 3.10 to 3.13 summarize the results of L8 glass tests. The effects on 7-day PCT results by the addition of 6 wt% ZrO_2 into a base glass of SiO2 56.78, Na_2O 20.0, Al_2O_3 9.0, but with different amounts of B_2O_3 and CaO, are shown in Figure 3.10. The addition of 6 wt% ZrO_2 created the lowest sodium release in the glass with 6 wt% B_2O_3 (L8-1), the highest release was in the glass with 6 wt% CaO (L8-2), and intermediate release was in the glass with 3 wt% B_2O_3 and 3 wt% CaO (L8-3). The silicon release and leachate pH data showed the same trend.

Figure 3.11 shows the effect on durability by addition of 6 wt% Fe_2O_3 into a base glass of SiO_2 56.78; Na_2O 20.0, Al_2O_3 9.0, but with different amounts of B_2O_3 and CaO. The sodium release was lower when 6 wt% of Fe_2O_3 was added to the glass with 6 wt% B_2O_3 (L8-4) than when the same amount of Fe_2O_3 was added to a glass with 6 wt% CaO (L8-5). It was interesting to see that the lowest sodium release occurred in the glass with 3 wt% B_2O_3 and 3 wt% CaO (L8-6). This was different from the results of the ZrO_2 glasses discussed above, where the lowest release occurred in the B_2O_3 glass (L8-1), not in the mixture glass (L8-3).

However, the actual sodium release, 0.67 g/m2, of the Zr glass, L8-3, was very similar to 0.62 g/m2 of the Fe glass, L8-6, with equal amounts of B_2O_3 and CaO. Also, the 6 wt% CaO-containing glasses had similar sodium releases of 1.03 and 1.16 g/m^2 for L8-2 (ZrO_2 glass) and L-5 (Fe_2O_3 glass), respectively. The obvious difference was between L8-1 (ZrO_2 glass) and L8-4 (Fe_2O_3 glass); the sodium release of 0.35 g/m^2 of L8-1 was a factor of 2.9 different from the 1.02 factor of L8-4. Another difference among the ZrO_2 glasses and Fe_2O_3 glasses was that the sodium release trend was the same as the silicon release among ZrO_2 glasses (Figure 3.10), while the sodium and silicon release trends were different among Fe_2O_3 glasses (Figure 3.11). The leachate pH trend among Fe_2O_3 glasses was similar to that of ZrO_2 glasses, as shown in Figure 3.11c; i.e., CaO glass had the highest pH, B_2O_3 glass the lowest, and CaO-B_2O_3 glasses the intermediate.

Glass L8-8 and Glass L6-549 were similar in that all had SiO_2 59.8, B_2O_3 5.0, Na_2O 20.0, Al_2O_3 9.0, and 2.22 wt% Others, and were different in that L6-549 had 4 wt% CaO and L8-8 had 4 wt% MgO. Figure 3.12 clearly shows that the CaO glass, L6-549, was greater than a factor of 2.2 more durable than the Mg glass, L8-8, in terms of both sodium and silicon releases. However, the leachate pH, 11.65, of CaO glass, L6-549, was slightly higher than the 11.29 of the MgO glass, L8-8.

Figure 3.13 summarizes the composition effects on durability by 6 wt% addition of different oxides to a base glass with SiO_2 56.78, Na_2O 20.0, Al_2O_3 9.0, B_2O_3 6.0, and Others 2.22. The sodium releases shown in Figure 3.13a and the silicon releases in Figure 3.13b were similar. The results show that the order of oxides (at the same mass addition) in improving glass durability in this particular glass system was:

Al2O > ZrO2 > mixture (ZrO2+Fe2O3) > CaO > SiO2 > Fe2O3 > B2O3.

The effects of these oxide additions on leachate pH were minor, as shown in Figure 3.13. This order of durability improvement was consistent with the current understanding of glass chemistry (Feng 1989, 1994; Ellison 1994).

Durability Ranking by PCT

The durability ranking in Table 3.1 was established according to PCT sodium releases. The most durable glass was the glass with the least sodium content, 15 wt%, while the least durable glass was the one with the highest level of sodium, 35 wt%. The PCT data in Figures 3.14 and 3.15 show that at the same alumina, silica, and sodium levels, the order of glass systems based on durability ranked as follows:

Boron-only (L4) > Mixture (L6) > Calcium-only (L5).

This order of durability was consistent with our current understanding of glass chemistry. Alumina increases glass durability by converting the nonbridging oxygen bonds generated by alkalis into bridging oxygen bonds through formation of tetrahedral alumina in the glass structure (Bobkova 1983; Feng 1988; Ellison 1994). There are still plenty of NBO bonds in these high-sodium glasses (Na_2O = 20 wt%) after charge-balancing by available alumina in the glass. The addition of boron oxide (at the expense of SiO_2, [i.e., SiO_2 was replaced by B_2O_3 on the equal weight basis]) into such a high-sodium glass will convert more NBO bonds into BO bonds by forming tetrahedral boron, resulting in an increase in chemical durability. Addition of calcium oxide (at the expense of SiO_2) also increased durability through oxygen-sharing between alkali and alkaline earth. The NBO bonds convert to hybrid NBO and BO bonds. The addition of CaO can improve glass durability if there are sufficient NBO bonds in the glass for such a conversion. The improvement is less than that seen by the addition of boron oxide, which promotes direct conversion of NBO to BO. Another

beneficial effect of the boron addition is that the boron release into the static glass leachate can lower the solution pH due to the boric acid buffering capability, which lowers the corrosion process. The PCT pHs of the boron-only glasses were observed to be 1 to 2 pH units lower than the corresponding calcium-only glasses.

3.1.2 Vapor Hydration Test Results

Vapor hydration tests on eleven compositions are being conducted at Argonne National Laboratory (ANL) (Bakel 1994). Tables 3.3a and 3.3b show the glass compositions (wt %) and their associated identification numbers (assigned by ANL and PNNL). PNL-A (or LD6-5412) was selected for use in both long-term PCT and the accelerated vapor hydration tests. The other ten glasses (PNL-B through PNL-K) were tested only under accelerating conditions of the vapor hydration test.

All eleven glasses are being tested using the ANL vapor hydration test method to generate secondary phases within a short period of time. Monolithic samples are exposed to a saturated waste vapor environment. These tests are being conducted at temperatures of 70, 120, 150, 175, and 200°C to determine the effect of temperature on the alteration phases generated and the corrosion rate under these conditions. The long-term corrosion rate and identification of secondary phases generated during glass corrosion as a function to temperature will determined. A quantitative measure of the corrosion rate is given by the overall generation of the alteration material. The thickness of the alteration layer (including secondary phase formation and the sodium-depleted layer) is used to approximate the rate of alteration at different reaction times.

For a detailed description of the test conditions, refer to the ANL interim report, "Long-Term and Accelerated Testing of Candidate Waste Forms for Low-Level Hanford Waste for FY94" (Bakel 1994). Most of the information reported in this summary was obtained from the interim report (Bakel 1994) for fiscal year 1994, while limited data and discussion obtained through monthly reports were also provided.

Table 3.3a. Glass Compositions (Oxides in wt%) and Identifications

PNL ID	LD6-5412	L4-906	L4-909	L4-6012	L4-9012
ANL ID	PNL-A	PNL-B	PNL-C	PNL-D	PNL-E
SiO_2	55.91	62.78	59.81	59.78	56.78
Na_2O	20.0	20.0	20.0	20.0	20.0
B_2O^3	5.0	9.0	9.0	6.0	9.0
CaO	4.0	0.0	0.0	0.0	0.0
Al_2O_3	12.0	6.0	9.0	12.0	12.0
Others	3.09*	2.22**	2.22**	2.22**	2.22**

Table 3.3b. Glass Compositions (Oxides in wt%) and Identifications

PNL ID	L4-12012	L5-096	L5-0912	L6-546	L6-549	L6-5412
ANL ID	PNL-F	PNL-G	PNL-H	PNL-I	PNL-J	PNL-K
SiO_2	53.78	62.78	56.78	62.78	59.78	56.78
Na_2O	20.0	20.0	20.0	20.0	20.0	20.0
B_2O_3	12.0	0.0	0.0	5.0	5.0	5.0
CaO	0.0	9.0	9.0	4.0	4.0	4.0
Al_2O_3	12.0	6.0	12.0	6.0	9.0	12.0
Others	2.22**	2.22**	2.22**	2.22**	2.22**	2.22**

* Cr_2O_3 (0.04), K_2O (1.46), MoO_3 (0.15), SrO (0.11), I (0.13), Cs_2O (0.15), MgO (0.003), P_2O_5 (0.19), F (0.29), Fe_2O_3 (0.003), MnO (0.002), SO_3 (0.21), and Cl (0.35).

** Bi_2O_3 (0.014), K_2O (0.327), P_2O_5 (1.188), Cl (0.093), Cr_2O_3 (0.036), MnO (0.007), SO_3 (0.32), F (0.213), Fe_2O_3 (0.004), Nd_2O_3 (0.012), ZrO_2 (0.005).

Secondary Phases Observed

Four secondary phases (referred to as Phases A, B, C, and D) were observed and identified. From X-ray diffraction data, the d-spacings measured for Phase A were similar to those of both gobbinsite [$Na_5(Al_5Si_{11})0_{32}\cdot 11H_2O$] and phillipsite ($K_2Na_4Al_6Si_{10}O_{32}\cdot 12H_2O$); the chemical compositions were also similar. Morphology considerations lead to Phase A being identified as gobbinsite.

The d-spacings measured for Phase B were in good agreement with those of analcime [$Na(AlSi_2O_6)\cdot H_2O$].

Phase C had composition and d-spacings similar to those of Phase A, but a different morphology. Based on the morphology, Phase C was identified as phillipsite.

Phase D was the only secondary phase that contained a high concentration of calcium, the primary sink for calcium in these systems. Although the compositional analysis of Phase D showed there to be no aluminum, the XRD results were in very good agreement with sodium-aluminum-silicate.

Table 3.4 shows the measured alteration thickness and the phases present on PNL-A at each test temperature and time. Several measurements were taken; an average value is reported on the layer thickness due to large variances about the perimeter of the sample. The hydration test, performed at 70°C and terminated after 56 days, had only a few scattered fine-grained particles. Several crystals of Phase A (possibly gobbinsite) were found in the 120°C tests conducted for 28 days, while no secondary phases were found on the sample reacted for 56 days. No measurable alteration layer was present in either test.

In tests conducted at 150°C, all four phases were observed (Phase A only detected in the 7-day test). During the early stages of the tests, only fine-grained particles were observed on the glass surface. As reaction times increased at 150°C, Phase A particles scattered on the glass surface; the formation of a measurable sodium-depleted layer and Phases B, C, and D were identified.

In tests conducted at 175°C, alteration layers (sodium-depleted) and an outer crust of Phase B, C, and D were observed after 1 day. As the reaction times increased, a thick surface layer of these three phases (primarily Phase B) was observed.

Secondary phases generated on PNL-A reacted at 200°C were large, abundant, and well-formed. All samples developed a thick outer crust composed of Phase B (primary phase), Phase C, and Phase D.

Corrosion of PNL-A resulted in the formation of a sodium-depleted layer beneath the original sample surface and several secondary phases which nucleated on the outer surface of the sodium-depleted layer. The initial stage of corrosion involved the dissolution of material at the glass surface, primarily ion-exchange reactions with water. This generally resulted in an increase in the solution pH, which then facilitated the slower hydrolysis reaction to release boron and silicon. The formation of the sodium-depleted layer observed in the 150°C tests (and higher) was consistent with the two different reaction (ion-exchange and hydrolysis) rates and the experimentally observed solution analysis. The silicon and boron were released nearly stoichiometrically, while sodium was released to a greater extent. As the solution concentration became more concentrated, the effects of secondary precipitation played a role in the overall dissolution once solution saturation has been reached.

Table 3.4. Alteration Phases on PNL-A After the Vapor Hydration Tests (Bakel 1994)

Temperature (°C)	Time (days)	Layer (μm)	Phase A	Phase B	Phase C	Phase D
70	56	0	-	-	-	-
120	28	0	+	-	-	-
120	56	0	-	-	-	-
150	3	0	-	-	-	-
150	7	0	+	-	-	-
150	11	200	-	+	+	+
150	14	200	-	+	+	+
150	18	>	-	+	+	+
150	21	>	-	+	+	+
150	28	>	-	+	+	+
175	1	200	-	+	+	+
175	2	800	-	++	+	+
175	3	1000	-	++	+	+
175	5	800	-	++	+	+
175	7	>	-	++	+	+
175	14	>	-	++	+	+
175	18	>	-	++	+	+
175	21	>	-	++	+	+
175	28	>	-	++	+	+
200	3	>	-	++	+	+
200	7	>	-	++	+	+
200	14	>	-	++	+	+

0 = indicates no measurable layer observed
- = indicates this phase was not observed
+ = indicates this phase was observed
> = indicates that the sample was completely altered
++ = indicates this phase was observed to be the most abundant phase.

Estimating the Corrosion (or Alteration) Rate

From the layer thickness, the corrosion rate (or rate of alteration) of the PNL-A was estimated. From Table 3.4, it can be seen that the corrosion of the glass (alteration layer thickness) occurred very quickly at temperatures of 150°C or higher, but more slowly at lower temperatures. Samples reacted in tests at 70°C and 120°C or 150°C (through 7 days) did not form a measurable alteration layer. An upper corrosion rate for tests at 70°C and for tests at 120°C with layers less than 0.2-μm thick (the minimal detectable thickness) after 56 days was 4×10^{-3} μm/day.

Although tests at 150°C conducted for 7 days or less did not produce a measurable layer, both the 11- and 14-day tests yielded approximately a 200-μm-layer thickness. In both cases, the alteration layer was dominated by the sodium-depleted layer. Assuming the layer thickness was 0.2 μm after 7 days, the glass initially corroded at a rate of less than 3×10^{-2} μm/day. The dissolution rate for longer-term tests (> 18 days) was 50 μm/day, which was consistent with that measured between 7 and 11 days.

In the tests conducted at 175°C, if the assumption was made that the corrosion rate could be expressed based on the initial three days, a rate of about 300 μm/day was calculated. However, since the glass was completely dissolved after 5 days, the rate of dissolution was estimated to be about 500 μm dissolved in 5 days, or 100 μm/day. This was about twice the calculated rate of the tests at 150°C. It was noted that since the same alteration phases are formed at 150°C and 175°C, the same reaction mechanisms are likely to occur.

Vapor hydration tests at 200°C were conducted for 3, 7, and 14 days. All samples were completely corroded. A lower limit of the corrosion rate was calculated to be approximately 170 μm/day, since about 500 μm of glass were totally dissolved within 3 days. Due to the same secondary phase formations at this temperature compared to the lower temperatures, it was suggested that the corrosion mechanism did not change over this temperature range.

These limited data can be used to estimate the corrosion rate at lower temperatures. These initial estimates are based on limited data to demonstrate how the data will be used as more data becomes available at the lower temperatures. Based on a plot of the measured corrosion rate as a function of temperature, the data are well fit by a straight line with the formula log rate = 6.74 - 2.13(1000/T). Extrapolation of the line to 120°C predicted a corrosion rate of about 20 μm/day (about 50 g/m^2/day); extrapolation to 90°C predicted a corrosion rate of about 8 μm/day (about 20 g/m^2/day); and extrapolation to 20°C predicted a corrosion rate of about 0.3 μm/day (about 0.8 g/m^2/day).

The long-term corrosion rate extrapolated at 20°C (0.8 μm/day, based on the vapor hydration test) was about 800 times that measured for the initial 30 days in the PCT at 20°C (about 0.001 g/m^2/day, based on sodium release). This suggests that the eventual formation of secondary phases at 20°C will increase the corrosion rate of PNL-A by a factor of about 800.

Vapor Hydration of PNL-B Through PNL-K

Vapor phase tests with the remaining ten glasses (PNL-B through PNL-K) were performed at 150°C for reaction times of 7, 14, and 28 days. The tests should demonstrate the use of a limited number of vapor hydration tests at a single temperature to differentiate the long-term durabilities of glasses of different compositions.

Table 3.5. Alteration Layer Thickness Measured (in μm) on Samples from Vapor Hydration Test Run at 150°C for 7, 14, and 28 Days

	Alteration Layer Thickness (μm)			Glass Composition (wt%)			Zeolite Phase A, B, and C			Phase D		
Glass	7 day	14 day	28 day	B_2O_3	CaO	Al_2O_3	7 day	14 day	28 day	7 day	14 day	28 day
B	0	300	0	9	0	6	-	-	-	-	-	-
C	0	0	0	9	0	9	-	-	-	-	-	-
D	0	0	300	6	0	12	-	-	-	-	-	-
E	0	0	0	9	0	12	-	-	-	-	-	-
F	0	0	0	12	0	12	-	-	-	-	-	-
G	30	100	300	0	9	6	+	+	+	+	+	+
H	40	50	>	0	9	12	+	+	+	+	+	+
I	50	>	>	5	4	6	+	+	+	+	+	+
J	300	>	>	5	4	9	+	+	+	-	+	+
K	0	400	>	5	4	12	-	+	+	-	+	+
A	0	200	>	5	4	12	-	+	+	-	+	+

0 = indicates that no measurable alteration layer was observed in SEM
> = indicates that the monolith was completely altered
- = indicates this phase was not observed
+ = indicates this phase was observed.

Table 3.5 summarizes the observed alteration of the ten glasses in terms of the sodium-depleted layer thickness, the presence or absence of zeolite secondary phases (Phases A, B, or C), and the calcium-bearing Phase D. The results showed an obvious trend wherein glasses containing calcium corrode in the tests and glasses without calcium were not corroded. It was not surprising that the same secondary phases formed in the calcium-bearing glasses and in PNL-A, due to the similarities in composition (see Table 3.4). This suggests that the reaction mechanisms in the corrosion of glasses tested at ANL thus far are similar.

Within the group of calcium-bearing glasses (PNL-A, -G, -H, -I, -J, and -K), those with the higher aluminum contents (-H, -K, and -A) were somewhat more durable than those with lower aluminum contents (-G, -I, and -J) based on the alteration layer thickness. The extent of reaction also correlated to the boron content of the glass. It was noted that the compositions of PNL-A and PNL-K differed only in the "Others" added to the glass. These two glasses showed very similar corrosion behaviors, suggesting that the "Others" component did not affect corrosion.

The vapor hydration tests results showed the following durability order for the different glass systems at similar silicon, alumina, and sodium contents:

Boron-only > Mixture = Calcium-only.

The limited data cannot distinguish the durability order between the calcium-only system and the mixture system (boron and calcium). In general, this order is similar to the order observed from PCTs and may also provide evidence that the results from short-term vapor hydration tests are similar to those from PCTs. The vapor hydration test in saturated vapor provided very high S/V conditions (only a few layers of water molecules were adsorbed on the glass surface). The beneficial effects of boron oxide on glass structure and on leachate pH were retained in the same way as in the static PCTs, but the higher S/V and higher temperature in vapor test conditions promoted faster reaction progress.

3.1.3 Viscosity and Electrical Conductivity Results

Table 3.6 and Appendix E lists the viscosity data for all of the LLW glasses measured so far. Table 3.6 contains interpolated data from actual viscosity measurements by using Arrhenius temperature dependence. For each glass, the temperatures (°C) at 10 and 5 Pa.S, and the viscosities at temperatures from 1000 to 1450 (°C) are listed.

Electrical conductivity measurements were conducted by the following procedures, GDL-ECC ("Electrical Conductivity Calibration Procedure, Rev. 0") and GDL-ELC ("Electrical Conductivity Measurement Procedure, Rev. 0"). Measurements were automated, using a General Purpose Interface Board and an IBM PC to collect data. Procedures GDL-AECC, Rev. 0 and GDL-AEC, Rev. 0 ("Automated Electrical Conductivity Calibration" and "Measurement Procedures for Molten Glass") were used for these measurements. A probe with two platinum-10% rhodium blades was inserted into the glass to a known depth and the resistance of the glass between the blades was determined by a resistance meter.

Table 3.6. Viscosities of LLW Glasses

		Temp(°C)		Viscosity(Pa*S) at Various Temperature(°C)											
Vendor	Glass ID	10Pa*S	5Pa*S	A	B	1000	1050	1100	1150	1200	1250	1300	1350	1400	1450
PNL	L4-1215	1311	1411	-9.36	18472	172.8	99.8	60.1	37.4	24.1	16.0	10.9	7.6	5.4	3.9
PNL	L4-129	1243	1337	-9.66	18145	98.5	57.5	34.9	21.9	14.2	9.5	6.5	4.6	3.3	2.4
PNL	L4-615	1471	1582	-9.29	20219	729.4	400.3	229.5	136.8	84.5	53.8	35.3	23.8	16.4	11.5
PNL	L4-912	1357	1459	-9.44	19139	269.2	152.5	90.1	55.2	35.0	22.8	15.3	10.5	7.4	5.3
PNL	L4-96	1296	1390	-9.90	19152	170.6	96.6	57.1	35.0	22.1	14.4	9.7	6.7	4.7	3.4
PNL	L5-1215	1347	1430	-11.88	22972	475.7	240.6	127.8	71.0	41.1	24.6	15.2	9.7	6.4	4.3
PNL	L5-129	1317	1401	-11.51	21960	311.4	162.3	88.7	50.6	29.9	18.4	11.6	7.6	5.0	3.4
PNL	L5-615	1481	1578	-10.99	23321	1522.2	761.8	401.0	220.8	126.6	75.3	46.3	29.3	19.1	12.7
PNL	L5-96	1353	1445	-10.60	20986	357.6	191.8	107.7	62.9	38.2	23.9	15.4	10.2	6.9	4.8
PNL	L6-3312	1438	1543	-9.79	20706	644.9	348.8	197.3	116.1	70.9	44.7	29.0	19.3	13.2	9.2
PNL	L6-5412	1359	1458	-9.82	19789	305.0	169.5	98.3	59.3	37.0	23.8	15.7	10.7	7.4	5.3
PNL	L6-5415	1385	1484	-9.97	20336	406.5	222.3	127.0	75.5	46.5	29.5	19.3	13.0	8.9	6.3
PNL	L6-546	1308	1403	-9.90	19294	191.5	108.0	63.5	38.8	24.5	15.9	10.6	7.3	5.1	3.7
PNL	L6-549	1329	1425	-9.86	19480	230.9	129.5	75.8	46.0	28.9	18.7	12.5	8.5	6.0	4.2
PNL	L6-6612	1284	1377	-10.08	19281	158.6	89.5	52.6	32.1	20.3	13.2	8.8	6.1	4.2	3.0
PNL	L6-669	1261	1351	-10.15	19103	128.2	72.7	43.0	26.4	16.7	10.9	7.3	5.0	3.5	2.5
PNL	L7-15	1504	1608	-10.23	22271	1428.3	737.5	399.5	226.0	132.9	80.9	50.8	32.9	21.8	14.8
PNL	L7-25	1232	1324	-9.73	18110	89.5	52.3	31.8	20.0	13.0	8.7	5.9	4.2	3.0	2.2
PNL	L7-30	1139	1222	-10.07	17467	38.5	22.9	14.2	9.1	6.0	4.0	2.8	2.0	1.4	1.1
PNL	L7-35	1051	1125	-10.83	17391	17.0	10.1	6.3	4.0	2.7	1.8	1.3	0.9	0.6	0.5
PNL	L8-1	1397	1487	-11.19	22536	671.2	343.8	184.9	103.9	60.7	36.7	23.0	14.8	9.8	6.6
PNL	L8-2	1416	1500	-12.43	24893	1237.9	591.3	298.1	157.6	87.1	50.0	29.7	18.3	11.6	7.5
PNL	L8-3	1404	1491	-11.70	23481	847.4	422.1	221.2	121.3	69.3	41.1	25.2	15.9	10.3	6.9
PNL	L8-4	1276	1351	-12.65	23162	255.5	128.5	67.9	37.6	21.6	12.9	8.0	5.1	3.3	2.2
PNL	L8-5	1362	1452	-10.92	21620	429.4	226.0	124.7	71.7	42.8	26.4	16.8	11.0	7.4	5.1
PNL	L8-6	1348	1447	-9.64	19347	260.2	146.5	86.0	52.4	33.1	21.5	14.3	9.8	6.9	4.9
PNL	L8-7	1357	1451	-10.40	20714	352.9	190.8	107.9	63.5	38.8	24.4	15.9	10.6	7.2	5.0
PNL	L8-8	1385	1486	-9.79	20044	386.8	213.4	122.9	73:6	45.6	29.2	19.2	13.0	9.0	6.3

Table 3.6. Viscosities of LLW Glasses, continued

		Temp(°C)		Viscosity(Pa*S) at Various Temperature(°C)											
Vendor	Glass ID	10Pa*S	5Pa*S	A	B	1000	1050	1100	1150	1200	1250	1300	1350	1400	1450
PNL	LD4-912	1325	1424	-9.57	18983	207.7	118.2	70.1	43.1	27.4	18.0	12.1	8.3	5.9	4.2
PNL	LD5-912	1371	1457	-11.69	23002	588.7	297.4	157.9	87.7	50.7	30.3	18.8	12.0	7.8	5.3
PNL	LD6-5314	1379	1474	-10.41	21006	440.7	236.2	132.5	77.4	46.9	29.4	19.0	12.6	8.5	5.9
PNL	LD6-5412	1323	1416	-10.37	20232	249.7	136.9	78.5	46.8	28.9	18.4	12.1	8.1	5.6	3.9
PNL	LD6-5510	1296	1384	-10.78	20525	208.9	113.6	64.6	38.2	23.4	14.8	9.7	6.5	4.4	3.1
PNL	LD6-5510c	1294	1399	-8.78	17371	129.6	77.4	48.0	30.8	20.3	13.8	9.6	6.8	5.0	3.7
PNL	LDM-0912	1348	1439	-10.72	21110	350.9	187.5	104.9	61.1	36.9	23.1	14.9	9.8	6.7	4.6
PNL	LDM-1	1365	1450	-11.80	23101	571.4	287.9	152.4	84.4	48.7	29.1	18.0	11.4	7.5	5.0
PNL	LDM-2	1345	1433	-11.12	21727	381.2	200.0	110.0	63.1	37.6	23.2	14.7	9.6	6.4	4.4
PNL	LDM-3	1376	1464	-11.40	22600	571.3	292.1	156.8	88.0	51.3	31.0	19.4	12.4	8.2	5.5
PNL	LDM-4	1161	1232	-12.43	21133	64.4	34.4	19.2	11.2	6.8	4.2	2.7	1.8	1.2	0.8
PNL	LDM-5412	1310	1410	-9.42	18563	174.1	100.3	60.2	37.4	24.0	15.9	10.8	7.5	5.3	3.9
PNL	LRM-0912	1381	1473	-10.88	21810	517.8	271.0	148.7	85.1	50.6	31.1	19.7	12.9	8.6	5.9
PNL	LRM-1	1334	1419	-11.48	22158	372.7	193.1	104.9	59.5	35.1	21.4	13.5	8.7	5.8	4.0
PNL	LRM-2	1380	1471	-10.86	21751	505.7	265.1	145.7	83.5	49.7	30.6	19.5	12.7	8.5	5.8
PNL	LRM-3	1411	1498	-11.83	23804	956.8	472.0	245.2	133.3	75.6	44.5	27.1	17.0	11.0	7.2
PNL	LRM-4	1165	1232	-13.32	22472	75.9	39.0	21.0	11.8	6.9	4.2	2.6	1.7	1.1	0.8
PNL	LRM-5412	1356	1464	-8.82	18113	223.6	130.6	79.3	49.9	32.4	21.6	14.8	10.4	7.5	5.4
PNL	SSHTM-1	1333	1410	-12.91	24429	535.0	259.1	132.3	70.8	39.5	22.9	13.8	8.5	5.4	3.6
GDI	Duratek	1096	1163	-12.58	20381	30.8	16.8	9.6	5.7	3.5	2.2	1.5	1.0	0.7	0.5
PEI	PEI	1327	1414	-11.15	21515	315.2	166.4	92.1	53.1	31.8	19.7	12.6	8.2	5.5	3.8
VTI	VECTRA I	1224	1318	-9.49	17657	79.7	47.2	29.0	18.5	12.1	8.2	5.7	4.0	2.9	2.1
WSTC	WSTC	1216	1306	-9.94	18233	80.0	46.5	28.2	17.7	11.4	7.6	5.2	3.6	2.6	1.9

A single rotation through a programmed loop of current frequencies at 0.1, 1, 10, and 100 kilohertz that passed the currents quickly through the glass was used to measure resistance. The series of measurements was taken once every 60 seconds after temperature stability had been reached in the furnace. Measurements continued for an established time at each temperature, and the furnace would cool to the next designated temperature. Temperatures ranged for 900°C to 1550°C. Because electrical conductivity is generally less sensitive to glass alteration by volatilization or crystallization than viscosity, no replicate points were taken.

To normalize temperature and to compare the glasses, a simple Arrhenius relation was used,

$$\ln (EC) = A + B/T$$

where A and B are coefficients. A and B values fitted by using experimental data are given in Table 3.7. Also given is the R^2, which in is a measure of fitness. $R^2 = 1.0$ is a perfect fit. Based on literature and HLW glass electrical conductivity measurement, 10 kilohertz data closely represents the true conductivity.

Table 3.7. Electrical Conductivities of LLW Glasses

Glass ID	Electrical Conductivity (S/m)							Fitted Paramters		
	900°C	1000°C	1100°C	1200°C	1300°C	1400°C	1500°C	B	A	R^2
L6-3312	13.8	19.8	27.1	35.4	44.8	55.0	66.1	-5432	7.25	1.00
L6-5412	12.8	19.8	28.7	39.6	52.5	67.2	83.6	-6499	8.09	1.00
L6-5415	14.0	20.6	28.8	38.3	49.2	61.4	74.6	-5802	7.58	1.00
L6-546	13.4	19.6	27.2	36.1	46.2	57.5	69.7	-5726	7.47	1.00
L6-549	14.5	21.0	28.7	37.7	47.7	58.8	70.8	-5486	7.35	1.00
L6-6612	12.3	18.3	25.7	34.5	44.6	55.9	68.3	-5948	7.58	1.00
L6-669	16.3	23.8	32.9	43.4	55.4	68.6	82.9	-5635	7.60	0.99
L7-15	22.9	36.8	55.3	78.5	106.5	139.5	177.1	-7091	9.18	1.00
L7-25	24.3	38.3	56.7	79.5	106.7	138.4	174.2	-6834	9.01	1.00
L7-30	45.5	58.4	72.4	87.2	102.5	118.1	134.0	-3748	7.01	1.00
L7-35	78.6	109.0	144.0	183.2	226.1	272.0	320.6	-4873	8.52	1.00
L8-1	13.3	18.6	24.7	31.7	39.3	47.6	56.3	-5003	6.85	1.00
L8-2	11.6	18.1	26.4	36.7	48.9	63.0	78.8	-6655	8.12	1.00
L8-3	11.9	21.0	34.0	51.6	74.3	102.4	136.0	-8439	9.67	0.99
L8-4	15.1	24.4	36.8	52.6	71.8	94.4	120.3	-7207	8.85	1.00
L8-5	16.4	23.0	30.7	39.3	48.8	59.1	70.0	-5029	7.09	1.00
L8-6	16.7	25.4	36.3	49.4	64.6	81.9	101.1	-6242	8.14	1.00
L8-7	15.9	21.4	27.7	34.6	42.0	49.8	57.9	-4490	6.59	1.00
L8-8	14.2	24.1	37.8	55.7	78.3	105.7	137.8	-7880	9.37	1.00
LDM-1	13.6	20.7	29.6	40.3	52.7	66.9	82.5	-6239	7.93	1.00
LDM-4	14.0	24.3	38.9	58.5	83.4	114.1	150.6	-8236	9.66	1.00
LRM-1	16.6	27.8	43.1	63.2	88.1	118.1	153.1	-7711	9.38	1.00

3.1.4 Statistical Models for PCT Na Release

First-, second- and third-order mixture models were fitted to the natural logs of PCT-normalized Na release values (g/m^2) averaged over duplicate 7-day PCT results for the glasses of L1-9 through L8-8 (42 glasses). The following sections discuss the results of the fitted models.

Correlation Coefficients Among the Mixture Components

The pair-wise correlation coefficients among the nine mixture components were checked before model development because highly correlated mixture components can cause problems in model fitting. If two mixture components are highly correlated, then the fitted mixture model will not be able to separate the effects from the two components; therefore, the results may be misleading. The pair-wise correlation coefficients were computed and are given in Table 3.8.

The possible range of correlation coefficients is -1 to 1. The values -1 and 1 indicated perfect negative and perfect positive linear correlation, respectively, while the value zero indicates that two components are completely uncorrelated. According to Table 3.8, the correlation coefficient between Na_2O and Other is 0.999, which means the two components were almost perfectly correlated. Such highly correlated components should not be treated as two independent terms in a model. Therefore, the two components were combined to form a new component, "NaPlus," which is the sum of Na_2O and Other. Other correlation coefficients large enough to be potentially bothersome are highlighted in bold type in Table 3.8.

First-Order Mixture Model

The first-order mixture model using mass fractions was fitted to the natural logs of Na-PCT released values for glasses L1-9 through L8-8. The model coefficients and three R^2 statistics are given in Table 3.9. The three R2 statistics, R^2, R_{2adj}, R^2_{press}, are described in Section 6 of Hrma, Piepel, et al. (1994).

The three R^2 statistics were used to evaluate fitted mixture models. Generally, R^2 statistics take values between 0 and 1 and large R^2 values (i.e., close to 1) are desired. Among the three R^2 statistics, typically $R^2 > R^2_{adj} > R^2_{press}$. More than a minor difference between R^2 and R^2_{adj} or R^2_{press} was considered to be an indication of problems. The three R^2 values of the first-order model indicated that the model fit the data reasonably well, but there was considerable room for improvement.

Table 3.8. Pair-Wise Correlations Among the Mixture Components

SiO_2	B_2O_3	Na_2O	CaO	Al_2O_3	MgO	Fe_2O_3	ZrO_2	Other
SiO_2	1.000							
B_2O_3	-0.305	1.000						
Na_2O	**-0.505**	-0.004	1.000					
CaO	-0.279	**-0.580**	-0.022	1.000				
Al_2O_3	**-0.585**	0.106	0.007	0.134	1.000			
MgO	0.043	0.045	-0.030	-0.142	-0.078	1.000		
Fe_2O_3	-0.073	-0.040	-0.061	-0.075	-0.159	-0.047	1.000	
ZrO_2	-0.073	-0.040	-0.061	-0.075	-0.159	-0.047	-0.009	1.000
Other	**-0.505**	-0.004	**0.999**	-0.022	0.006	-0.030	-0.060	1.000

Table 3.9. Coefficients for First-Order Mixture Model

Component	Coefficient
SiO_2	-2.2176
B_2O_3	-15.0909
NaPlus	18.3060
CaO	-7.2121
Al_2O_3	-19.0564
MgO	-0.5179
Fe_2O_3	-10.0727
ZrO_2	-16.2908
$R^2 = 0.8088$, $R^2_{adj} = 0.7694$, $R^2_{press} = 0.7140$	

All eight mixture components except MgO had significant effects on the PCT-normalized Na release. Among them, NaPlus had the largest positive effect, while Al_2O_3, ZrO_2, and B_2O_3 showed the largest negative effects. The estimated coefficient for MgO may not be very informative because the estimate was based on a single glass (L8-8) containing MgO. The plot of predicted versus measured PCT Na release for the first-order model is displayed in Figure 3.16. The plot indicates that the first-order model has reasonably accuracy but noticeable imprecision.

Second-Order Mixture Model

To obtain the "best"-fitting second-order mixture model, a statistical procedure was used to select the second-order terms. Based on the R^2, R^2_{adj}, and C_p values, the procedure provided the candidates for the "best" model selected from all possible model forms with a certain number of terms. The C_p statistic measures the bias of a model. If a model had negligible bias, the C_p value should have been close to the number of terms in the model. All second-order terms involving components MgO, Fe_2O_3, or ZrO_2 were

excluded from the selection, because each of these three components appeared in only a few (one or four) L8 glasses. Such limited information cannot support the second-order terms involving these components.

The second-order mixture model with the best three R^2 and C_p values is given in Table 3.10. The model fit PCT Na-release data fairly well. The second-order model provided a better fit than the first-order model, based on comparing the R^2 statistics of the two models. The plot of predicted versus measured PCT Na release, shown in Figure 3.17, also indicates that the second-order model had a better prediction capability than did the first-order model.

Third-Order Mixture Model

Third-order mixture models were also investigated to explore the possibility of further improvement for model fitting. The same statistical procedure was used to select the second- and third-order terms. Again, all second- and third-order terms involving MgO, Fe_2O_3, and ZrO_2 were excluded from the selection for the same reason.

The third-order mixture model with the best R^2 and C_p values is given in Table 3.10a. The R^2 statistics of the third-order model were slightly increased compared to the second-order model. The plot of predicted versus measured PCT Na release in Figure 3.18 also shows that better predicted values were obtained by the third-order model for a few points (e.g., point #9, glass L4-96 and point #19, glass L5-96). However, the improvement gained by upgrading the model from the second-order to the third-order is quite limited.

Table 3.10. Coefficients for Second-Order Mixture Model

Term	Coefficient	Term	Coefficient
SiO_2	-67.9445	MgO	40.7025
B_2O_3	-7.2450	Fe_2O_3	23.9476
NaPlus	41.6355	ZrO2	17.7295
CaO	22.1563	SiO_2 x SiO_2	81.2173
Al_2O_3	8.5533	B_2O_3 x B_2O_3	222.9915
$R^2 = 0.9563$, $R^2_{adj} = 0.9440$, $R^2_{press} = 0.9241$			

Table 3.10a. Coefficients for Third-Order Mixture Model

Term	Coefficient	Term	Coefficient
SiO_2	-32.7543	Fe2O3	16.6262
B_2O_3	-4.2742	ZrO2	10.4081
NaPlus	33.2717	B2O3 x B2O3	217.5201
CaO	14.8293	SiO_2 x SiO_2 x SiO_2	50.6837
Al_2O_3	4.0427	SiO_2 x B_2O_3 x Al_2O_3	-156.7852
MgO	33.4808		
$R^2 = 0.9627$, $R^2_{adj} = 0.9507$, $R^2_{press} = 0.9290$			

3.2 Minor Component Study of LLW Glasses

In addition to its high sodium content, some of the Hanford Site LLW has high enough concentrations of minor components, including Cl, F, P_2O_5, SO_3, and Cr_2O_3 to be concerned about their impacts on the glass properties. These troublesome minor components could cause problems during waste-glass vitrification. Minor component study of LLW glass is an important part of the LLW glass formulation program at PNNL. The study addresses crucial issues relevant to the glass formulation and the melter evaluation, including solubilities of these minor components in LLW glass, glass composition effect on the solubilities, effects of the minor components in glass on waste processibility, and their impacts on chemical durability of final glass waste forms. Results of the minor component study of LLW glasses are summarized in a letter report. Crucial parts in that report are summarized here, and new results obtained since that report was written are also included to provide information necessary for vendor glass formulation.

3.2.1 Solubility of Minor Components

Solubility limits of minor components in glass were defined by their concentration levels at which both quenched and annealed glasses were homogeneous, amorphous to X-ray, and free from crystals or a second amorphous phase under an optical microscope. However, the true solubility limits may be higher at temperatures at which glasses are processed. A good example can be found in fluorine-spiked glass. The high fluorine-containing melts were transparent, but became either translucent or opalescent once the molten glasses cooled. This suggests that fluorine is soluble in the melt at the glass-processing temperature, but becomes over-saturated at lower temperatures. A similar observation was seen in the case of phosphate-spiked glass. Accordingly, solubility data should be considered as lower bounds of these limits in general, which provide a safety margin for both glass formulation and the actual waste vitrification process.

Table 3.11 lists the nominal compositions of L6-5412 and L4-9012 glasses, which were most extensively used in the minor component study. Solubility limits of halide (Cl, F), phosphate (P_2O_5), sulfate (SO_3), and chromium oxide (Cr_2O_3) were determined in L6-5412 base glass at 1300, 1350, and 1400°C, as well as in L4-9012 glass at 1350°C only. Table 3.12 summarizes the solubility limits of minor components in these glasses.

As shown in L6-5412 glass, within experimental error the solubility limits were insensitive to the change of the glass-processing temperature from 1300 to 1400°C. Effects of melt duration and the batch-size variation on the solubility limits were examined using L6-5412 glass at 1300°C. Results confirmed the validity of solubility data obtained from small-size batch melts for a shorter time.

The effect of glass composition on the solubilities of some of the minor components was apparent, except for Cl. Compared to L6-5412 glass, F solubility increased by about 30%, but by more than 120% for P_2O_5 solubility in L4-9012 glass. Solubility of Cr_2O_3 also increased in L4-9012 glass by about 100%, while solubility of SO_3 decreased by about 40%.

Table 3.11. Nominal Compositions (wt%) of LLW Glasses Used in Minor Component Study

Oxide	L6-5412	L4-9012	Oxide	Others
SiO2	56.78	56.78	Bi2O3	0.014
B2O3	5.00	9.00	Cl	0.092
Na2O	20.00	20.00	Cr2O3	0.036
CaO	4.00	0.00	F	0.213
Al2O3	12.00	12.00	Fe2O3	0.005
Others	2.22	2.22	K2O	0.327
			MnO	0.007
			Nd2O3	0.012
			P2O5	1.187
			SO3	0.320
			ZrO2	0.005
Total	100.00	100.00	Subtotal	2.217

Table 3.12. Measured Solubility Limits (wt%) of Minor Components in LLW Glasses as a Function of Glass Processing Temperature

Glass	L6-5412			L4-9012
Minor Component	1300 C	1350 C	1400 C	1350 C
Cl (#)	0.56 (0.03)	0.57 (0.03)	0.52 (0.03)	0.49 (0.04)
F (#)	0.77 (0.02)	0.92 (0.02)	0.91 (0.02)	1.18 - 1.45
P2O5 (#)	1.94 (0.16)	2.10 (0.16)	2.28 (0.17)	5.8 (*)
SO3 (#)	0.75 (0.06)	0.75 (0.07)	0.75 (0.07)	0.47 (0.04)
Cr2O3 (&)	0.46	0.48 (0.02)	0.48 (0.02)	1.04 (0.07)

(#) Values in aparenthese are one standard deviation, except for Cr2O3 case.
(&) For Cr2O3, values in apparenthese are differences between
Na- and K- fussion methods used in ICP.

A limited amount of chlorine can be incorporated into silicate glass melt by substitution for BO (Sun and Silverman 1945), which lies in its larger ionic radius, 1.81 Å, compared to oxygen, 1.38 Å. According to Cl solubilities in L6-5412 and L4-9012 glasses, the change of B_2O_3 seemed to slightly decrease or have no influence on Cl solubility.

Fluorine, on the other hand, was expected to be more soluble in glass because its smaller ionic radius, 1.31-1.33 Å, makes the substitution easier. However, at high F concentration, NaF and CaF_2 precipitated from the glass. Reviewing F solubilities in L6-5412 and L4-9012 glasses, it can be seen that by removing CaO, the increase in F solubility was substantial. However, F solubility could have been strongly affected by Na in LLW glasses.

A significant increase in P_2O_5 solubility in L4-9012 was directly related to the removal of CaO, which prevented glass from forming $Na_2Ca_4(PO_4)_2SiO_4$ crystals. At a fixed level of CaO (4 wt%), concentration of Na_2O also influences the solubility of P_2O_5 significantly. Experimental results reported by a subcontractor of Rensselaer Polytechnic Institute (Crichton and Tomozawa 1995) demonstrated that by increasing Na_2O from 20 wt% to 25 wt%, the phosphate solubility was increased from 2.1 wt% to 6.3 wt%. On the other hand, phosphate solubility was reported to decrease with an increase in Al_2O_3 content at a given CaO content level (4 wt%). With a complete removal of Al_2O_3 from L6-5412 glass, the phosphate solubility increased up to 8.5 wt%, as compared to 2.1 wt% P_2O_5 for L6-5412 glass with 12 wt% Al_2O_3 (Crichton and Tomozawa 1995). Although either increasing Na_2O or decreasing Al_2O_3 are beneficial to the phosphate solubility, an impact of the composition change on glass durability must be considered for optimization of glass formulation.

Compared to L6-5412 glass, SO_3 was much less soluble in L4-9012 glass, which may be attributed to an overall reduction of NBO concentration in glass due to both a removal of CaO and an increase in B_2O_3, according to Holmquist (1966) and Papadopoulos (1977). It is not fully understood if an increase in solubility of Cr_2O_3 in L4-9012 glass is related to the change of CaO or to B_2O_3. The recent EXAFS (extended X-ray absorption fine structure) data show that in LLW glasses, Cr_2O_3 has a form of 6-fold Cr^{3+} in the glass network. Combining the EXAFS results with a previously published model (Singh and Nath 1981), it seems that increasing BO concentration in glass favors Cr_2O_3 dissolution in glass. Comparing glass compositions between L6-5412 and L4-9012, the latter has higher B_2O_3 and no CaO, and hence is expected to have a higher concentration of BO, which in turn results in higher solubility of Cr_2O_3. Further investigation into the relationship between the BO and Cr_2O_3 solubility is necessary to support the current understanding.

3.2.2 Volatilization of Minor Components

Figure 3.19 presents total weight losses for L6-5412 base glass and glasses with minor components versus minor component-loading at various temperatures. Clearly, volatility of the base glass and glasses with either P_2O_5 or Cr_2O_3 was negligible. However, the weight loss in glasses with additions of Cl, F, and SO_3 were significant once their concentrations in batch were in excess of their solubility limits. The volatility is in the order $Cl > SO_3 \approx F$. For a batch with 5.0 wt% Cl, the total weight loss was found to be more than the chlorine loading in the batch, suggesting that Cl also promotes volatilization of other constituents identified as B_2O_3 and Na_2O.

Figure 3.20 presents a comparison of weight losses between L6-5412 and L4-9012 glasses with minor components. It is evident that L4-9012 glasses with minor components exhibited higher volatility than L6-5412 glasses, indicating that B_2O_3 in glass also promoted minor component volatility, probably during the initial batch melting stage since melting temperature of boric acid is as low as 236°C.

Weight-loss data presented in this study are for the melts under a static melting atmosphere. However, the weight loss of L6-5412 glass melted at 1300°C is reported to increase with a flow-rate of atmosphere above the melt (Crichton et al. 1995). In this case, the loss was presumably associated with B_2O_3 and Na_2O, and the rate of weight loss appeared to be mainly governed by the transportation of the alleged species away from the melt surface (Crichton et al. 1995). Accordingly, it is important to evaluate further the impact of air flow-rate on the volatility of glasses with additions of Cl, F, and SO_3.

3.2.3 Effect of Minor Components on Crystalline Phase Formation

Various crystalline phases were found in glasses with minor components in excess of their solubility limits, some of which formed in the bulk of glass and others which segregated from the melt, either on the top of the melt, or at the interface between the melt and the crucible wall.

In glasses spiked with Cl over its solubility, a spherical crystalline phase, NaCl, precipitated from the melt and then accumulated toward the top of the melt. The crystallization and consequent segregation toward the top of the melt is considered to occur at glass-processing temperatures, based on the morphology and distribution of NaCl crystals in the melt. However, once F is above its solubility, the glass was opalescent, the extent of which depended on concentrations of NaF and CaF_2 formed in a melt (in L4-9012 glass, only NaF existed). The crystallization of NaF and CaF_2 was found to occur during melt cooling, suggesting that at the glass-processing temperature, F solubility should be higher than the values defined under the current specification. The reasons to use lower solubility value can be found in the previous report.

Glass containing phosphate in excess of its solubility also became opalescent upon melt cooling; this was caused by crystallization of Na_3PO_4 and $Na_2Ca_4(PO_4)_2SiO_4$ (in L4-9012 glass, only Na_3PO_4 existed). At 1300°C, L6-5412 glass with 10 wt% P_2O_5 exhibited an additional phase segregation on the top of the melt. In this case, the segregated layer contained two distinctive phases, one rich in P and Ca, and another rich in Si. At 1350°C or 1400°C, a phase-segregated layer was not observed for melts of the same glass, suggesting these melts were likely outside of a glass immiscibility boundary for this particular glass system (Tomozawa 1979).

In L4-9012 glass with 6.0 wt% P_2O_5, opalescence became visible to the eye. As previously addressed, removal of CaO increased P_2O_5 solubility significantly. One concern regarding CaO-free glass was whether the presence of SrO in LLW glass would affect the phosphate solubility and hence its crystallization. A preliminary study was conducted using L4-9012 glass with addition of both 6.0 wt% P_2O_5 and 1 wt% SrO. The melt was held at 1350°C for 2 h. Both quenched and annealed glass samples were visually examined. No distinguishable appearance existed between L4-9012 glasses with and without SrO, suggesting that a small amount of SrO in glass is unlikely to affect the solubility of P_2O_5 in glass.

A primary crystalline phase was Na_2SO_4 segregating from melts containing over-saturated SO_3. The segregated sulfate accumulated either on the top of the melt or at the interface between the melt and the crucible wall. In addition, phases containing high P and Ca were found both in and near the segregated sulfate phase. Furthermore, in a melt of LD6-5510 glass (with 0.3 wt% SO_3), which was made from simulant and glass additives, sulfate segregation was severe, and chromium content in the segregated sulfate was higher as compared with chromium in the glass matrix (undetectable by EDS). The sulfate segregation in this case is probably associated with an earlier batch melting under a reducing atmosphere due to the presence of a reductant in the simulant (possibly NO_x). Further investigation is necessary to clarify the real cause.

Crystals, Cr_2O_3, in the bulk of glass formed in melts with over-saturated chromium oxide. No crystal settlement was found in L6-5412 glass with 2.0 wt% Cr_2O_3, which was melted at 1350°C for 40 h. However, it is important to realize that the result should not be viewed as a general picture for LLW glasses. Specific attention must be paid if a glass contains certain amounts of either Fe_2O_3 or NiO, or MnO. Under these circumstances, spinel-like crystals are likely to form, and the tendency of the crystal settlement should be investigated.

Reviewing the above results, a general conclusion can be drawn that two types of phase segregation exist in these minor components. For F, P_2O_5, and Cr_2O_3, the phase segregation takes place within the glass melt and no accumulation takes place on the top of the melt surface. (The segregated layer on the top of 10 wt% P_2O_5 melt is related to amorphous phase-separation phenomenon.) For Cl and SO_3, however, the segregated phases tend to accumulate first on the top of the melt, forming molten salt layers and then evaporate as the melting proceeds.

This study also found interactions between sulfate and phosphate, or between sulfate and chromium oxide, during glass batch melting. Results show that segregation of SO_3 tends to extract P_2O_5 and Cr_2O_3 from the melt, bringing them to the top of the melt. The similar phase-segregation phenomenon related to minor component interaction has been reported in high-level waste glasses (Li et al. 1995; Sullivan et al. 1995). In addition, the effect of minor component interaction, particularly between P_2O_5 and SO_3, was studied using L6-5412 (5 wt% B_2O_3 - 4 wt% CaO - 12 wt% Al_2O_3); L4-9012 (9 wt% B_2O_3 - 9 wt% Al_2O_3), L4-909 (9 wt% B_2O_3 - 9 wt% Al_2O_3); and L5-0912 (9 wt% CaO - 12 wt% Al_2O_3) glasses, which was done by using the same amounts of P_2O_5 (2.5 wt%) and SO_3 (1.0 wt%) in all batches. Table 3.13 summarizes XRF-analyzed concentrations of these minor components in glass and the results of visual inspections for the quenched glass samples (these glasses were melted at 1350°C for 2 h). Except for L5-0912 glass, remaining glasses, spiked with both P_2O_5 and SO_3, were phase-separated, showing both molten sulfate segregation in the early stage of batch melting and various degrees of opalescence in the bulk of quenched glasses, possibly due to amorphous phase separation. Among these glasses, the phase separation in the bulk of L4-9012 appeared to be the strongest.

The sample opalescence was considered to be related to amorphous phase separation, related to cluster formation of R-O-P-O and R-O-S-O (Darab et al. 1995). Results in Table 3.13 suggest that the phase separation was promoted by SO_3, based on the following reasons. First, at 2.5 wt% P_2O_5, phosphate phase separation in L4-9012 was not expected because P_2O_5 was well below its solubility limit (5.8 wt%). For L6-5412, the phase separation was also unlikely since P_2O_5 was at its solubility limit (2.5 wt%) and no phase separation was observed in L6-5412 with the single addition of 2.5 wt% P_2O_5. However, these samples did show phase separation and it was the worst in L4-9012 glass. For L5-0912, the phosphate phase segregation was expected, but it was not observed. Therefore, the phase separation observed here cannot be explained in terms of solubility of P_2O_5, but seems to be well correlated with solubility of SO_3. The SO_3 solubility in L6-5412 is higher than that in L4-9012 glass. In L5-0912 glass, retained SO_3 was 1 wt%, the same as the batched concentration, and yet no segregated Na_2SO_4 was found, indicating even higher SO_3 solubility, above 1 wt% SO_3, in this glass. The overall impression was that the solubility of SO_3 in glass was a limiting factor in the amorphous phase separation.

3.2.4 Effect of Minor Components on Glass Melt Viscosity

Glass melting temperature, T_{10}, as specified at 10 Pa.s melt viscosity, was determined in L6-5412 and L4-9012 glasses with minor component additions, which are summarized in Table 3.14. Figure 3.21

illustrates the change in the melting temperature, T_{10}, of glass spiked with minor components at their solubility limits. Overall, F significantly reduced T_{10}. On the other hand, Cl and P_2O_5 increased T_{10}, and the effect of Cl was the largest. SO_3 appeared to increase T_{10} also. However, a mixed effect of Cr_2O_3 on T_{10} was observed. In L6-5412 glass, Cr_2O_3 increased T_{10}, while in L4-9012 glass, T_{10} decreased initially with the addition of Cr_2O_3 and then increased at higher Cr_2O_3 content. Compared to glasses with Cr_2O_3 at its solubility, it appears that precipitation of Cr_2O_3 in the melt increased the melt viscosity or the melting temperature (Table 3.14).

Table 3.13. Measured Concentrations (wt%) of Phosphate and Sulphate in LLW Glasses and Visual Inspection of Phase Separation

Glass	L6-5412	L4-9012	L4-909	L5-0912
P2O5 (#)	2.24 (0.21)	2.20 (0.19)	2.05 (0.18)	2.29 (0.23)
SO3 (#)	0.88 (0.07)	0.57 (0.05)	0.68 (0.06)	1.00 (0.08)
Phase Separation	slightly	significant	intermediate	non

(#) Values in parentheses are one standard deviation.

Table 3.14. Glass-Melting Temperature (°C) at the Melt Viscosity of 10 Pa•S for LLW Glasses with Minor Component Additions

Minor Component (wt%)	L6-5412	Minor Component (wt%)	L4-9012
base glass	1351		1345
Cl		Cl	
0.40 wt%	1363	0.49 wt%	1352
0.56 wt%	1374		
F		F	
0.77 wt%	1216	1.18<X<1.45	1216
P2O5		P2O5	
1.94 wt%	1361	5.8 wt%	1366
SO3		SO3	
0.5 wt%	1357	0.47 wt%	1342
0.75 wt%	1361	0.56 wt%	1348
Cr2O3		Cr2O3	
0.48 wt%	1354	1.04 wt%	1320
0.79 wt%	1361	1.19 wt%	1342

(#) Values in Bold phase are for the minor components at their solubility limits.

In addition, T_{10} values of L6-5412, L4-9012, and L5-0912 glasses spiked with 1 wt% SO_3 and 2.5 wt% P_2O_5 (batch compositions) were also determined. For L6-5412 glass, addition of P_2O_5 and SO_3 increased T_{10} further, compared to an individual increase in T_{10} when P_2O_5 and SO_3 were added separately. However, for L4-9012 glass, the addition of P_2O_5 and SO_3 seemed to have no effect on the base glass-melt viscosity, or T_{10}. No viscosity data are available for L5-0912 glass spiked separately with these two minor components at their solubility limits (the solubility limits have not been determined yet). However, available viscosity data suggested that P_2O_5 and SO_3 in L5-0912 had a smaller effect on the glass-melting temperature when compared with the effect on L6-5412 glass. Overall, the results suggested that the effect of mixed minor components on glass viscosity is nonlinear with respect to their concentrations.

3.2.5 Effect of Minor Components on Glass Chemical Durability

The static 7-day PCT and the single-pass flow-through test were used to evaluate chemical durability of L6-5412 glasses with the minor components at their solubility limits; the PCT was also performed on the samples with minor components above their solubility limits. Figure 3.22 illustrates the release of sodium as determined by both the PCT and the SPFT. Results from both tests showed that P_2O_5, SO_3, and Cr_2O_3 decreased glass durability; Cr_2O_3 had the largest effect (Li et al. 1995). Glass with 0.48 wt% Cr_2O_3 showed an increase in either sodium release (PCT) or sodium leaching rate (SPFT) by about 20%. Apparent durability of glass with F addition is increased, based on the PCT data; i.e., a reduction of sodium release by about 10% at F solubility, but by about 30% above the solubility. The apparent durability increase was considered to be a result of lower solution pH. Without the pH influence, the flow-through test showed that F-spiked glass was the least durable, and that its sodium-leaching rate was 100% higher than that of the base glass. Judging results from both the PCT and SPFT, Cl-spiked glass appeared to be as durable as the base glass.

3.3 Phase I Vendor Glass Study

Phase I is a "proof of principle" test to demonstrate that a melter system can process a simulated highly alkaline, high nitrate/nitrite content aqueous LLW feed and produce a glass product of consistent quality. Seven melter vendors participated in the Phase I evaluation, including the following: joule-heated melters from GTS Duratek, Incorporated (GDI), Envitco, Incorporated (EVI), Penberthy Electromelt, Incorporated (PEI), and Vectra Technologies, Incorporated (VTI); gas-fired cyclone burner from BabCock & Wilcox (BCW); plasma torch-fired, cupola furnace from Westinghouse Science and Technology Center (WSTC); and electric arc furnace with top-entering vertical carbon electrodes from U.S. Bureau of Mines (UBM). A detailed technology review on this phase I study has been reported (Wilson 1995).

3.3.1 Phase I Glass Compositions and Waste

The waste used for the Phase I study is the nominal composition of the double-shell slurry feed (DSSF) as shown in Table 1.1. The nominal glass compositions are shown in Table 3.1. These glasses include five PNNL glasses, LD4-912, LD5-912, LD6-5412, LD6-5510, and LD6-5314. Some of the vendors of Phase I used PNNL composition for their testing. U.S. Bureau of Mines used PNL LD6-5510 in an arc furnace with top-entering vertical carbon electrodes. Babcock & Wilcox used PNL LD6-5510 in its small-boiler simulator-cyclone furnace. The simulator-cyclone furnace uses a slurry composed of the LLW simulant plus glass formers that are injected into a horizontal, gas-fired cyclone burner. Envitco, Incorporated used LD4912 in its ceramic-lined, joule-heated melter that uses molybdenum rod electrodes.

The other four vendors developed their own glass compositions. GTS Duratek, Incorporated used a composition similar to most high-level waste borosilicate glass that melt at 1150°C or below, to be able to melt the glass in their ceramic, refractory-lined, joule-heated melter that uses Inconel® plate electrodes. Penberth Electromelt, Incorporated used boron-free aluminosilicate-glass composition in their ceramic refractory-lined, cold-top, joule-heated melter with side-wall molybdenum electrodes. Vectra Technologies, Incorporated used a composition similar to PNNL LD6-5510 (replacing 3 wt% SiO_2 with 3 wt% B_2O_3 and replacing 2.1 wt% CaO with MgO) in its water-jacketed and joule-heated furnace with vertical top-entering molybdenum electrodes. Westinghouse Science and Technology Center used a high-alumina borosilicate glass in a plasma-torch-fired, cupola furnace.

From the limited comparison between the nominal compositions and the analyzed composition of the crucible melts performed in this laboratory, our crucible melts composition were usually similar to nominal compositions, as shown in Appendix A. However, the analyzed compositions from some of the glasses produced by Phase I vendors were very different from those of the target compositions (see Appendix A). Most of the discrepancies were between sodium and boron compositions; i.e., the analyzed composition of a vendor composition had sodium contents of 12 wt%, which was 40 wt% less than the targeted 20 wt% due to severe volatilization of some particular melting operation. The products with 40% less sodium will be, of course, more durable and this will have a great impact on the PCT results discussed below.

3.3.2 Phase I Glass Durability and Viscosity

The measured PCT releases for some major components of Phase I glasses are listed in Table 3.15; the completed PCT releases are tabulated in Appendix B. These Phase I glasses were all much more durable than the high-level nuclear waste EA glass (designated "EA" glass in Table 3.15). The BCW and UBM glasses should have similar durabilities as the PNNL LD6-5510 glasses, since they have the same nominal composition; the deviation from the measured PNNL LD6-5512 durability is an indication of the deviation in glass composition. The analyzed BCW and UBM glass compositions had much lower sodium and boron contents due to volatilization during melting, as shown in Appendix B. The relative durabilities of the Phase I glasses, shown in Figure 3.23, were measured by 7-day PCT and in Figure 3.24, were measured by single-pass flow-through tests. It is interesting to see that the durability order measured by PCT is different than that measured by SPFT tests. The PEL glass was the least durable glass measured by PCT sodium release (Figure 3.23); it was the most durable glass according to SPFT tests (Figure 3.24). This opposite durability order was also observed through testing other LLW glasses with these two types of tests, performed under the current conditions. However, the detailed investigation indicates that PCT results are more sensitive to glass composition change and can be understood according to glass chemistry, while SPFT at pH 12 is not useful for glass composition optimization but its results are understandable based on solution chemistry.

Table 3.15. Phase I Vendor Glass Compositions

	LD4-912	LD5-912	LD6-5412	LD6-5510	LD6-5314	GDI	PEI	WSTC	VTI	EVI	BCW	UBM
Na2O	20.00	20.00	20.00	20.00	20.00	18.82	18.82	18.82	20.00	20.00	20.00	20.00
K2O	1.46	1.46	1.46	1.46	1.46	3.68	1.44	1.44	1.46	1.46	1.46	1.46
Al2O3	12.00	12.00	12.00	10.00	14.00	6.14	6.00	18.22	10.00	12.00	10.00	10.00
B2O3	9.00		5.00	5.00	5.00	6.15		9.45	8.00	9.00	5.00	5.00
CaO		9.00	4.00	5.00	3.00	7.80	9.77	4.65	2.90		5.00	5.00
Fe2O3						7.50	1.00		1.00			
Li2O								0.83				
TiO2						1.00						
ZrO2						5.09	2.00	2.10				
SiO2	55.91	55.91	55.91	56.91	54.91	42.23	59.22	42.90	52.90	55.91	56.91	56.91
MgO									2.10			
Other	1.63	1.63	1.63	1.63	1.63	1.59	1.75	1.59	1.64	1.63	1.63	1.63
Total	100.00	100.00	100.00	100.00	100.00	100.00	100.00	100.00	100.00	100.00	100.00	100.00
Glass										LD4-912	LD6-5510	LD6-5511
PCT B,g/m2	0.35		0.11	0.13	0.10	0.60		0.15	0.46		0.05*	0.10*
PCT Na,g/m2	0.32	1.23	0.38	0.52	0.26	0.72	1.70	0.25	0.55	0.32*	0.13*	0.32*
PCT Si,g/m2	0.13	0.22	0.10	0.12	0.09	0.21	0.26	0.08	0.18		0.05*	0.08*
PCT pH	10.55	12.03	11.39	11.48	11.05	11.46	12.14	10.82	11.12		10.44*	11.06*
T(C) at 10 PaS	1325	1371	1323	1296	1379	1096	1327	1216	1224	"	"	"
* These PCT results were obtained from glasses made from the melters that are significantly different from target compositions.												

Table 3.16. Phase II Vendor Glass Nominal (Top) and Analyzed (Bottom) Compositions for M-DSSF Waste

OtherD Oxide	waste (wi)
Cr2O3	0.15
Cs2O	0.53
Fe2O3	0.01
K2O	5.31
MgO	0.01
MnO2	0.01
MoO3	0.54
SrO	0.38
P2O5	0.69
SO3	0.79
Cl	2.38
F	3.02
I	0.47
Total	14.29

Glass Name		LDM-1	LDM-2	LDM-5412	LDM-0912	LDM-3	LDM-4
oxide	DSSF(Mod) waste (wi)	glass (gi)	glass (gi)	glass (gi)	glass (gi)	glass (gi)	glass (gi)
SiO2	0.00	50.14	52.14	55.14	55.14	52.14	44.14
B2O3	0.00	2.00	0.00	5.00	0.00	6.00	6.00
Na2O	74.02	20.00	20.00	20.00	20.00	20.00	20.00
CaO	0.01	2.00	6.00	4.00	9.00	0.00	6.00
Al2O3	11.69	12.00	12.00	12.00	12.00	12.00	10.00
ZrO2	0.00	4.00	0.00	0.00	0.00	6.00	4.00
Fe2O3	0.00	6.00	6.00	0.00	0.00	0.00	6.00
Li2O	0.00	0.00	0.00	0.00	0.00	0.00	0.00
OtherD	14.29	3.86	3.86	3.86	3.86	3.86	3.86
Total	100.01	100.00	100.00	100.00	100.00	100.00	100.00

OtherD Oxide	waste (wi)
Cr2O3	
Cs2O	
Fe2O3	
K2O	
MgO	
MnO2	
MoO3	
SrO	
P2O5	
SO3	
Cl	
F	
I	
Total	

Glass Name		LDM-1	LDM-2	LDM-5412	LDM-0912	LDM-3	LDM-4
oxide	DSSF(Mod) waste (wi)	glass (gi)	glass (gi)	glass (gi)	glass (gi)	glass (gi)	glass (gi)
SiO2		50.06	51.87	53.56	55.30	53.50	43.70
B2O3		2.01		5.01		6.31	6.25
Na2O		21.05	20.30	21.22	19.92	18.85	20.36
CaO		1.78	6.24	3.94	9.60	0.12	6.48
Al2O3		12.17	12.08	12.05	12.22	12.44	10.06
ZrO2		4.02	0.01			5.27	3.82
Fe2O3		6.21	6.19	0.06	0.06	0.05	6.14
Li2O							
OtherD		2.70	3.31	4.18	2.89	3.45	3.18
Total		100.00	100.00	100.00	100.00	100.00	100.00

Table 3.17. Phase II Vendor Glass Nominal (Top) and Analyzed (Bottom) Compositions for M-RI Waste

OtherR Oxide	waste (wi)
Cr2O3	0.14
Cs2O	0.60
Fe2O3	0.01
K2O	0.12
MgO	0.00
MnO2	0.04
MoO3	0.61
SrO	0.44
P2O5	9.95
SO3	3.98
Cl	0.14
F	1.04
I	0.54
Total	17.61

Glass Name		LRM-1	LRM-2	LRM-5412	LRM-0912	LRM-3	LRM-4
oxide	Rem.Inv (Mod waste (wi)	glass (gi)	glass (gi)	glass (gi)	glass (gi)	glass (gi)	glass (gi)
SiO2	0.00	48.54	51.54	54.54	54.54	51.54	43.04
B2O3	0.00	2.00	0.00	5.00	0.00	6.00	6.00
Na2O	78.93	20.00	20.00	20.00	20.00	20.00	20.00
CaO	0.01	2.00	6.00	4.00	9.00	0.00	6.00
Al2O3	3.46	12.00	12.00	12.00	12.00	12.00	10.00
ZrO2	0.00	4.00	0.00	0.00	0.00	6.00	4.00
Fe2O3	0.00	6.00	6.00	0.00	0.00	0.00	6.00
Li2O	0.00	1.00	0.00	0.00	0.00	0.00	0.50
OtherR	17.61	4.46	4.46	4.46	4.46	4.46	4.46
Total	100.01	100.00	100.00	100.00	100.00	100.00	100.00

OtherR Oxide	waste (wi)
Cr2O3	
Cs2O	
Fe2O3	
K2O	
MgO	
MnO2	
MoO3	
SrO	
P2O5	
SO3	
Cl	
F	
I	
Total	

Glass Name		LRM-1	LRM-2	LRM-5412	LRM-0912	LRM-3	LRM-4
oxide	Rem.Inv (Mod waste (wi)	glass (gi)	glass (gi)	glass (gi)	glass (gi)	glass (gi)	glass (gi)
SiO2		47.42	48.20	53.41	53.19	54.21	41.74
B2O3		2.02		5.09	0.03	6.25	6.01
Na2O		21.23	22.13	20.27	20.42	17.75	20.22
CaO		1.82	6.13	4.23	9.41	0.19	6.19
Al2O3		12.19	11.41	11.86	11.79	12.37	9.77
ZrO2		3.99				4.97	3.82
Fe2O3		6.24	5.87	0.05	0.05	0.05	5.98
Li2O		1.02					0.49
OtherR		4.05	6.25	5.09	5.11	4.20	5.78
Total		100.00	100.00	100.00	100.00	100.00	100.00

The melting temperatures (at 10 Pa.S) of the Phase I glasses are listed in Table 3.15. The temperatures were between 1096° to 1379°C. The GDI composition had the lowest melting temperature; LD6-5314 had the highest melting temperature. The viscosity data from temperature 1000° to 1450°C are tabulated in Table 3.6. The relative melting temperatures of Phase I compositions are also shown in Figure 3.25.

3.4 Phase II Vendor Glass Study

The Phase II glass formulation supports the overall Phase II vendor testing to allow for more comprehensive testing of equipment and procedures for selected promising technologies. This includes testing the capability of the melter technology to handle wastes with high contents of F, Cl, P, and S. These data will identify melter systems with the greatest flexibility to process feeds with these components and provide data on concentration limits for these components that can be realistically processed by vitrification.

To accommodate the highest contents of F, Cl, P, and S in the Phase II glasses, the Phase II formulations were developed based on the following:

- the available minor component solubility data in LLW glasses as presented in Section 3.2;
- the expansion from the Phase I glass compositions;
- waste loading at the equivalent of 20 wt% Na_2O but at higher minor component concentrations in the simulants;
- the exploration of the trade-off between melt temperature vs durability (e.g., 100 poise temperature vs PCT response) to determine how much difference there might be among viscosity and implied volatility with respect to durability;
- the examination of the effect of different sources of glasses formers (ZrO_2 and Fe_2O_3 as well as SiO_2 and B_2O_3);
- the search for a good-quality glass, i.e., a glass with good long-term durability and reasonable viscosity; and
- the provision of much wider melting temperature ranges, from approximately 1100 to 1450°C, to give the vendors more flexibility.

3.4.1 Phase II Glass Composition and Wastes

The simulated wastes used for the Phase II study are the modified DSSF (M-DSSF) and the modified remaining inventory (M-RI), as shown in Table 1.1. The M-DSSF simulant had 3 wt% F and 2.4 wt% Cl, which represented the highest possible fluorine and chlorine contents in the LLW waste streams. The M-RI had 9.95 wt% of P_2O_5 and 3.98 wt% SO_3, which represented the highest possible phosphorus and sulphur contents in the LLW streams. The 25 wt% waste-loading requirement translated to 0.75 wt% F and 0.6 wt% Cl in the glass formulations with M-DSSF, which are similar to the solubility limits of F and Cl in LLW glasses shown in Table 3.12. A 25 wt% loading of M-RI meant 2.48 wt% P_2O_5 and 0.995 wt% of SO_3 in

glass formulations with M-RI, which exceeded some solubility limits in some glasses, especially for SO_3 as shown in Table 3.12. Table 3.13 shows the interactions of SO_3 and P_2O_5 and the minimum interactions observed in L6-5412 and L5-0912.

Based on these considerations for the solubility of minor components S, P, Cl, and F, 12 glass formulations were tested as Phase II compositions shown in Tables 3.16 and 3.17. These 12 glasses are divided into two groups: six LDM-glasses, made from M-DDSF waste and six LRM-glasses, made from M-RI waste.

LRM-5412 was based on LD6-5412; the only difference between these two glasses is the difference in waste composition. LRM-5412 used the M-RI waste and had high contents of P_2O_5 and SO_3. This glass was expected to be able to accommodate 25 wt% of M-RI without phase segregation and phase separation according to the results presented in Section 3.2.

LRM-1 was modified from LRM-5412 by replacing 3 wt% B_2O_3, 2 wt% CaO, and 6 wt% SiO_2 with 6 wt% Fe_2O_3, 4 wt% ZrO_2, and 1 wt% Li_2O. LRM-1 was supposed to have had better chemical durability, especially in terms of the long-term durability due to the reduction of CaO and addition of ZrO_2 and lower melting temperature.

LRM-0912 was based on L5-0912 which was shown to be able to accommodate high levels of P_2O_5 and SO_3. LRM-2 was improved from LRM-0912 by replacing 3 wt% CaO and 3 wt% SiO_2 with 6 wt% Fe_2O_3. The durability, especially the long-term durability, was supposed to be improved and the melting viscosity should have been similar.

LRM-3 was supposed to be a glass with good chemical durability, especially in terms of long-term durability, by eliminating CaO and keeping the correct amounts of ZrO_2, B_2O_3, and Al_2O_3.

LRM-4 was supposed to be a glass with good short- and long-term chemical durability, but could be melted at a temperature below 1200°C.

The LDR-1, LDM-2, LDM-3, LDM-4, LDM-0912, and LDM-5412 glasses were formulated for the same purposes as were the corresponding LRM-glasses discussed above.

3.4.2 Phase II Glass Melting

LRM-5412 was melted at 1350°C; the glass was green in color and homogeneous. No phase segregation was observed during melting. LRM-1 was melted at 1345°C; the glass was black-brown in color. During the first hour of melting, a yellow layer was observed on top of the glass and some yellow material (probably Na_2SO_4) was found at the top interface between the cooled glass and the Pu crucible and also on part of the center surface, as shown in Figure 3.26, after the second one-hour melting at 1345°C. The measured temperatures at 10 Pa.S for LRM-5412 and LRM-1 were 1356 and 1334°C, respectively, as shown in Table 3.6.

LRM-0912 was melted at 1375°C and a layer of white materials was observed on top of the melt after 30 minutes melting (Figure 3.27a); the white layer disappeared after one hour of melting (Figure 3.27b). Bubbles formed in the melt during cooling, as shown in Figure 3.27b. The glass was reground and melted for

the second hour at 1375°C. The glass was dark green in color, free of white layers, but had some small bubbles. LRM-2 was melted at 1360°C and a yellow layer was observed on top of the melt during the first 30 minutes. Bubble formation was observed after the crucible was removed from the furnace after the first one-hour melting, as shown in Figure 3.28. The second melting at the same temperature still produced bubbles after one hour of melting, as shown in Figure 3.28d. A small amount of yellow materials, similar to those observed in LRM-0912, around the glass at the interface with the Pt crucible was observed. The glass was dark-brown in color. The measured 10 Pa.S temperatures were 1381 and 1380°C, respectively. The observed bubble formation was due in part to the low melting temperatures (1375 and 1360°C were both below the measured 10 Pa.S temperatures of 1381 and 1380°C, respectively). The escaping bubbles were slow in highly viscous melts.

LRM-3 was melted at 1440°C and no phase segregation was observed during either first or second melting as shown in Figure 3.29. However, the glass was cloudy and yellow-green in color. The cloudiness suggested phase separation during cooling; the crystallinity is being investigated. The measured 10 Pa.S temperature was 1411°C.

LRM-4 was melted at 1140°C and a light brown layer was observed on top of the melt after 30 minutes melting during the first melting, as shown in Figure 3.30. The light-brown surface layer gradually dissolved in the melt as the melting duration increased, as shown in Figure 3.30. This disappearance of the light-brown surface layer was not due to volatilization, as indicated by the high retention of SO_3 and P_2O_5 contents in the melted glass analysis results.

All of the six LDR-glass series were melted smoothly without obvious phase segregation and separation. The melting temperature for LDR-5412 was 1290°C and the glass was light-green in color. The measured 10 Pa.S temperature was 1310°C. The melting temperature for LDR-1 was 1310°C and the glass was black-yellow in color. The measured 10 Pa.S temperature was 1365°C. The melting temperature for LDR-0912 was 1381°C and the glass was yellow-green in color. The measured 10 Pa.S temperature was 1348°C. The melting temperature for LDR-2 was 1320°C and the glass was yellow-black in color. The measured 10 Pa.S temperature was 1345°C. The melting temperature for LDR-3 was 1410°C and the glass was green in color. The measured 10 Pa.S temperature was 1376°C. The melting temperature for LDR-4 was 1130°C and the glass was black in color. The measured 10 Pa.S temperature was 1161°C.

The detailed measurements of viscosities for Phase II glasses are shown in Figures 3.31 and 3.32. The comparison of the melting temperature, at 10 Pa.S, among Phase II glasses are shown in Figure 3.33. This figure demonstrates that the LDR-glasses usually had lower melting temperatures due to the F content in the M-DSSF waste than did the corresponding LMR-glasses, due to the P and S contents in the R-RI waste. LD5-0912 had a melting temperature (at 10 Pa.S) of 1371°C, as shown in Table 3.6. The melting temperatures for LDM-0912 and LRM-0912 were 1348° and 1381°C, respectively. The addition of 0.8 wt% F and 0.6 wt% Cl reduced the melting temperature by over 20°C, while the addition of 2.5 wt% P_2O_5 and 1.0 wt% SO_3 increased the melting temperature by 10°C. LD6-5412 had a melting temperature (at 10 Pa.S) of 1323°C, as shown in Table 3.6. The melting temperatures for LDM-5412 and LRM-5412 are 1310° and 1356°C, respectively. The addition of 0.8 wt% F and 0.6 wt% Cl reduced the melting temperature by 13°C while addition of 2.5 wt% P_2O5 and 1.0 wt% SO_3 increased the melting temperature by 33°C.

3.4.3 Solubilities of F, Cl, S, and P in Phase II Glasses

The nominal concentrations of F and Cl in the LDR-glasses were 0.82 and 0.64 respectively, which were expected to be close to the solubility limits reported in Section 3.2 and caused no difficulties in crucible melting as discussed above. The actual contents of F and Cl in LDR-glasses have not been analyzed yet.

Table 3.18. Sulfur and Phosphorus Contents in Phase II Glasses (wt%)

Glass	LRM-5412	LRM-1	LRM-0912	LRM-2	LRM-3	LRM-4
Nominal SO_3	1.01	1.01	1.01	1.01	1.01	1.01
Analyzed SO_3	0.87	0.76	1.01	0.74	0.59	0.93
Nominal P_2O_5	2.52	2.52	2.52	2.52	2.52	2.52
Analyzed P_2O_5	2.67	2.72	2.67	2.60	2.82	2.62
Glass	LDM-5412	LDM-1	LDM-0912	LDM-2	LDM-3	LDM-4
Nominal SO_3	0.21	0.21	0.21	0.21	0.21	0.21
Analyzed SO_3	0.69	0.22	0.26	0.23	0.21	0.26
Nominal P_2O_5	0.19	0.19	0.19	0.19	0.19	0.19
Analyzed P_2O_5	0.62	0.46	0.24	0.28	0.28	0.27

The SO_3 and P_2O_5 contents were similar to the nominal composition in the LDM-glasses. The P_2O_5 contents in LRM-glasses were also the same as the nominal composition, as shown in Table 3.18. Among the LRM-glasses, LRM-0912, and LRM-4 composition were able to accommodate almost 100% of the SO_3 and P_2O_5 added to the batching mixture under crucible-melting conditions without significant phase segregation and phase separation. LRM-3 was least capable of retaining SO_3 under the crucible-melting condition because it had the least NBO bonds available in this formulation. LRM-5412, LRM-1, and LRM-2 had slightly lower SO_3 contents than did the targeted values due to volatilization.

Another special property of our crucible melting is the high oxidizing conditions. The chemicals used in the crucible melting are high valance oxides such as Fe_2O_3; the contact of laboratory air with the small volume of melt in the crucible was good and resulted in a strong oxidizing condition. The analysis of the ratio of Fe(II) to total Fe for the Fe-containing phase II glasses is shown in Table 3.19 for LRM-1, LRM-2, LRM-4, LDM-1, LDM-2, and LDM-4, respectively. The majority of irons are still in the Fe(III) state. In general, more Fe(II) were present in LRM glasses than were in LDM-glasses, which may be an indication

Table 3.19. Redox State of Phase II Glasses Measured by Fe(II)/Fe Ratio

Glass	Wt % Fe(II) in Glass	Wt% Fe (total) in Glass	Ratio of Fe(II)/Fe
LRM-1	0.2669	3.5585	0.075
LRM-2	0.3190	2.9045	0.110
LRM-4	0.0868	3.6249	0.024
LDM-1	0.2144	3.4041	0.063
LDM-2	0.2346	3.4618	0.068
LDM-4	0.0730	2.9329	0.0249
LDMS-1	0.1159	4.2328	0.0274
LDMSM-1	0.0694	3.9936	0.0174
LRMS-1	0.1651	4.1961	0.0394
LRMSM-1	0.0355	4.0224	0.0088
NIST Obsidian	0.9268	1.3156	0.7045
NIST Obsidian	0.9117	1.2523	0.7280
NIST Obsidian -- NIST Values			0.7050

of the reduction of iron by sulfur in the LRM-glasses. Another obvious trend was that the glasses melted at high temperature were more reduced, as seen from the comparison of the ratios of Fe(II)Fe between low-temperature glass, LRM-4, with LRM-1 and LRM-2, or by comparison between LDM-3 with LDM-1 and LDM-2. One should be aware of that when the melting condition becomes a reducing one, it may affect the solubilities of minor components, as well as processing difficulties such as foaming and decreasing durabilities. This is especially true for those Fe-containing formulations where iron will be reduced to Fe(II).

3.4.4 Phase II Glass Durability

The 7-day PCT durability of the Phase II glasses is shown in Figures 3.34 and 3.35 for sodium and silicon releases. The complete PCT results are tabulated in Appendix B. All of the Phase II glasses were much more durable than the EA glasses. The highest 7-day PCT sodium releases were from LDM-0912 and LRM-0912, 1.2 and 1.02 $g/m^2/7$ d. Compared with 6.6 $g/m^2/7$ d, these glasses were still a factor of 6 more durable than EA glass. The most durable glasses were LDM-3, which had a sodium release of 0.29 $g/m^2/7$ d, which was a factor of 23 more durable than EA glass. Within the LDM-glass group the durability order is:

LDM-3 > LDM-1 > LDM-5412 > LDM-4 > LDM-2 > LDM-0912.

The durability order for the LRM-glasses is:

LRM-3 > LRM-5412 > LRM-1 > LRM-4 > LRM-2 > LRM-0912.

The comparison between LRM-glass and LDM-glass is complicated. The durabilities for LDM-3, LDM-4, and LDM-1 are better than those of the corresponding LRM-3, LRM-4, and LRM-1. This may be an indication that the addition of F and Cl into glasses will be more beneficial than the addition of SO_3 and P_2O_5 under PCT conditions, which are consistent with the results presented in Section 3.2. However, the durabilities for LDM-0912 and LDM-2 are worse than those of LRM-0912 and LRM-2, while both LDM-0912 and LRM-0912 are less durable than the base glass L5-0912. We interpret this to mean that the addition of either F and Cl or SO_3 and P_2O_5 into calcium oxide-containing glasses decreases glass durability and that the addition of F plus Cl is worse than the addition of SO_3 and P_2O_5. The durability of LDM-5412 and LRM-5412 was similar and was also similar to the durability of base glass L6-5412. This was probably due to the opposite effects with the addition of these minor components into boron-only glasses (improving durability) and into calcium-only glasses (decreasing durability) in a glass with almost equal amounts of boron and calcium oxides. These durability results on LRM-5412 and LDM-5412 were also consistent with the results discussed in Section 3.2, where opposite effects were observed with the addition of F and Cl and small effects were observed with the addition of SO_3 and P_2O_5.

3.4.5 Phase II Glass Melting from Simulant Solutions

The Hanford Site LLW streams will likely be in the form of sludge after it is separated from high-level waste. There is a need to explore the differences of glass melting from dry chemicals and sludge. The work described below is one of such efforts. Only preliminary information was available when this report was prepared; a detailed discussion on this topic will be included in the year-end report of the LLW glass formulation program.

Four compositions were prepared and melted with simulant waste slurries added as the "Others" component. The resulting glasses were characterized for chemical composition by ICP, durability by PCT, and viscosity. Two glasses, LRMS-1 and LRMSM-1, were based on the LRM-1 composition, and two glasses, LRMS-1 and LRMSM-1, were based on the LDM-1 composition. The simulant solution (slurry) for the "Others" in the LRM-1-based compositions came from the M-RI simulant (Table 1.1), while the slurry of "Others" in LDM-1-based glass compositions was from the M-DSSF simulant (Table 1.1). The difference between LRMS-1 and LRMSM-1 is that LRMSM-1 has additional 3 wt% of metal ion mixture of Cu, Zn, Pb, Sn, Cr, Mn, Ni, Mo, Sb, As, Bi, and Cd, although both were made from simulant solutions. The same difference exists between LDMS-1 and LDMSM-1. The detailed nominal and analyzed compositions of these four glasses are in Appendix A2. The detailed procedure for the preparation of the simulant solutions and the metal mixture solutions are described in details in (Lokken 1995).

Each batch was made from dry chemicals, either oxide or carbonate, except for the "Others" mixture and the metal additions. Simulant solutions were agitated by either shaking the container vigorously or heating the solution on a hot plate and stirring with a impeller to dissolve particles. The solutions were then measured using a graduated cylinder and hand-stirred into the dry chemicals in a 1L stainless-steel beaker. The resulting slurry was smooth with a creamy consistency.

The slurries were dried in a convection oven, heating from 120°C to approximately 200°C during the day. The slurry was checked occasionally for boiling. The samples were left, at a minimum, overnight at 200°C. They dried into a hard cake which was chipped out and put in a 500-cc platinum crucible and placed in a melting furnace at 650°C. The temperature was increased at 50°C intervals until foaming occurred, between 800° and 850°C. The temperature was held steady while foaming to allow NOx to escape. At times, the sample would be removed from the furnace to cool and allow the foam to subside and often the foamed samples needed to be pushed back into the crucible with a stainless-steel rod. When the foam ceased to rise, the crucible was removed from the furnace, the temperature was elevated to 1230° or 1250°C, and the crucible was placed back into the furnace.

Melting was then conducted following the same procedure as described in Section 2.2. General observations of the melts are that all glasses except LDMS-1 had a yellow segregated phase on their surface after the final melt. This yellow substance was soluble in water. When contrasting simulant melts with dry-chemical melts, the melt produced with simulants had more volatilization at melt temperature. Consequently, the viscosity is believed to increase the longer the melt was at temperature, due to the continued volatilization. All of the glasses were black except for the segregated yellow layer.

LDMS-1 was initially melted at 1250°C but lowered to 1230°C shortly after the melt began, due to low viscosity and high volatilization. No segregation of sulfur was observed. The viscosity was 10 Pa.S at 1376°C.

LDMSM-1 had the same starting composition as LDMS-1, but had the 3 wt% added metals. This glass was melted like LDMS-1, starting at 1250°C and then lowered to 1230°C. In both of the first and second melts, a thin layer of yellow segregate was observed on the glass surface. Volatilization and foaming were more prevalent in this melt than in LDMS-1. The viscosity was 10 Pa.S at 1323°C. Volatilization increased the viscosities of both LDMS glasses significantly during viscosity measurements.

LRMS-1 began its melt at 1230°C. During the second melt the volatilization was moderate and the glass appeared to be viscous, so the temperature was raised to 1275°C. The viscosity was estimated to be 12 Pa.S at the final pour, but the measured viscosity was 10 Pa.S at 1338°C. A yellow segregated layer was observed in both first and second melts.

LRMSM-1 had the same initial composition as LRMS-1, but with 3 wt% added metals. This glass was melted at 1230°C. Both melts had a pool of yellow segregate. The segregate poured quickly from the main melt and formed its own solid in two separate beads approximately 1-cm diameter and 0.5-mm thick. In addition, a yellow layer coated most of the surface of the poured glass. The viscosity was 10 Pa.S at 1297°C.

The redox states of these four glasses were analyzed in terms of the ratio of Fe(II) to total Fe, as shown in Table 3.19. It was surprising to find that the glasses made from simulant solutions were more oxidizing, i.e., with lower Fe(II)/Fe ratio, than were the glasses made from dry chemicals. The4e(II)/Fe ratio of 0.0274 of LDMS-1 was only 43% of the value of 0.063 of LDM-1 (made from dry chemicals) and the ratio, 0.0394 of LRMS-1, was also only 53% of the 0.075 of LRM-1 (made from dry chemicals). The metal-added glass had even lower Fe(II)/Fe ratios. These results may suggest a more oxidizing environment corrected by the simulant solutions during glass melting instead of the general perception that the simulant solution provides a more reducing condition.

The solubilities of SO_3 and P_2O_5 in these four glasses are tabulated in Table 3.20. LRMS-1 had a higher SO_3 solubility than that of LRM-1, which was consistent with the redox ratios discussed above, i.e., oxidized sulfur has higher solubility. The trend on phosphorus solubilities is not clear since the values in Table 3.20 are essentially within experimental errors.

The observed sulfur solubilities can be explained by the observed redox ratios, but the increased foaming and sulfur segregation in the melting with simulant solutions are still not clear. The melting viscosities shown in Table 3.6 are basically the same for glasses made from dry chemicals and from simulant solutions. Very minor differences were also observed in glass durability (Appendix B2) between glasses made from dry chemicals and from simulant solutions.

Table 3.20. Sulfur and Phosphorus Contents in Phase II Simulant Glasses (wt%)

Glass	LRM-1	LRMS-1	LRMSM-1	LDM-1	LDMS-1	LDMSM-1
Nominal SO_3	1.01	1.01	1.01	0.21	0.21	0.21
Analyzed SO_3	0.76	0.96	0.70	0.22	0.32	0.26
Nominal P_2O_5	2.52	2.52	2.57	0.19	0.19	0.18
Analyzed P_2O_5	2.72	2.43	2.39	0.46	0.29	0.28

3.5 Liquidus Temperature and Crystallization Kinetics

Crystallization will alter the glass properties such as durability (Kim et al. 1995). If excessive, crystallization may generate enough mechanical stress to fracture the glass, thus increasing surface area for leaching. Hence, crystallization rate may limit the acceptable cooling rates or compositions for LLW glass produced at Hanford.

The objective of this study is to characterize the glass-to-crystal transformation kinetics in simulated LLW glasses. Since crystallization rates are dependent on glass composition and test conditions, many glass compositions and test methods were employed. The preliminary results presented here include scoping studies using different methods on different glass compositions. Complete characterization of crystallization kinetics, including composition and nucleation effects, will be documented in the future.

3.5.1 Crystallization Process

This transformation is caused by the reduction of free energy (Gibbs free energy if constant pressure, temperature, and composition). Below the liquidus temperature (T_L) the crystal is a lower energy phase than the glass so crystallization is promoted. However, additional energy is produced at the glass-crystal interface from surface work.

This energy forms a barrier to the formation of very small crystallites (or nuclei), as seen in Figure 3.36. Nucleation is the process by which this barrier is overcome. The rate of nucleation is proportional to the driving force and rate of particle motion. A majority of glass systems nucleate heterogeneously on impurity particles, surfaces, and concentration fluctuations. Heterogeneous nucleation sites lower the thermodynamic barrier by decreasing the surface energy associated with nuclei formation.

Generally, crystallization occurs below the T_L and above the transition temperature (T_g) of glass, if cooled slowly enough. The crystal growth rate is directly linked to atomic mobility and hence, to temperature. At high temperatures growth is rapid and crystallinity quickly reaches equilibrium levels. At lower temperatures, growth is slower and equilibrium may not be achieved even with very long heat treatments. Figure 3.37 illustrates the temperature dependence for nucleation and growth.

3.5.2 Experimental Approach

The measurement procedures for transformation of glass to crystal include both isothermal transformation kinetics, which can be measured using a gradient furnace, or isotherm furnace in which samples are heat-treated isothermally at several temperatures for a range of times. The samples are then characterized for crystal volume fraction using OM and SEM with image analysis and/or XRD calibrated for quantitative measurements.

Nonisothermal transformations are measured in two common ways, the first way is to place the samples in a furnace with a scheduled heating or cooling rate. This rate can be constant (linear change in temperature with time), or logarithmic. Several samples are measured with varying rates and dwell-times. Like the isothermal method, the samples are then analyzed for crystal volume fraction.

The second method to measure nonisotherm transformation kinetics entails the use of thermoanalytical devices (DSC and DTA). By this method, small samples are heated or cooled at constant rates while

measuring the amount of enthalpy change in the sample. The crystallization exotherm is then characterized. The exotherm peak location and area are compared for samples with different rates. The total enthalpy (or peak area) is related to the amount of crystal formation and the peak location (measured as the temperature at the peak maximum) is related to crystallization rate.

For thorough analysis of crystallization kinetics, the above methods should be combined. Isothermal kinetics can be used to estimate nonisothermal crystallization and vice versa for some glasses (depending on crystallization mechanisms).

Transformation measurements on a range of glass compositions varied systematically can yield an effective method for estimating the effect of composition on crystallization kinetics. Several glass samples must be tested (~10) to elucidate these composition effects in the simple LLW glass systems. This amount of testing is beyond the scope of this study.

Nucleation rate is strongly dependent on the concentration on nucleation sites in glass. To characterize crystallization kinetics effectively in simulated LLW glass, one must ensure control of nucleating agents. Several methods can be used to study or control the nucleation in glass. The maximum crystal count is obtained by supplying nuclei up to the saturation level before crystal growth occurs. The nuclei can be supplied by heat-treating a glass with a high concentration of nucleating agents (or high surface area glass powder) in the nucleation temperature range (see Figure 3.37). The minimum crystal count is obtained by the removal of all nucleating agents, then equilibrating well above the liquidus temperature and quenching directly to the heat-treatment temperature.

3.5.3 Preliminary Test Results

Scoping studies of crystallization kinetics of simulated LLW glasses have been completed. Two glasses were selected and tested, L8-3 and L8-6. The former contains B_2O_3, CaO, and ZrO_2, and showed a great deal of crystals from a heat-treated sample, while the latter contains B_2O_3, CaO, Fe_2O_3, and ZrO_2 and showed a strong contrast (refractive index/color) between crystal and glass.

The high crystallinity sample (L8-3) was used to test the appropriateness of thermal analytical techniques. Using the DTA method, the sample must be cooled (or heated) at a number of rates. As the cooling rate increases, the crystallization exotherm becomes sharper and shifts to lower temperatures. When decreased, the exotherm becomes flatter and shifts to higher temperatures. If the sample is cooled (or heated) too quickly, crystallization won't occur and no exotherm will be visible. If too slow, the exotherm will be too broad and will disappear in the noise (will move out of instrument capabilities). The use of this method is directly related to the crystallization rate, amount of crystals formed, and enthalpy change upon crystallization. This method proved unsuccessful for L8-3 glass. Unsuccessful attempts were also made for two additional simulated LLW glasses.

The gradient furnace method was used to characterize L8-6 glass. It was found that the contrast between crystal and glass was not adequate to rely upon optical microscopy methods; XRD was successfully employed.

This sample was also used to identify the effects of nucleation on crystallinity. It was found that crushed glass surfaces provided an adequate source of nuclei to the glass at low temperatures. At high temperatures, the glass powder would sinter before the surfaces formed stable nuclei.

Glass samples with different nuclei concentrations have been heat-treated at the same growth temperature for 24 hours. Three powdered glass samples were used, as follows: (1) heated to equilibrate above T_L, then quenched directly to the growth temperature; (2) heated from powder directly to the growth temperature (through the nucleation temperature); and (3) heated at a nucleation temperature (just above T_g), then raised to the growth temperature. The results show a dramatic effect of nuclei on the total crystallinity.

3.5.4 Liquidus Temperature (T_L) Measurement

Liquidus temperature measurements were completed on 17 select Hanford low-level waste glasses. To determine T_L, two experimental methods were used: gradient furnace temperature and isothermal heat treatment. The Glass Development Laboratory's standard test procedures GDL-GFC, Rev 0 and GDL-LQT Rev 0 were used for gradient furnace measurements; GDL-HRT Rev 0 was used for the isothermal heat treatments.

To measure T_L by the gradient furnace method, a Thermcraft gradient furnace was used with a gradient of approximately 1°C/mm in the sample test zone. Samples were placed in a 95% Pt - 5% Au boat, 6 mm wide by 6 mm high by 15 to 30 cm long. The samples were placed in the gradient furnace for 24 hours, removed, and annealed in a box furnace. Samples were thin sectioned and observed using optical microscopy.

Liquidus temperature obtained using the isothermal heat treatment method was accomplished by placing the sample in a 95% Pt - 5% Au boat, 6 mm high by 12 mm wide by 12 mm long. A platinum lid was placed over the top of the boat and the sample placed in a Del Tech Furnace at a designated temperature for 24 hours. The sample was rapidly cooled to room temperature or placed in an annealing oven after the heat treatment was completed. Samples were observed using a metallurgical microscope to examine the glass and determine if the sample had crystals. Additional isothermal heat treatments were made until the T_L was measured within 4 to 5 degrees of the last sample that had crystals present. For closer observation, select samples close to T_L were thin sectioned and examined using a high-powered microscope.

Examination of the crystals in most of the glasses proved to be very difficult. The crystals were clear, in most cases, and matched the appearance of the glass; only with very careful examination and adjustments to lighting were the crystals observed. Some of the samples examined by using the scanning electron microscopy (SEM) were difficult to interpret. In sample L8-1, no crystals were detected by SEM although by optical microscopy it was a crystal rich sample. With other samples, SEM found crystals only after a slight contrast was made between the glass matrix and the crystal.

Crystal growth in the LLW glasses can be affected by contact with the glass surface, a nucleating site for crystals. This phenomenon was observed in the gradient furnace samples where the top surface of the glass had crystals at a much higher temperature than the sides or bottom of the glass which was in contact with the platinum. Further, most of the samples were prepared with chunks of glass. The surfaces of the glass particles or chunks precipitated what appeared to be crystals or bubbles; so small (0.5 microns) that they were only detected because of the cloudy appearance caused from the numerous inclusions in the area around the fused glass surfaces. In the gradient furnace samples this could be observes at the low temperatures where the viscosity was high, convections in the glass were low, and the outline of the glass particles could still be observed. Examination by SEM revealed spherical shapes which could be bubbles of phase separation. Additional study will be needed to determine if there are soluble phases (perhaps Na_2SO_4) which are in these inclusions but are washed out as the sample is being cut and polished for examination.

Three categories will be used to examine the T_L data: calcium silicate, borosilicate, and calcium borosilicate glass systems. Eight calcium silicate glasses were measured:

Glass	Obseved T_L (°C)	Observed Crystal Type	SEM	Method
L8-2	1048	Lathe		GF
L8-5	1009	CC		GF
L5-069	[960]	+		GF and Iso
L5-096	[<955]	+		GF and Iso
L5-0615	1051	CR	(Na, Ca, P, Si)	GF
L5-0129	[1015]	+		GF
L5-01212	1078	CC	(Ca, Si, O)	GF and Iso
L5-01215	1079	CF, Hex	(Ca, Si, O)	GF and Iso
			(Na, Al, Si, O)	

Note: All temperatures in [] are preliminary estimates of T_L.
GF = Gradient Furnace Method
Iso = Isothermal Heat Treatment
CC = clear cubic crystal; CR = clear round crystal; Hex = hexagonal; Lathe = long, flat crystal; CF = clear with facets on the surface of the crystal; + = need more experimental study before determiniation can be made.
SEM = compositional analysis generated using energy-dispersion spectroscopy; ND = not detected.

L8-2 has 9 wt% Al_2O_3 and 6 wt% ZrO_2 and CaO. The lathe-like crystal was observed among the masses of small crystal-type inclusions commonly observed in this sample. The lathe-like crystals probably contain zirconium, which has a strong effect on increasing T_L. L8-5 is the same composition as L8-2, except 6 wt% Fe_2O_3 is substituted for 6 wt% ZrO_2. With the lack of zirconium in this sample, the T_L has decreased. In the last four glasses, the highest T_L exists for the measured LLW glasses. L5-0129 has 9 wt% Al_2O_3 while L5-0615, L5-01212, and L5-01215 have 12 and 15 wt% alumina present. The high alumina also has a strong effect on increasing T_L. Calcium has some effect on modifying T_L, which can be seen when comparing L5-069 (6 wt% CaO) with L5-0129 (12 wt% CaO). In the L5-01215, two crystal types were identified by SEM just below T_L. This glass has a 3 wt% increase in Al_2O_3 over L5-01212, only a slight increase in T_L but a change in crystal type.

Four borosilicate glasses were measured:

Glass	T_L (°C)	Crystal Type	Method
L8-1	1044	CC	ND
L8-7	[<780]	None	GF
L4-6015	[<780]	None	GF and Iso
L4-12015	[<800]	+	GF and Iso

L8-3 has 3 wt% CaO and B_2O_3, 6 wt% ZrO_2, and 9 wt% Al_2O_3. In L8-6 the zirconia is substituted for 6 wt% Fe_2O_3. Both of these glasses show a rather low T_L. The last two glasses show a rather average T_L for LLW glasses. This suggests that the combination of B and Ca in the glass tend to moderate T_L. SEM was only able to find the one crystal type in L8-6 even though the clear cubic crystal was twice as numerous as the hexagonal, zirconium bearing crystal.

The sample L8-8 was also measured. This borosilicate glass had 4 wt% MgO and 9 wt% Al_2O_3. Both methods of measurement were performed on the glass with no crystals observed. Unusual formations at the bottom in bubbles and a phase separated layer on the surface are still being investigated.

The method of measurement has been noted for each of these glasses because the gradient furnace temperature method had strong convections present in the samples. For those samples with the strongest convection lines, the sample was rerun using the isothermal heat treatment method. This method is more precise but takes much more time due to the number of samples that need to be generated. The isothermal method was always used as the primary method for T_L in the data. Some of the gradient furnace temperature samples may have higher T_L because of these convections.

Further analysis by scanning electron microscopy and X-ray diffraction is need to fully evaluate this T_L data. Additional samples and further testing by the isothermal heat treatment method would also strengthen the data.

3.6 High Iron Glass Study

3.6.1 Introduction

Boron oxide has been recognized as an important component in a waste glass for lowering the melting temperature and melt viscosity without compromising the glass durability. However, inherent problems exist with the use of boron oxide. Volatility of boron throughout the batch reaction and glass-melting process, and potential phase separation are two important factors to consider. Since the refractory materials have been improved significantly, melters can now be operated at higher temperatures. In addition, lower level wastes are high in sodium oxide, which is an effective flux for lowering the glass melting temperature. Therefore, boron oxide can potentially be replaced by other trivalent oxides like Fe_2O_3 in a lower level waste formulation without sacrificing the chemical durability and increasing the melt temperature.

Through work funded by the Mixed Waste Integrated Program (MWIP), Merril et al. studied the feasibility of using high iron and boron-free glasses as a matrix for Hanford low-level tank wastes (Merril 1995). Nearly all glasses formulated are based on the system of oxides: Na_2O-Al_2O_3-Fe_2O_3-SiO_2. Some glass compositions contain high waste loading (up to 30 wt% Na20) with leach resistant comparable to high-level waste glasses. Viscosity of 10 Pa•s can be achieved at temperatures of 1350° to 1500°C. Most high iron glasses are homogeneous and non-crystalline.

3.6.2 Experimental

Glass development work involves determining the waste composition, glass formulation, bench-scale melting and glass property characterization, especially the glass processibility and durability. The LLW stream composes primarily of sodium nitrate, sodium nitrite, sodium hydroxide, and sodium aluminate. High sodium oxide loading glass formulation can result in considerable cost reduction to process, given the volume of LLW wastes.

Composition Design

A non-replicated, two-level factorial design was adopted to investigate the variation of glass durability with composition in this glass system Na_2O-Al_2O_3-Fe_2O_3-SiO_2. The centroid glass composition contains by weight: 25% Na_2O, 10%Al_2O_3, 10%Fe_2O_3 and 55%SiO_2. The three independent variables (Na_2O, Al_2O_3, and Fe_2O_3) vary 5 wt% above and below this base composition, with changes offset by corresponding changes in SiO_2. The centroid glass composition was melted in triplicate so that the experimental error could be estimated. These glass compositions (No. 1 through No. 11), along with some additional revised compositions (No. 12 through No. 18) are listed in Table 3.21.

Leach Test

The static leaching test was use to evaluate glass durability. The test procedure is similar to the PCT, with the following major differences: (1) glass particle size used was 250 to 400 μm compared, to 75 to 150 μm for PCT; (2) 24-hour test duration compared to 7-day or 28-day for PCT; (3) the test temperature is 40°C, compared to 90°C for PCT. The leaching rates of standard reference glasses were also measured under the same condition.

3.6.3 Results and Discussion

Compositional Effects

Analysis of leaching rates in relation to glass composition for No. 1 through No. 11 indicated that both Al_2O_3 and Fe_2O_3 help to reduce leaching. Al_2O_3 showed a stronger response at the same content level. The interaction effects among Na_2O, Al_2O_3, and Fe_2O_3 are less obvious. There is slight indication that Fe_2O_3 interacts with Na_2O to minimize the leaching rate.

Pairwise comparison is presented in Figure 3.38 and 3.39. In Figure 3.38, Na_2O and Al_2O_3 are kept the same for each pair, while 10wt% Fe_2O_3 is used to replace 10 wt% SiO_2. It can be seen from Figure 3.38 that the benefit of this replacement is more significant when the Na_2O content is high and the Al_2O_3 content is low. See Table 3.21 for glass compositions.

Figure 3.39 compares the effect of Al_2O_3 replacing Fe_2O_3 in each pair while the Na_2O and SiO_2 content are kept the same in each pair. The benefit of such a replacement is more for low Na_2O containing glass in terms of leaching rate ratio. For the compositions studied, Al_2O_3 is more effective for sodium containment that Fe_2O_3. However, the melting temperature increased at least 100°C in each case when 10 wt% Al_2O_3 replaced 10 wt% Fe_2O_3.

It is not surprising that the sodium leaching is inherently related to sodium content in a glass. Figure 3.40 shows the sodium release as a function of sodium content in simple dilution of a base glass (LLW91) or simple replacement of SiO_2 (Al_2O_3 and Fe_2O_3 are both at 15 wt% level). Comparing to reference glasses DWVP-EA reference glass and the approved reference material (ARM) glass, some high iron and boron-free glasses are quite promising in high sodium loading and low leaching rates. Leaching rates for DWVP-EA and ARM are represented as dashed lines in Figure 3.40.

Table 3.21. Selected Properties of High Iron, Boron Free Glasses

		10 Pa*S	Norm. Release	Composition (wt%)				
No.	Melt ID	Temp (°C)	(g/m^2)	Na_2O	SiO_2	Al_2O_3	Fe_2O_3	CaO
1	LLW81	1350	0.080	30.00	40.00	15.00	15.00	
2	LLW82	1550	0.012	20.00	50.00	15.00	15.00	
3	LLW83	1300	0.280	30.00	50.00	5.00	15.00	
4	LLW84	1450	0.086	20.00	60.00	5.00	15.00	
5	LLW85	1400	0.164	30.00	50.00	15.00	5.00	
6	LLW86	1600	0.030	20.00	60.00	15.00	5.00	
7	LLW87	1350	1.600	30.00	60.00	5.00	5.00	
8	LLW88	1500	0.181	20.00	70.00	5.00	5.00	
9	LLW89-1	1450	0.084	25.00	55.00	10.00	10.00	
10	LLW89-2		0.073	25.00	55.00	10.00	10.00	
11	LLW89-3		0.059	25.00	55.00	10.00	10.00	
12	LLW91		0.016	20.00	45.72	17.14	17.14	
13	LLW92		0.028	22.00	44.57	16.71	16.71	
14	LLW93		0.078	24.00	43.43	16.29	16.29	
15	LLW94		0.030	26.01	42.28	15.85	15.85	
16	LLW95		0.047	28.00	41.14	15.43	15.43	
17	LLW102	1450	0.023	25.00	45.00	15.00	15.00	
18	LLW104	1450	0.034	25.00	45.00	15.00	10.00	5.00
Ref	DWVP-EA		0.055					
Ref	ARM		0.022					

Note: This table is compiled using data from (Merrill 1995).

Table 3.22. Response Variables and the Associated Weighting Factors

Response Variable	Weighting Factor (%)
Durability	35
Homogeneity	25
Viscosity	25
Volatility	15

3.6.4 Conclusions

High iron glasses have less foaming and volatilization. Higher sodium loading can be achieved with high iron glasses. Compared with other trivalent oxides, especially Al_2O_3, Fe_2O_3 helps to lower melting temperature. Lowest leaching rate based on the study is when Al_2O_3 and Fe_2O_3 are presented in near equal amount and the total is about 30 wt%.

3.7 A Plackett-Burman Experimental Design Approach

Marra at Savannah River Technology Center used a self-directed optimization approach to develop a glass composition for plasma vitrification of a high sodium content nuclear waste (Marra 1995). This approach used four weighted response variables to access prospective compositions. Table 3.22 shows the four response variables and the weighting factor used. The weighting factors were determined based on perceived importance.

A priori criteria were established from which the response value would be experimentally measured or subjectively quantified. Durability was assessed by the 7-day PCT relatively to the EA glass limit for normalized sodium release. A range of "acceptable" viscosity values were defined to assess processibility and other related characteristics. The viscosity values for each glasses were predicted using a viscosity prediction model based on the concepts of glass structure (Kielpinski 1994). Homogeneity was visually assessed. Response values were determined based on glass homogeneity; crystalline phases only, glass only, or a glass with associated crystals. The volatility variable was based on the quantification of gall formation (or salt layer) on the melt surface. Since no gall layer was observed during testing, each composition received the maximum rating (1). The response variable was given a value of 0 to 1 (intermediate values usually based on a linear scale between extreme or "acceptable" values) and multiplied by the corresponding weighting factor. These values were added together to give a total "desirability quantity" for each composition. Based on the cumulative results, a simple algorithm was used to develop additional glass formulations and eventually to focus on the optimal composition.

Table 3.23. 10M Na^+ Simulant Composition

Oxide	Calcine Solid (wt%)
SiO_2	12.76
CaO	0.01
Cr_2O_3	0.16
Fe_2O_3	0.01
K_2O	5.78
MgO	0.01
MnO_2	0.01
MoO_3	0.60
Na_2O	72.56
SrO	0.43
Cs_2O	0.59
P_2O_5	0.75
NaI	0.62
NaCl	2.29
NaF	2.58
SO_3	0.84
Total	100

3.7.1 Experimental Considerations

Initially, twelve compositions were determined by a Plackett-Burman design. Glass formers additives included Al_2O_3, B_2O_3, CaO, Li_2O, ZrO_2, and SiO_2. Lithia was used to facilitate fritting. Preset high and low values of oxide ratios were determined for the initial 12 melts. A waste loading of 25% on a calcined oxide basis was used in the formulations. Table 3.23 shows the "waste" compositions which were added as a 10M Na^+ solution (obtained from Optima Chemical, Douglas, GA). The solution was a surrogate for the Hanford DSSF waste. All glasses were formulated using reagent-grade chemicals (either as oxides or carbonates) and melted at 1150°C for 2 hours in a covered alumina crucible and allowed to air cool.

Table 3.24. Ratios of Glass Additives for the 25 Glasses Tested

Composition	Round	Al_2O_3/SiO_2	B_2O_3/SiO_2	CaO/SiO_2	Li_2O/SiO_2	ZrO_2/SiO_2
1	1	0.23	0.22	0.07	0.08	0.16
2	1	0.23	0.22	0.11	0.08	0.05
3	1	0.23	0.09	0.11	0.02	0.16
4	1	0.35	0.22	0.11	0.02	0.05
5	1	0.35	0.09	0.11	0.08	0.16
6	1	0.35	0.22	0.07	0.02	0.05
7	1	0.35	0.22	0.07	0.08	0.16
8	1	0.23	0.22	0.11	0.02	0.16
9	1	0.23	0.09	0.07	0.08	0.05
10	1	0.23	0.09	0.07	0.02	0.05
11	1	0.35	0.09	0.07	0.02	0.16
12	1	0.35	0.09	0.11	0.08	0.05
13	2	0.20	0.09	0.11	0.005	0.02
14	2	0.32	0.09	0.07	0.005	0.13
15	2	0.20	0.22	0.07	0.005	0.02
16	2	0.20	0.22	0.07	0.06	0.02
17	3	0.15	0.25	0.07	0.00	0.08
18	3	0.27	0.25	0.11	0.04	0.08
19	3	0.27	0.12	0.11	0.00	0.00
20	3	0.18	0.25	0.11	0.06	0.00
21	4	0.27	0.30	0.07	0.03	0.00
22	4	0.30	0.17	0.11	0.00	0.11
23	4	0.23	0.27	0.07	0.05	0.13
24	4	0.32	0.14	0.07	0.00	0.13
"Best Average"	-	0.26	0.20	0.09	0.03	0.05

3.7.2 Ranking and Rating Methodology

The first twelve glasses were ranked according to the "desirability quantity." The four worst glass compositions were used to generate four new glasses by subtracting twice the average composition of the eight better glasses. The four new glasses were formulated, melted, characterized, and ranked with the eight better glasses. The new ranking then provided four poor glasses which were replaced by the same methodology as before. Four rounds (24 glasses) of this rank-and-replace methodology was used until the decision was made that further compositional development would not significantly improve or change the best eight glasses. The methodology used does not guarantee that the new formulations will be an improvement on the previous compositions. If fact, the new formulation may fall outside the compositional region of durable and/or processible glasses. However, as long as there is some progress with the new formulations, the rank-and-replace methodology will be pursued. An optimized composition was determined by averaging the eight best glasses following round 4. Table 3.24 shows the glass additive compositions for the 24 glasses tested in the study as well as the best average composition in terms of oxide ratios. For the 24 glass compositions see Appendix C.

3.7.3 Results

Rating and Ranking

Table 3.25 shows the ratings and rankings of the final 12 glasses after round 4. Glass compositions 4, 6, and 15 obtaining the maximum rating (1) for each response variable identified. For the rankings and respective response variable values after each round refer to Appendix D.

Durability and Viscosity

Tables 3.26 and 3.27 show the durability and viscosity results, respectively, for the final best eight glasses and the best average glass. The durability results are given as normalized PCT release (g/L) for various elements and for comparison purposes those values associated with the EA glass are also listed. Viscosities (poise) based on the model predictions are shown in Table 6.

Table 3.25. Ratings and Ranking After Round 4

Composition	Durability	Viscosity	Homogeneity	Volatility	Total
4	35	25	25	15	100
6	35	25	25	15	100
15	35	25	25	15	100
8	35	24.5	25	15	99.5
21	33.8	25	25	15	98.8
9	31.2	25	25	15	96.2
13	35	16.8	25	15	91.8
18	35	16.2	25	15	91.2
17	35	25	12.5	15	87.5
23	33.9	12.5	25	15	86.4
22	-*	25	12.5	15	-
24	-*	0	0	15	-

* Durability (PCT) not measured since composition did not form a glass.

Table 3.26. Normalized PCT Results for the Final Best Eight and Best Average Glasses

Composition	Rating	Na (g/L)	Si (g/L)	B (g/L)	Li (g/L)
8	35	0.568	0.123	0.449	0.231
6	35	0.502	0.134	0.549	0.270
4	35	0.609	0.112	0.630	0.284
13	35	0.610	0.079	0.726	0.185
15	35	0.685	0.099	0.940	0.364
Best Average	35	0.732	0.119	0.792	0.430
18	35	1.055	0.160	1.116	0.756
21	33.8	1.382	0.209	1.771	1.516
9	31.2	1.463	0.344	0.808	0.895
EA Glass	-	13.346	3.922	16.695	9.565

Table 3.27. Viscosity Results for the Final Best Eight and Best Average Glasses

Composition	Rating	Predicted Viscosity (poise)	Deviation from 100 poise
4	25	94.8	-5.2
Best Average	25	84.1	-15.9
15	25	116.0	+16.0
6	25	125.5	+25.5
9	25	65.9	-34.1
21	25	65.4	-34.6
8	24.5	59.2	-40.8
18	16.2	45.9	-54.1
13	16.8	159.8	+59.8

In an attempt to identify a centralized glass formulation (in terms of compositional space) for the best eight glasses, the glass formers concentrations were averaged to produce a best average composition (see Table 3.28).

Marra identified several general observations regarding the concentrations of glass formers and the interactions on glass quality (Marra 1994). These include the following:

(1) Typically, a low level of lithia coupled with an elevated level of boria constituted a good glass.

(2) In the initial Plackett-Burman compositions, a high level of alumina or zirconia, but not both, produced the better glasses. In the latter tests, moderate levels of alumina produced good glasses, so long as the boria levels were not excessive and the lithia levels were very low.

(3) Low zirconia levels were prevalent in the eventual eight best glasses.

(4) Calcia levels appeared to have no relationship to the quality of glass produced.

A nominal composition was also batched and melted with and without lithia additions. The latter was an attempt to minimize the total alkali content. Both formulations produced somewhat cloudy glasses with significant undissolved batch present.

3.7.4 Melter Run

To examine the feasibility of processing the waste compositions in a continuous melter, a small-scale vitrification campaign was performed. A joule-heated melter was operated for approximately 96 hours, producing approximately 80 lbs of simulated waste glass. Composition 4 was selected for this application. A melt temperature of 1150°C was maintained for the duration of the campaign. Some general observation during the melter campaign were reported. These include the following:

- Several deposits containing chlorine, sulfur, and phosphorous formed during the run. The salts likely caused the failure of several dome heaters in the pour chamber.

- The resulting glass product was blackish-brown due to the additional iron in the glass (requested by a Hanford customer). Based on optical microscopy, SEM/EDS, and X-ray diffraction, the glass was "generally homogeneous." A minor crystalline phase (sodium alumina silicate sulfate by XRD) was observed in one glass sample.

- Two samples form different can pours were tested by the 7-day PCT to assess durability. The normalized releases were well below the EA limit (see Table 3.29).

3.7.5 Low Boron Glass

Glass composition 4 was also used for the vitrification trials at the Westinghouse Waltz Mill Plasma Center. Significant volatility of sodium and boron was apparent following post-test analysis of the plasma melter cupola and off-gas system. Approximately 15% and the sodium and 20% of the boron were not incorporated in the glass.

Table 3.28. Best Average Glass Composition

Oxide	Glass Additive (wt%)	Final Glass (wt%)
SiO_2	61.1	46.08
Al_2O_3	16.1	15.35
B_2O_3	12.3	9.28
CaO	5.5	4.15
ZrO_2	3.3	2.49
Li_2O	1.7	1.28
Na_2O	-	19.06
K_2O	-	1.45
SO_3	-	0.21
P_2O_5	-	0.19
MoO_3	-	0.15
Cs_2O	-	0.15
SrO	-	0.11
Cr_2O_3	-	0.04
Fe_2O_3	-	0.004
MgO	-	0.002
MnO_2	-	0.002
Total	-	99.998

Table 3.29. Normalized PCT Release Results for the 774-A Melter Run

Composition	Na (g/L)	Si (g/L)	B (g/L)	Li (g/L)
Can 8	0.302	0.193	0.469	0.363
Can 9	0.287	0.204	0.438	0.540
EA	13.346	3.922	16.695	9.565

Table 3.30. Compositions of the Five Melted Glasses Containing No or Low Boron

Oxide	JH-1	JH-3	JM-2	JM-3	JM-5
SiO_2	43.12	43.12	53.17	53.93	52.42
Na_2O	19.05	19.05	19.06	19.06	19.06
Al_2O_3	17.91	17.91	12.26	12.26	12.26
B_2O_3	0	0	2.26	0	2.26
CaO	13.35	11.69	6.04	7.55	7.17
ZrO_2	2.11	2.11	3.02	3.02	3.77
Fe_2O_3	0.50	0.50	0.004	0.004	0.76
Li_2O	1.66	3.32	1.88	1.88	0
K_2O	1.45	1.45	1.45	1.45	1.45
SO_3	0.21	0.21	0.21	0.21	0.21
P_2O_5	0.19	0.19	0.19	0.19	0.19
MoO_3	0.15	0.15	0.15	0.15	0.15
Cs_2O	0.15	0.15	0.15	0.15	0.15
SrO	0.11	0.11	0.11	0.11	0.11
Cr_2O_3	0.04	0.04	0.04	0.04	0.04
MgO	0.002	0.002	0.002	0.002	0.002
MnO_2	0.002	0.002	0.002	0.002	0.002
Total	100.004	100.004	99.998	100.008	100.004

Ten potential glasses containing no or low boron were formulated of which five were melted. Table 3.30 shows the compositions of these five glasses. Three glasses were melted at 1150°C while the other two were melted at 1275°C. Compositions JM-3 and JM-5 formed homogeneous glass. JM-3 was successfully melted at both 1275°C and 1175°C (a remelt). However, at 1175°C the glass contained a significant amount of bubbles indicating that the viscosity was relatively high. Both melts of JM-3 were subjected to the 7-day PCT to assess the durabilities. Table 3.31 shows the results in terms on normalized elemental releases.

Table 3.31. Normalized PCT Results of JM-3 Glasses Containing No Boron

Composition	Na (g/L)	Si (g/L)	Li (g/L)
JM-3 (1275°C)	1.769	0.224	1.185
JM-3 (1175°C)	1.844	0.216	1.345
EA Glass	13.346	3.922	9.565

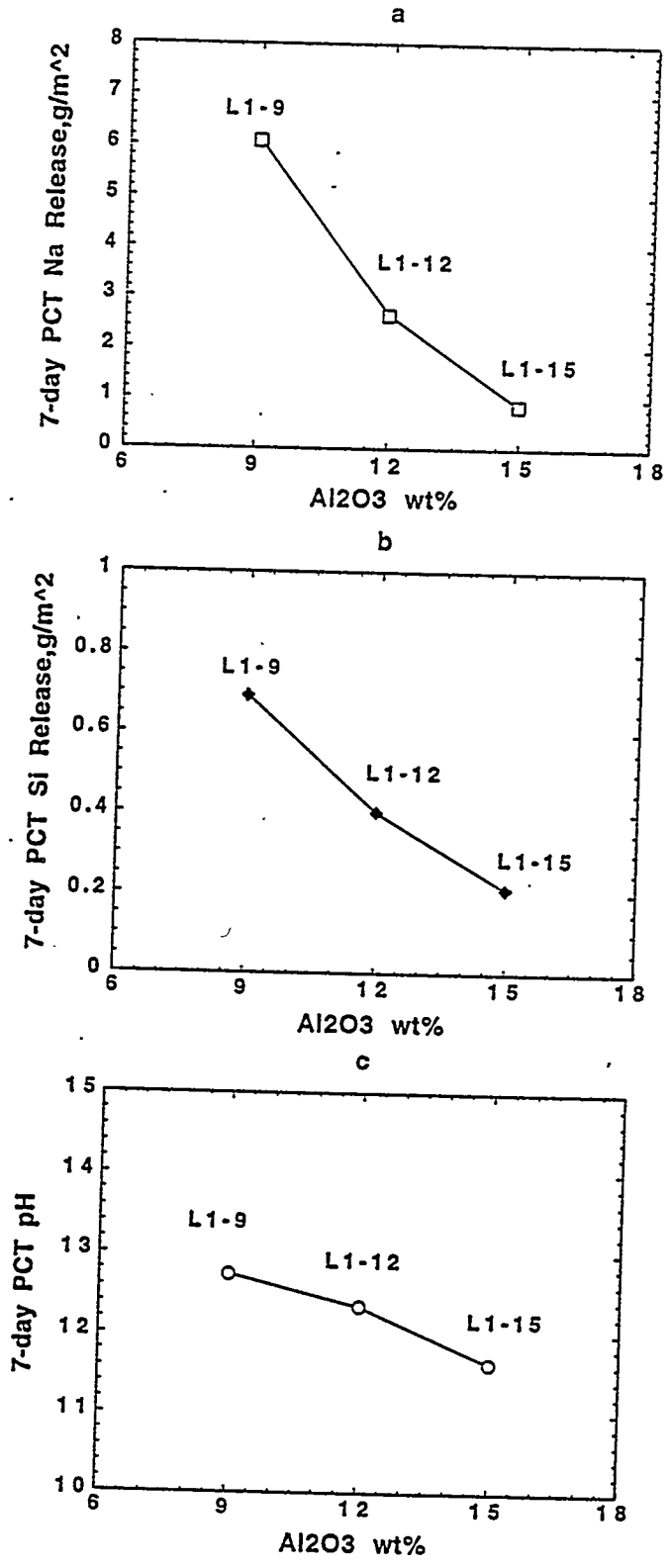

Figure 3.1. 7-Day PCT Results. Al_2O_3 increases at the expense of SiO_2 in glasses without B_2O_3 and CaO.

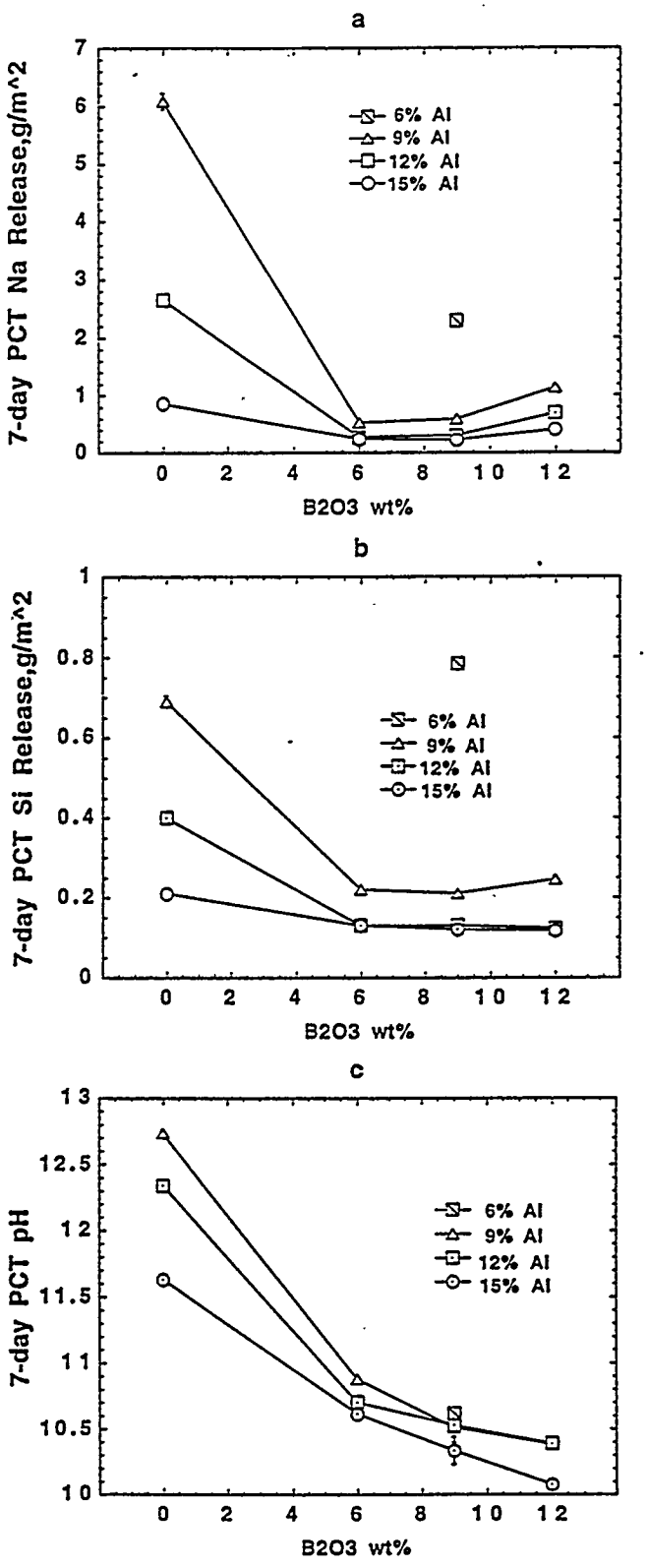

Figure 3.2. 7-Day PCT Results. B_2O_3 increases at the expense of SiO2 in glasses with different amounts of Al_2O_3.

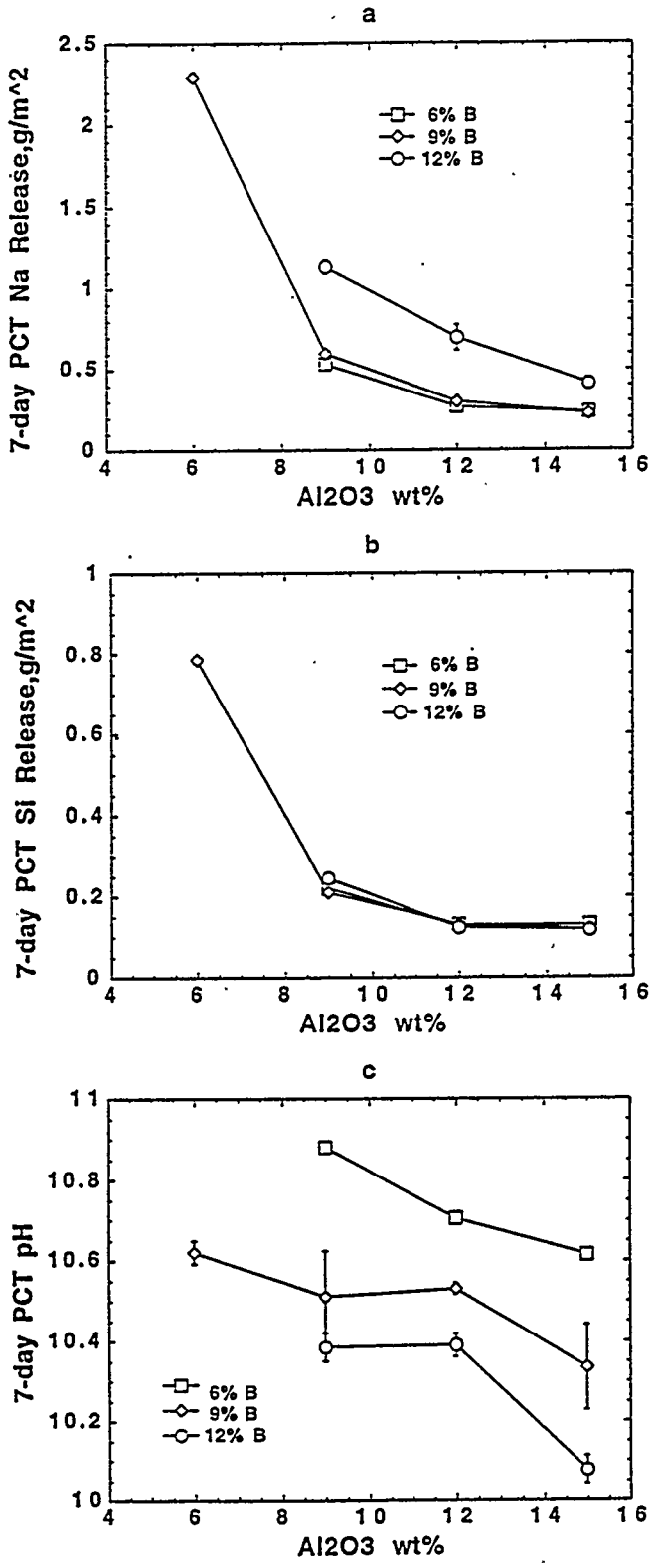

Figure 3.3. 7-Day PCT Results. Al_2O_3 increases at the expense of SiO_2 in glasses with B_2O_3.

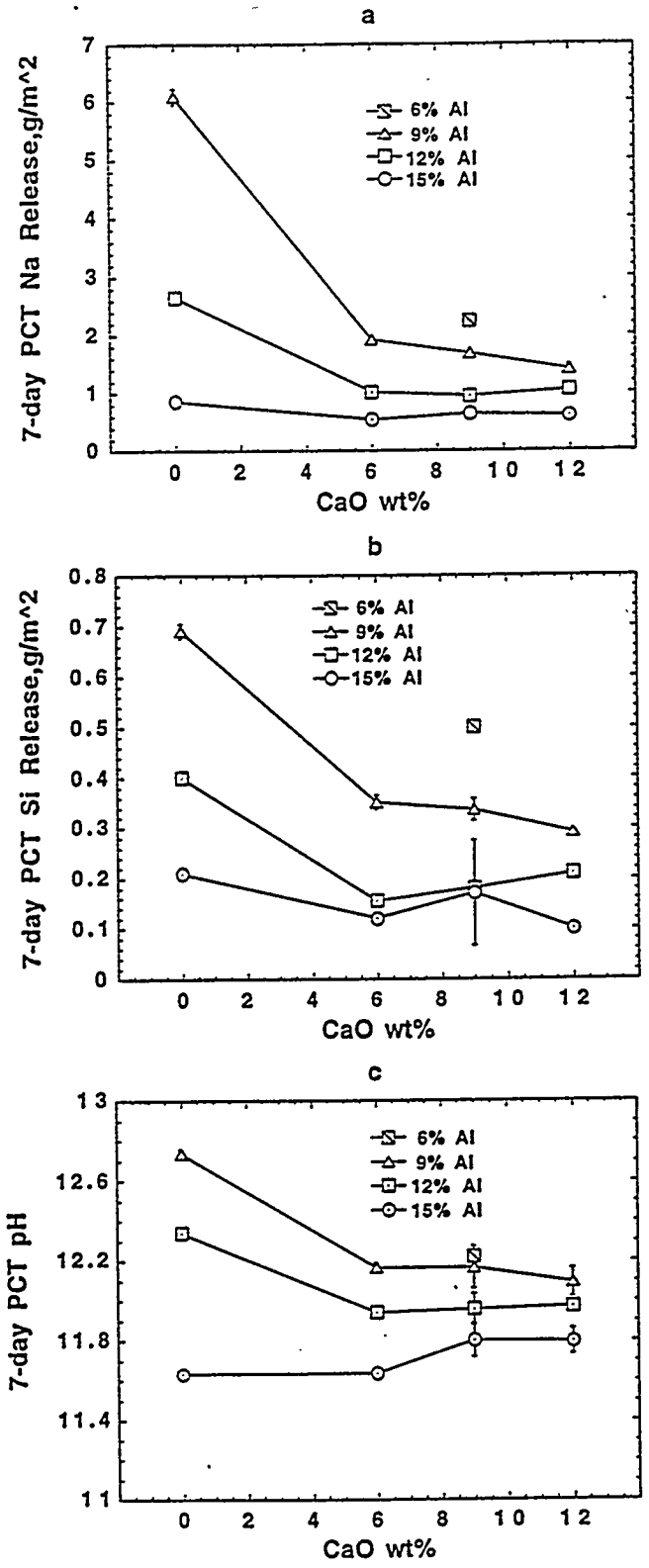

Figure 3.4. 7-Day PCT Results. CaO increases at the expense of SiO_2 in glasses with different amounts of Al_2O_3.

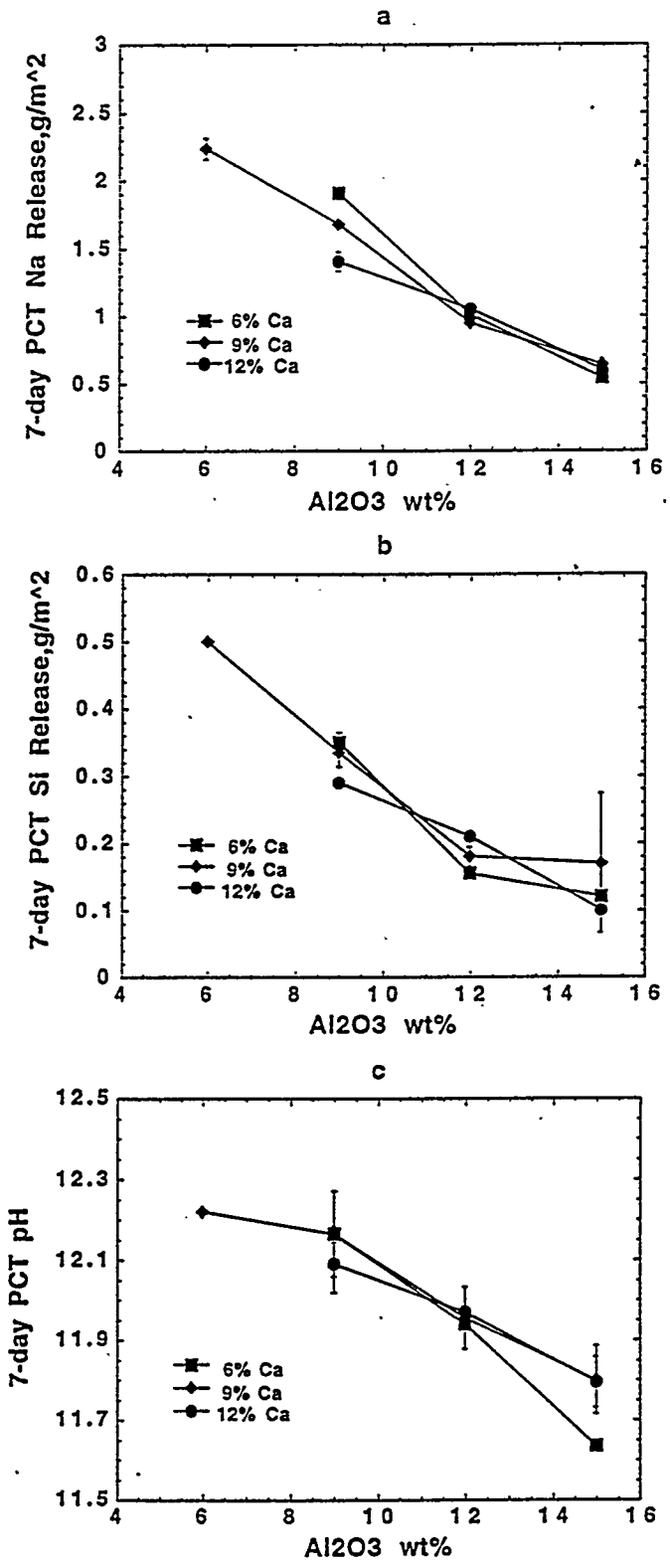

Figure 3.5. 7-Day PCT Results. Al_2O_3 increases at the expense of SiO_2 in glasses with CaO.

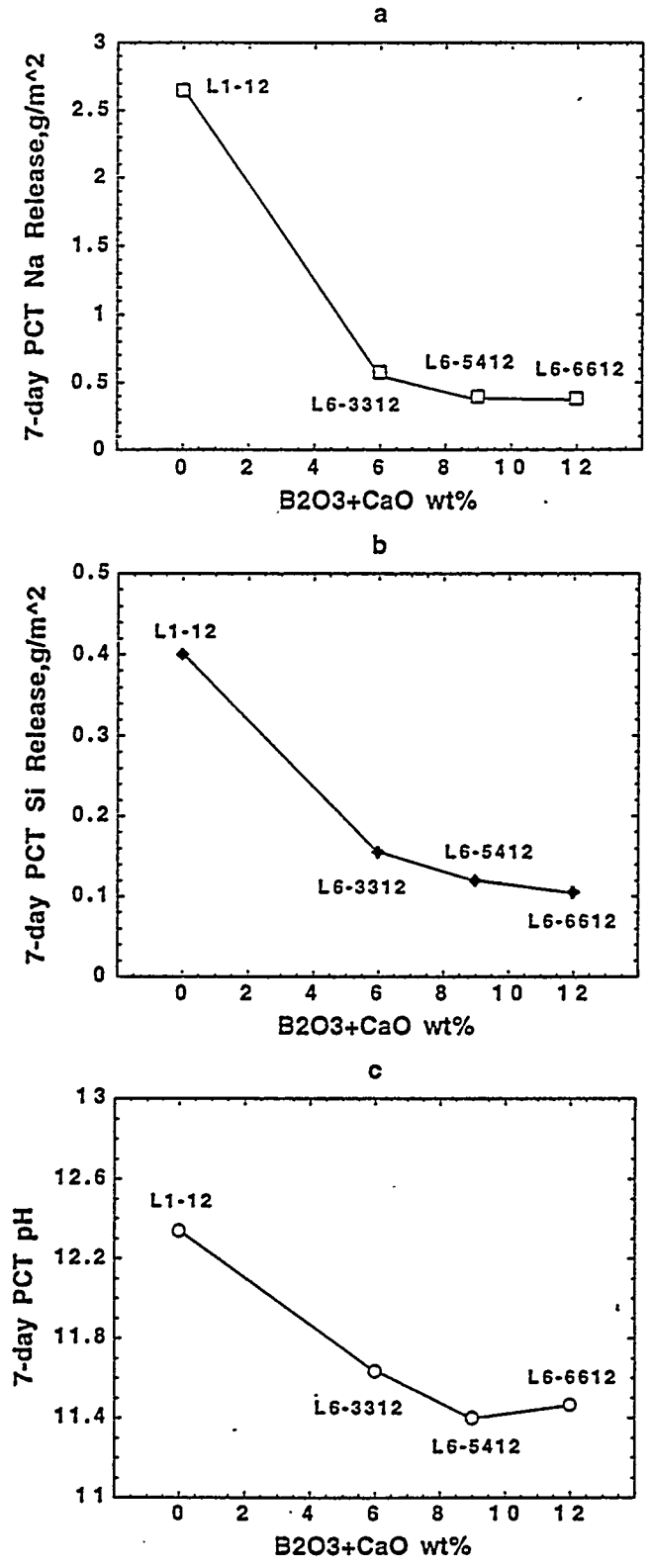

Figure 3.6. 7-Day PCT Results. The increase of B_2O_3 and CaO increase at the expense of SiO_2 in glasses.

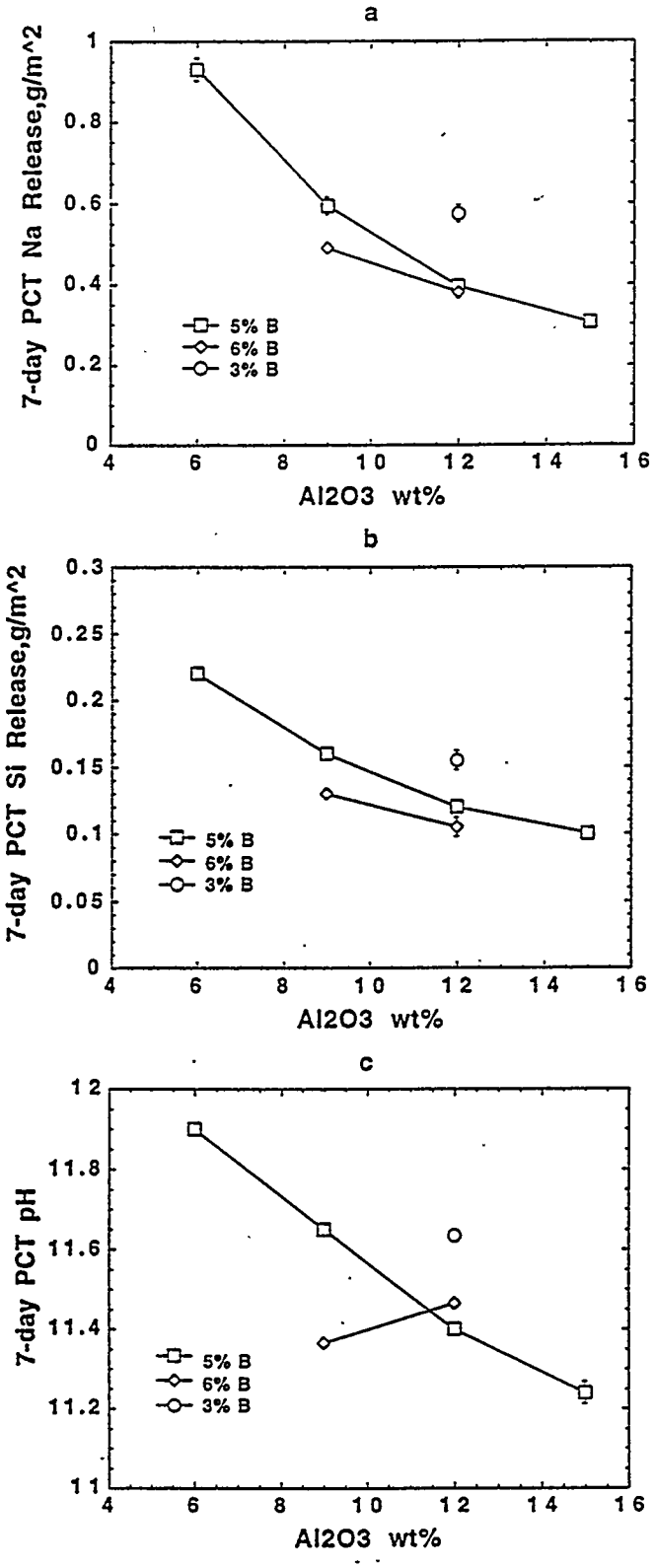

Figure 3.7. 7-Day PCT Results. Al_2O_3 increases at the expense of SiO_2 in glasses with mixture of B_2O_3 and CaO. Each glass has the same amount of CaO and B_2O_3.

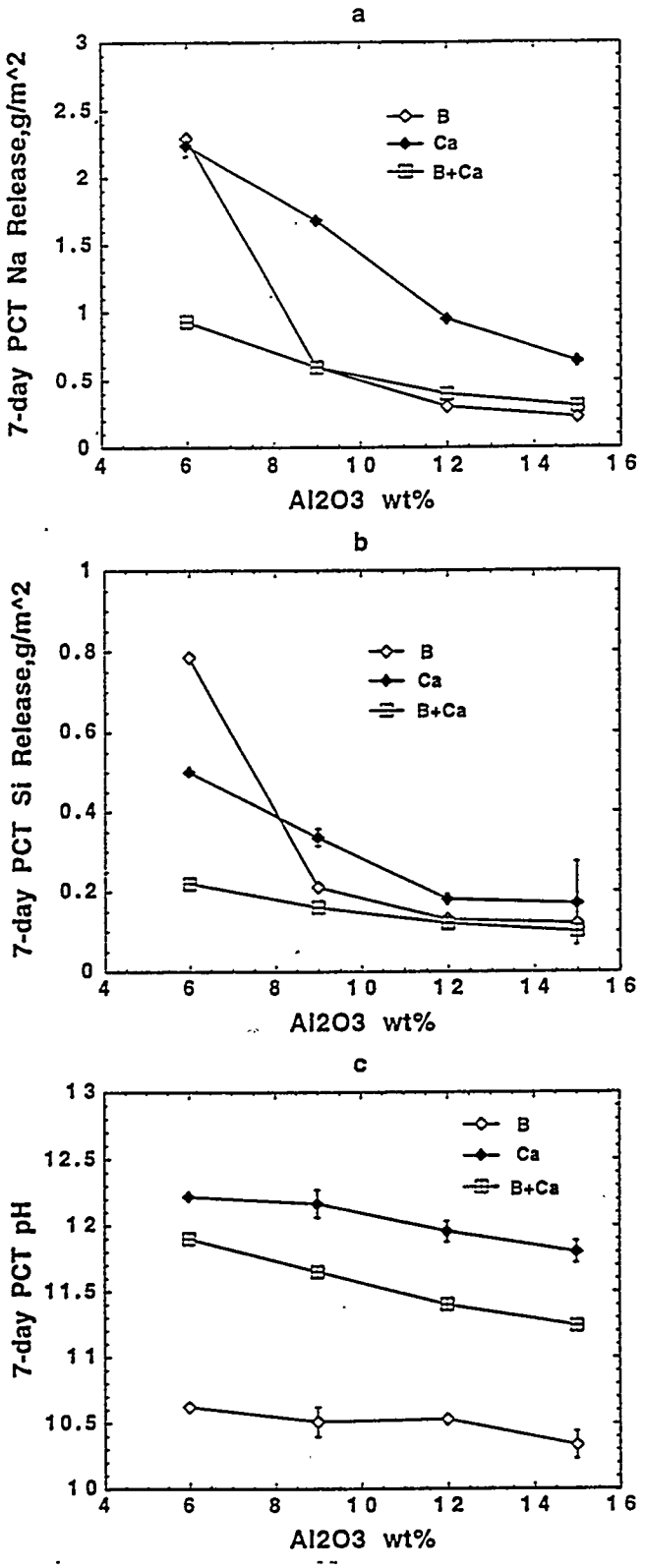

Figure 3.8. 7-Day PCT Results. Comparison of the relative effects of Al_2O_3 increase at the expense of SiO_2 among glasses with B_2O_3, CaO, and a mixture of both CaO and B_2O_3.

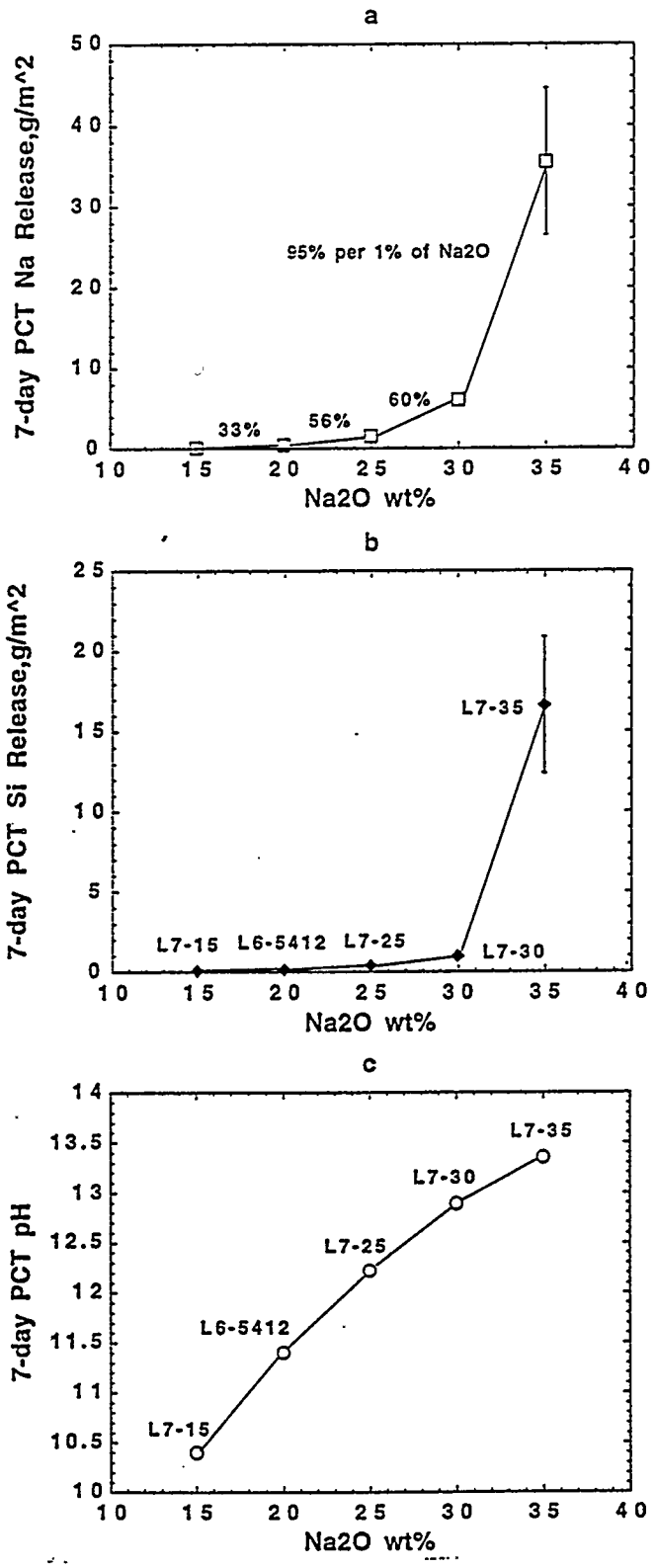

Figure 3.9. 7-Day PCT Results. Na_2O increases at the expense of all of the other components in glasses similar to L6-5412.

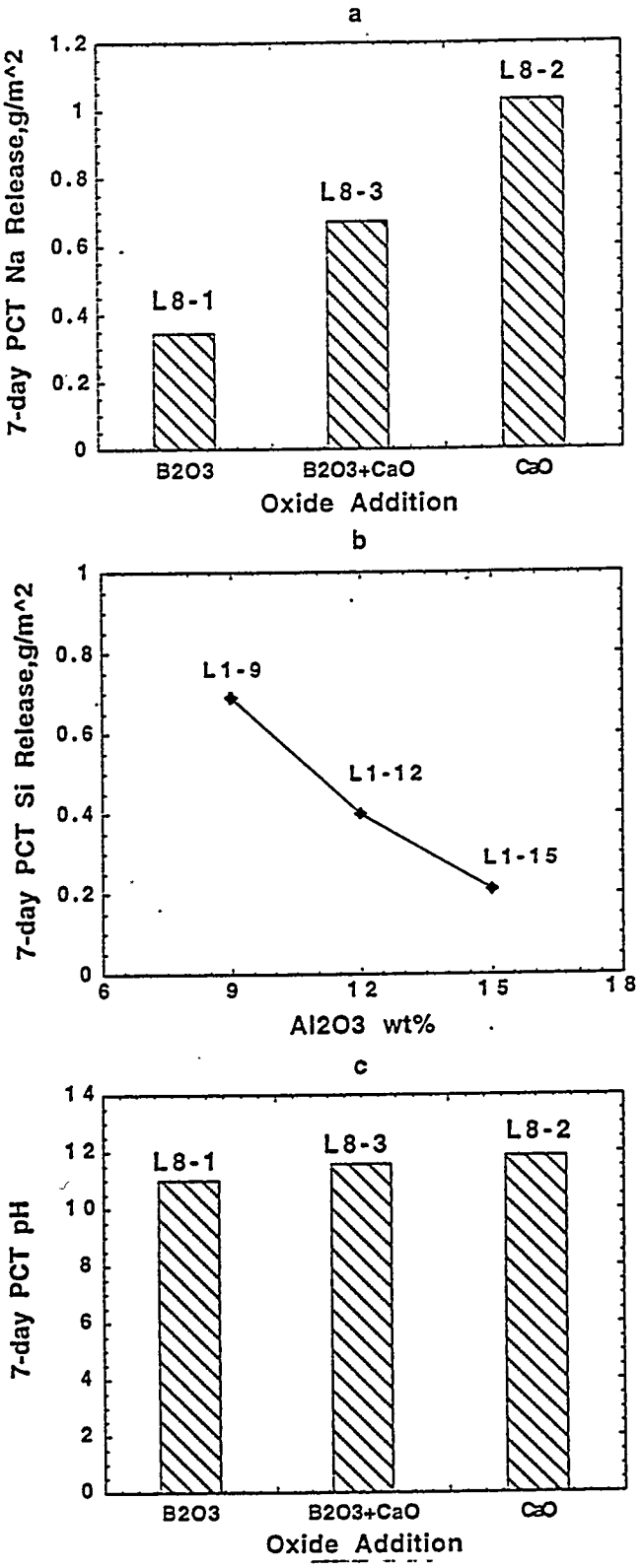

Figure 3.10. 7-Day PCT Results. 6 wt% of ZrO_2 addition to a base glass with SiO_2 56.78, Na_2O 20.0, Al_2O_3 9.0, but with different amounts of CaO and B_2O_3.

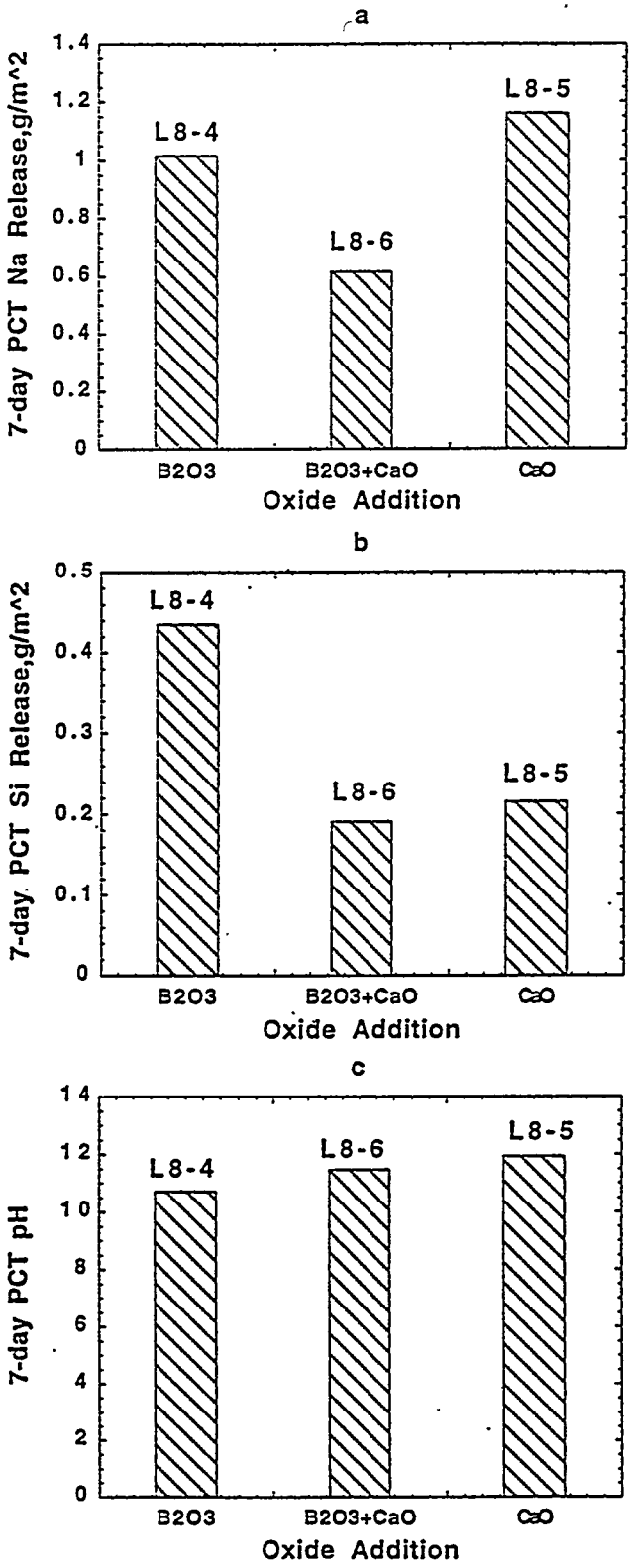

Figure 3.11. 7-Day PCT Results. 6 wt% of Fe_2O_3 addition to a base glass with SiO_2 56.78, Na_2O 20.0, Al_2O_3 9.0, but with different amounts of CaO and B_2O_3.

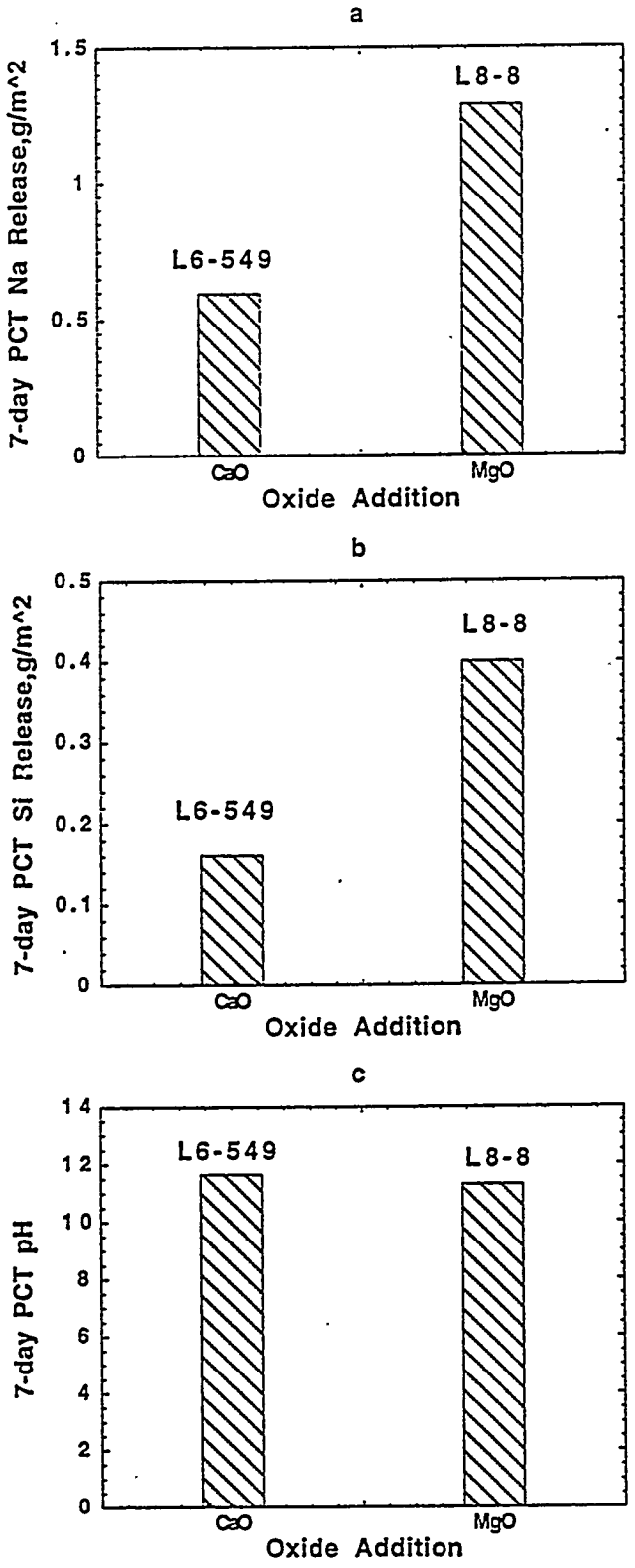

Figure 3.12. 7-Day PCT Results. Comparison of effects of 4 wt% addition of CaO with MgO in a glass with SiO_2 58.9, B_2O_3 5.0, Na_2O 20.0, and Al_2O_3 9.0.

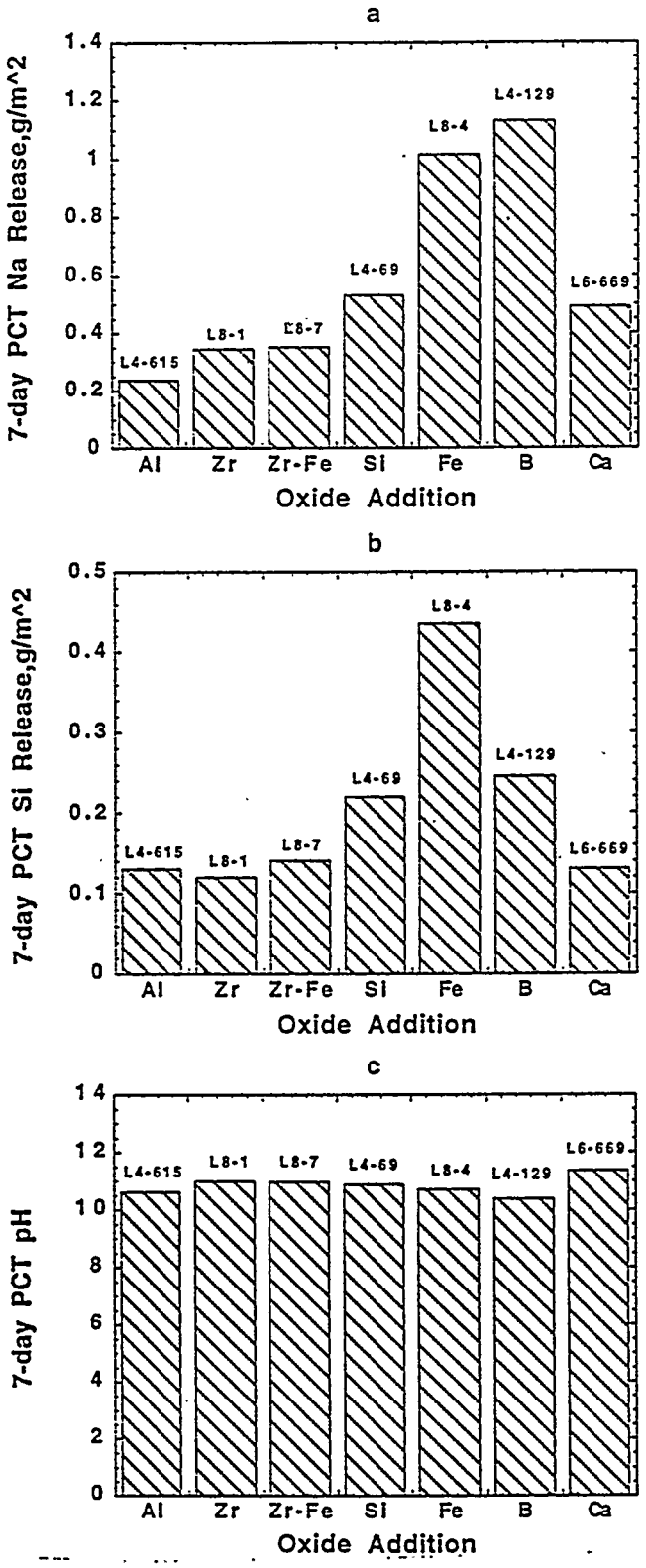

Figure 3.13. 7-Day PCT Results. 6 wt% addition to a base glass with SiO_2 56.78, Na_2O 20.0, Al_2O_3 9.0, B_2O_3 6.0, others 2.22.

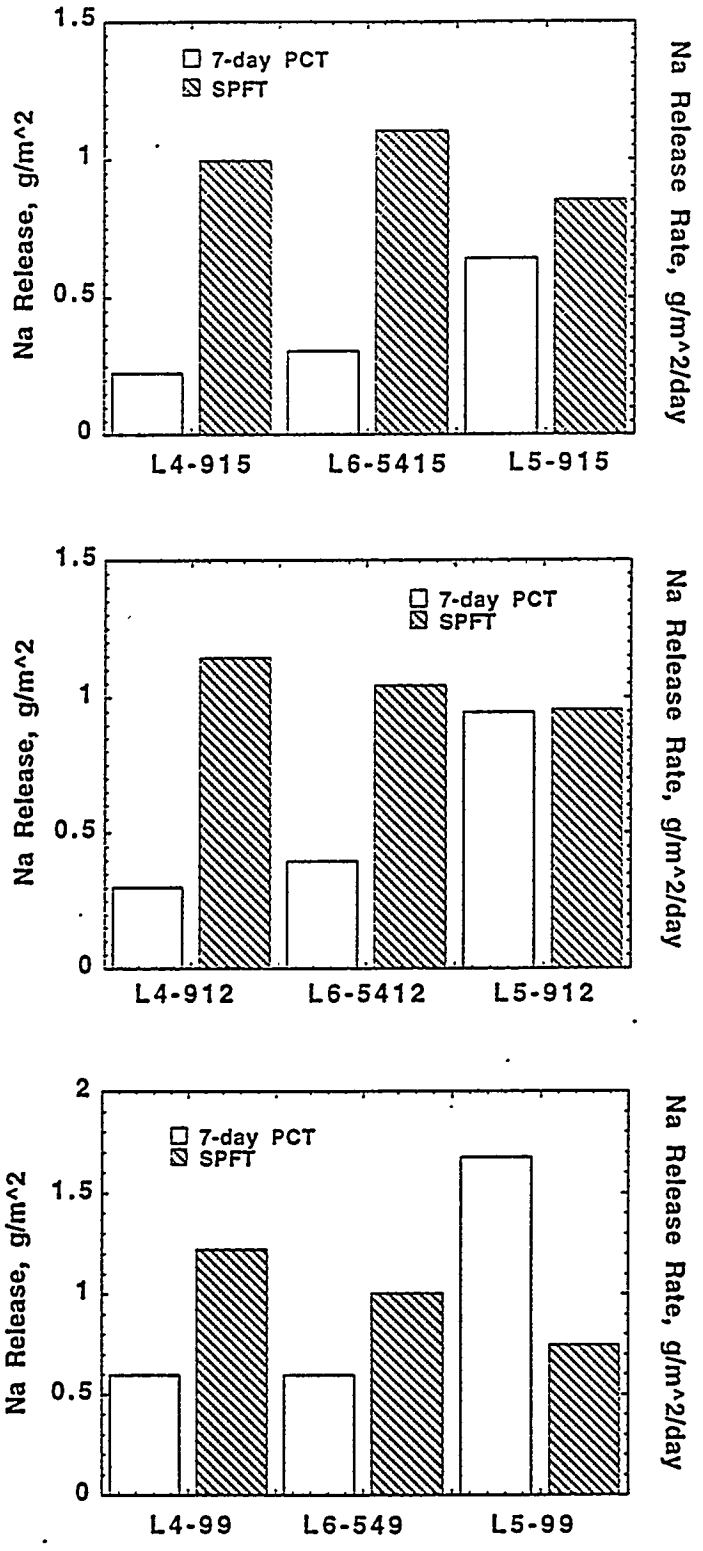

Figure 3.14. Comparison of Durability Using PCT (90°C) vs. Single-Pass Flow-Through (SPFT) Test (at 90°C and pH = 12.0)

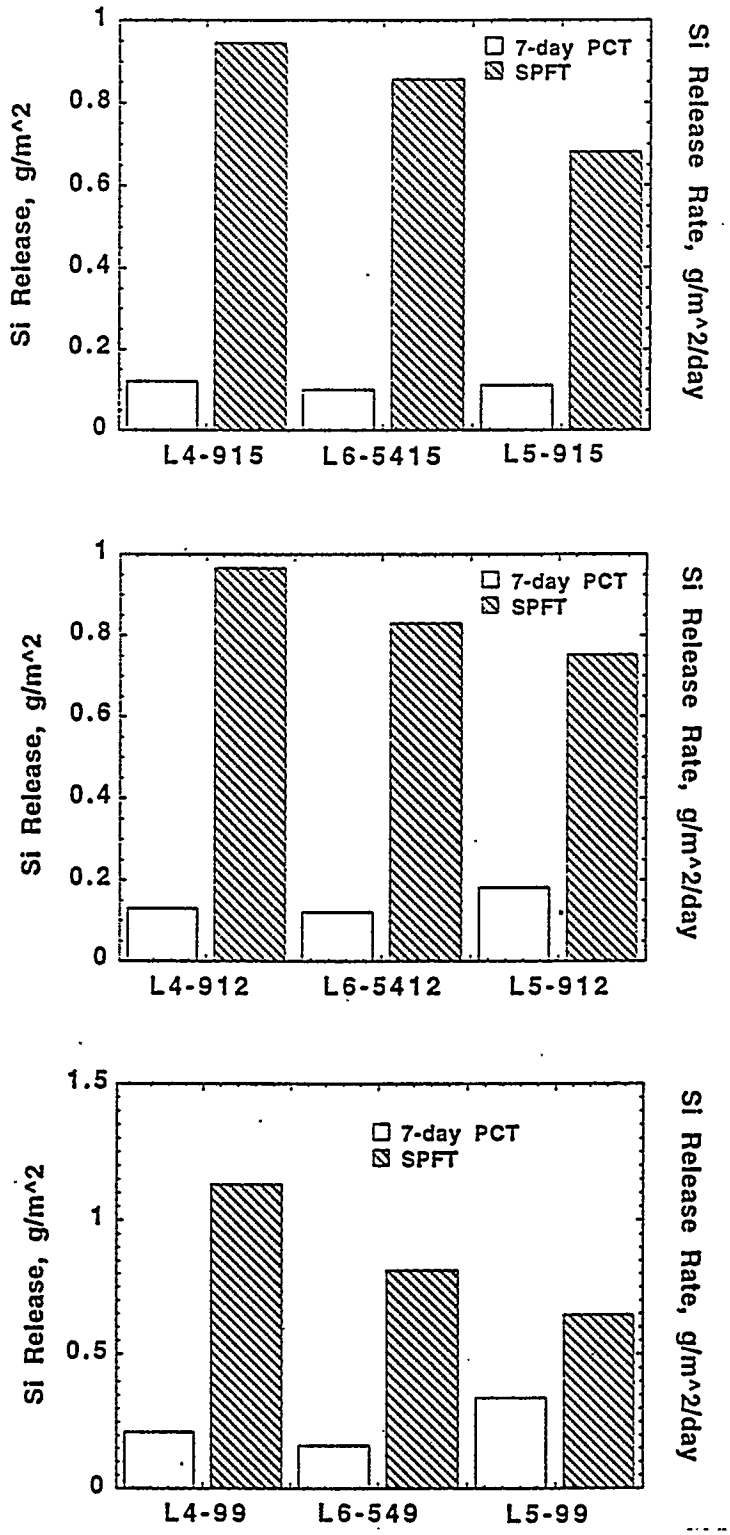

Figure 3.15. Comparison of Durability Using PCT (90°C) vs. Single-Pass Flow-Through (SPFT) Test (at 90°C and pH = 12.0)

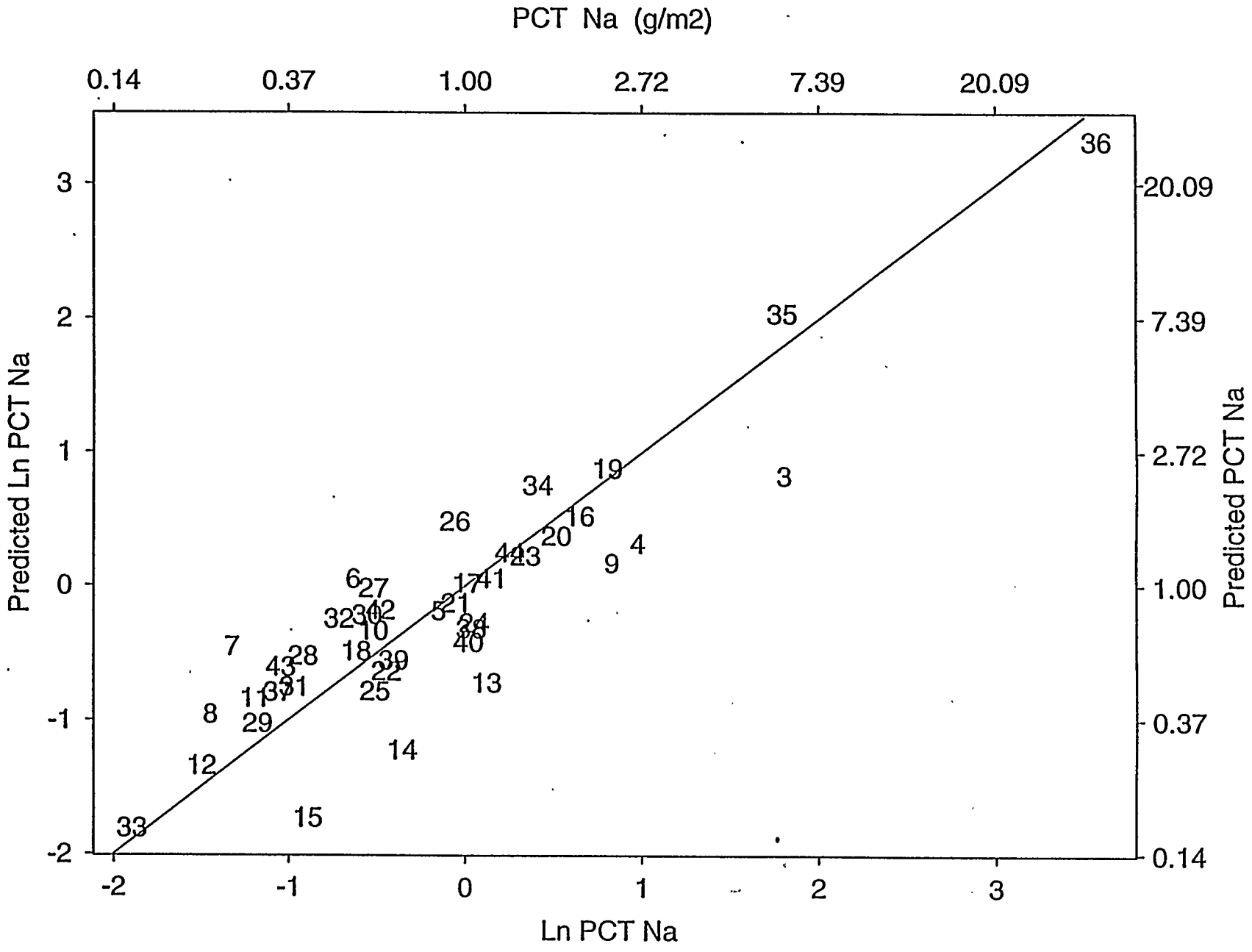

Figure 3.16. Predicted vs. Measured PCT Na Release for the First-Order Mixture Model

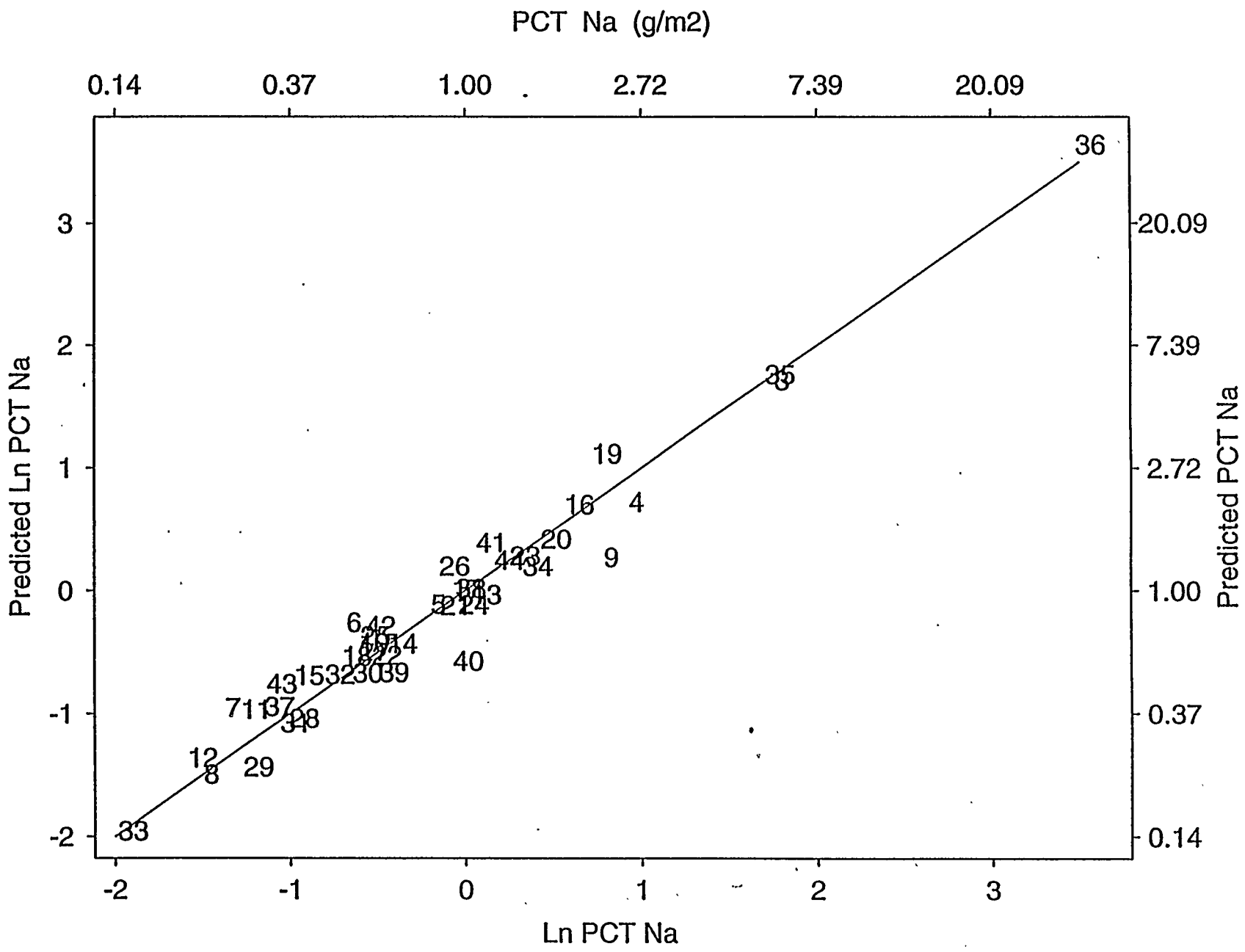

Figure 3.17. Predicted vs. Measured PCT Na Release for the Second-Order Mixture Model

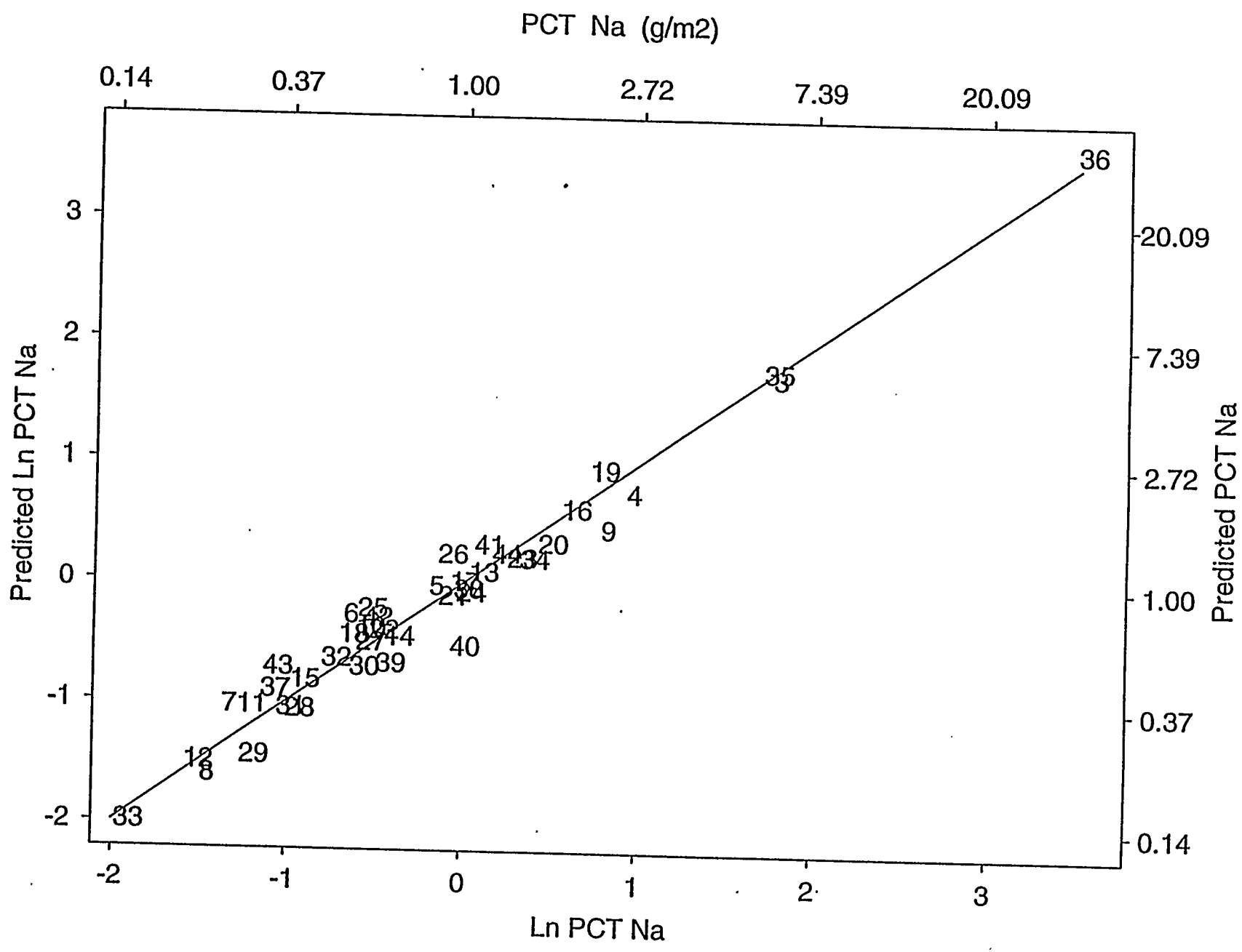

Figure 3.18. Predicted vs. Measured PCT Na Release for the Third-Order Mixture Model

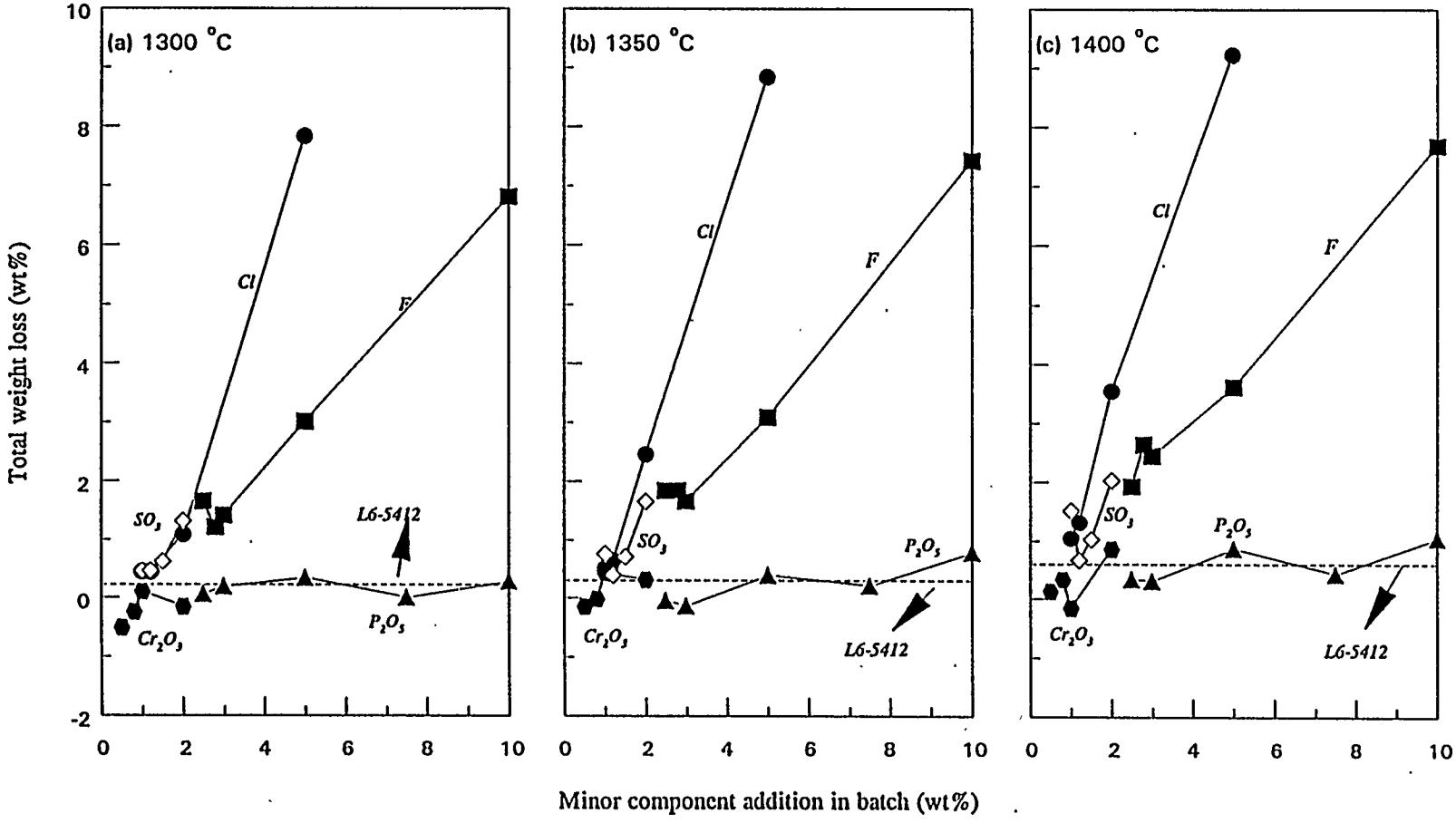

Figure 3.19. Weight Loss of L6-5412 Glasses with Addition of Minor Components at Various Glass-Processing Temperatures (2 h)

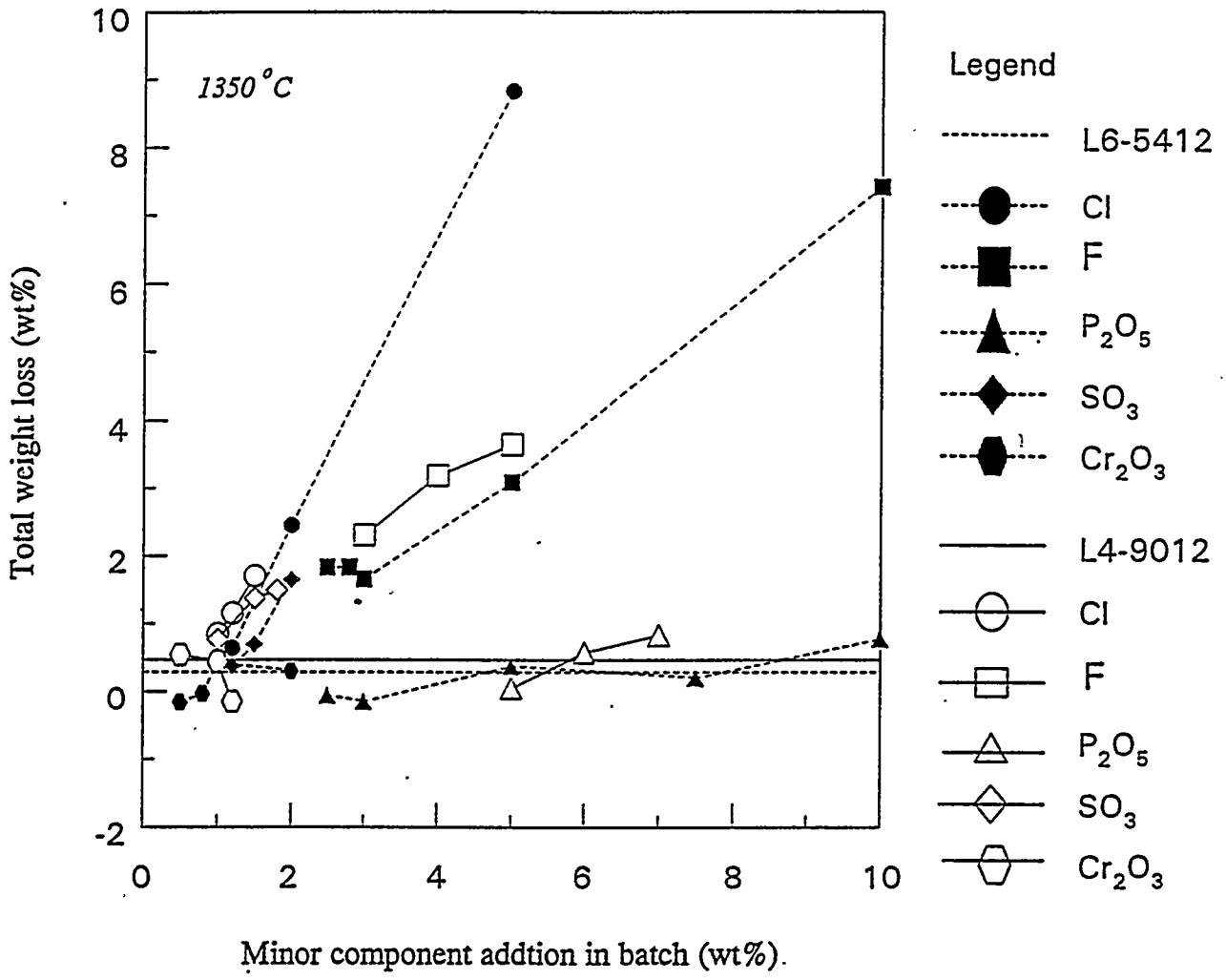

Figure 3.20. Comparison of Weight Losses Between L6-5412 and L4-9012 Glass Melts at 1350°C (2 h)

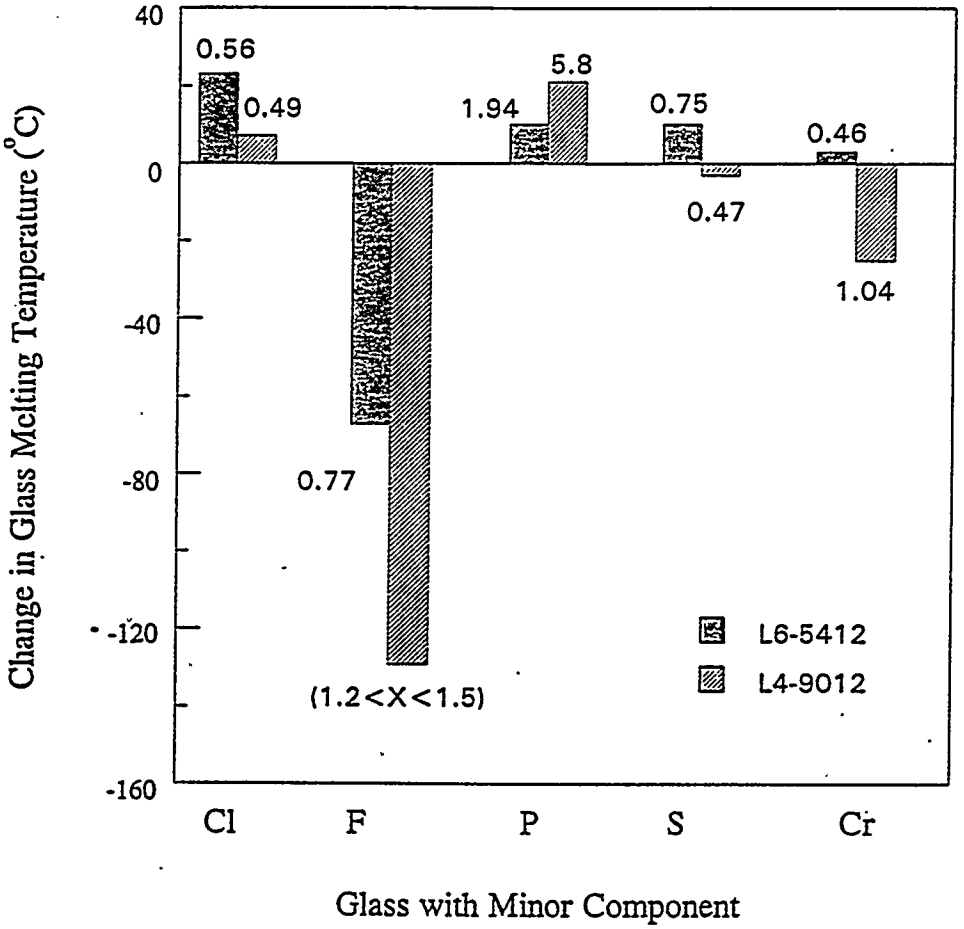

Figure 3.21. Effects of Minor Components on Glass Melting Temperature. (Numbers on the figure represent minor component concentration in glass, wt%.)

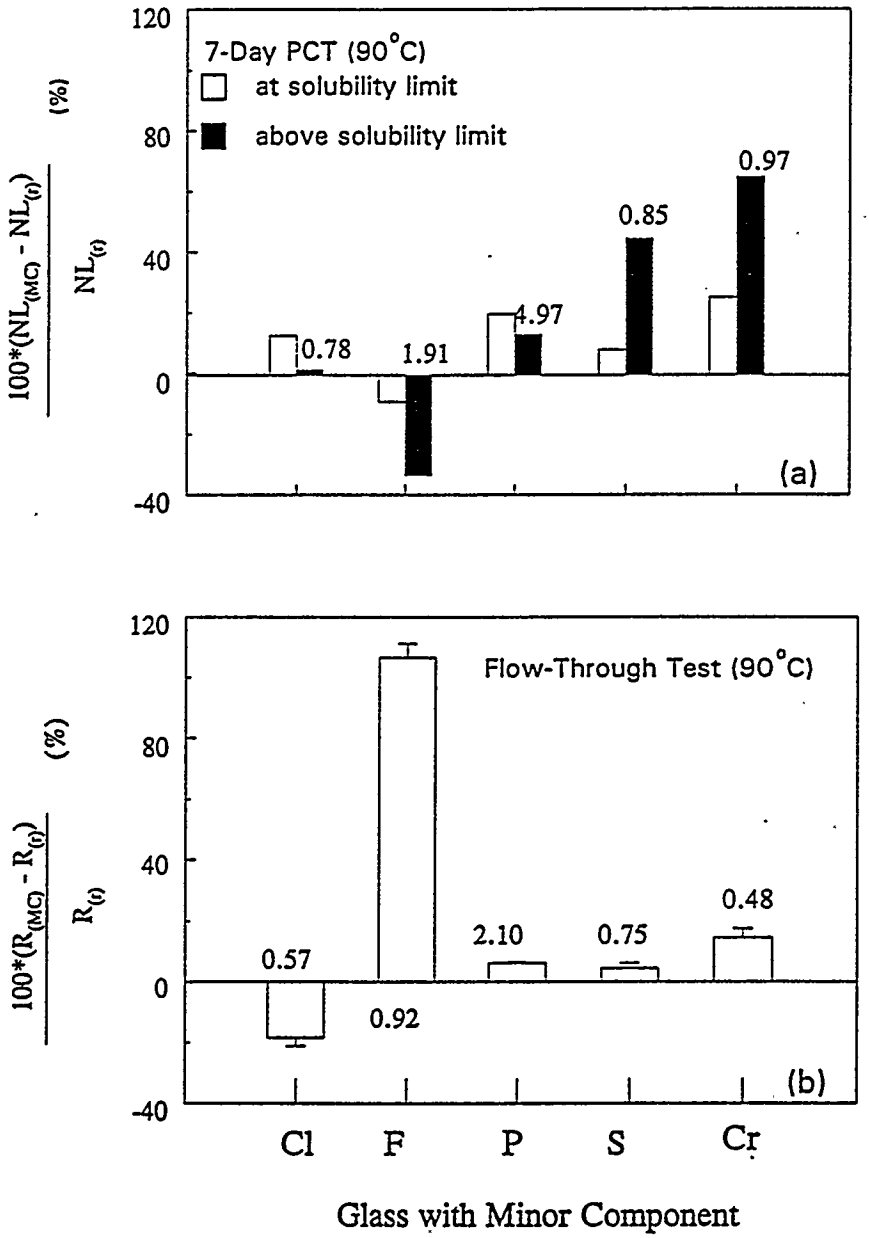

Figure 3.22. Chemical Durability of L6-5412 Glass with Additions of Minor Components, Which are Evaluated in Terms of (a) Amount of Na Release Using 7-Day PCT, and (b) Rate of Na Release Using Flow-Through Test (r and MC Refer to Glasses Without and With Spiking Minor Components). Numbers on the figures represent minor components concentrations in glass.

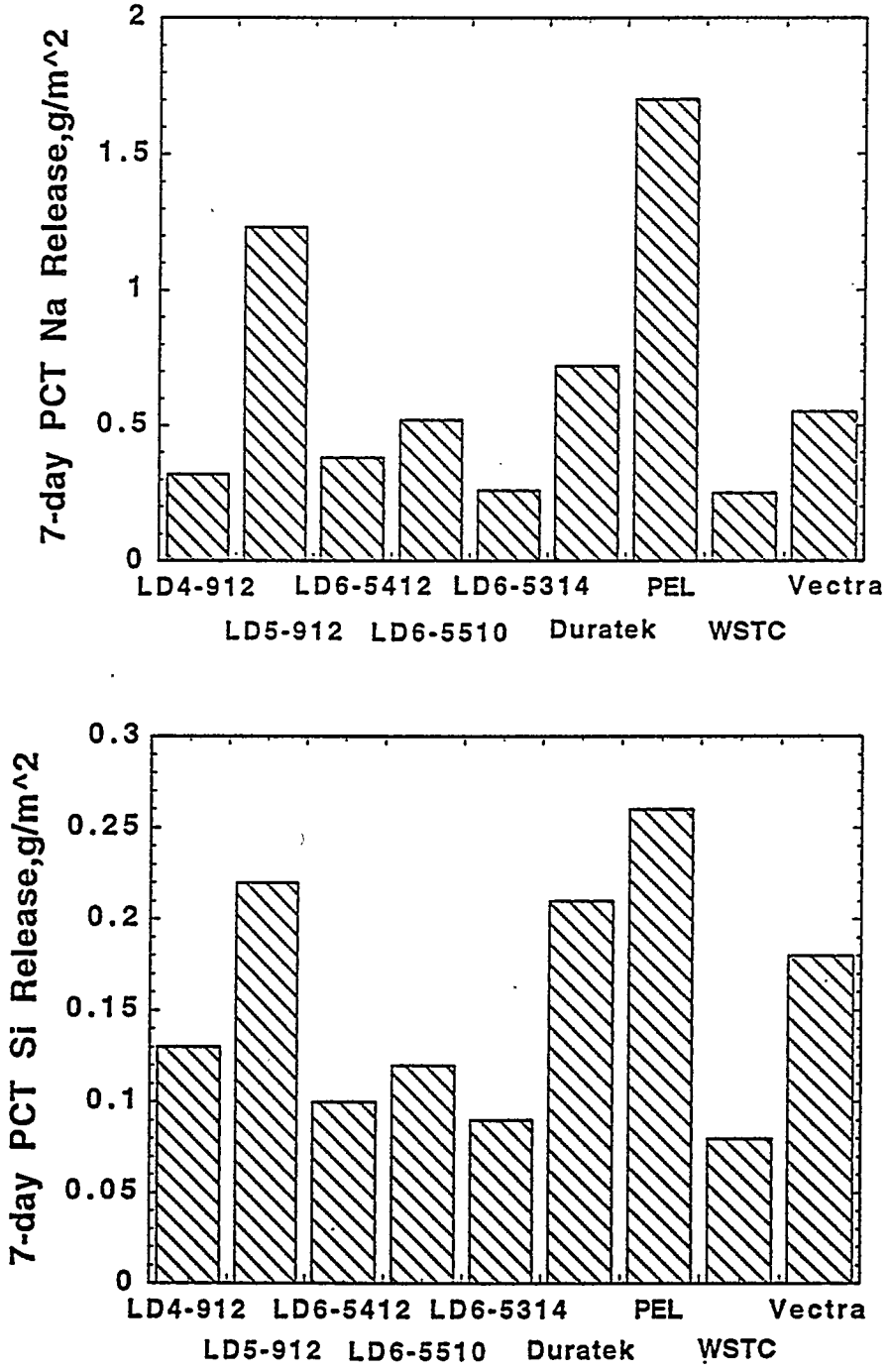

Figure 3.23. 7-Day PCT Results for Phase I Vendor Glasses Using DSSF Wastes

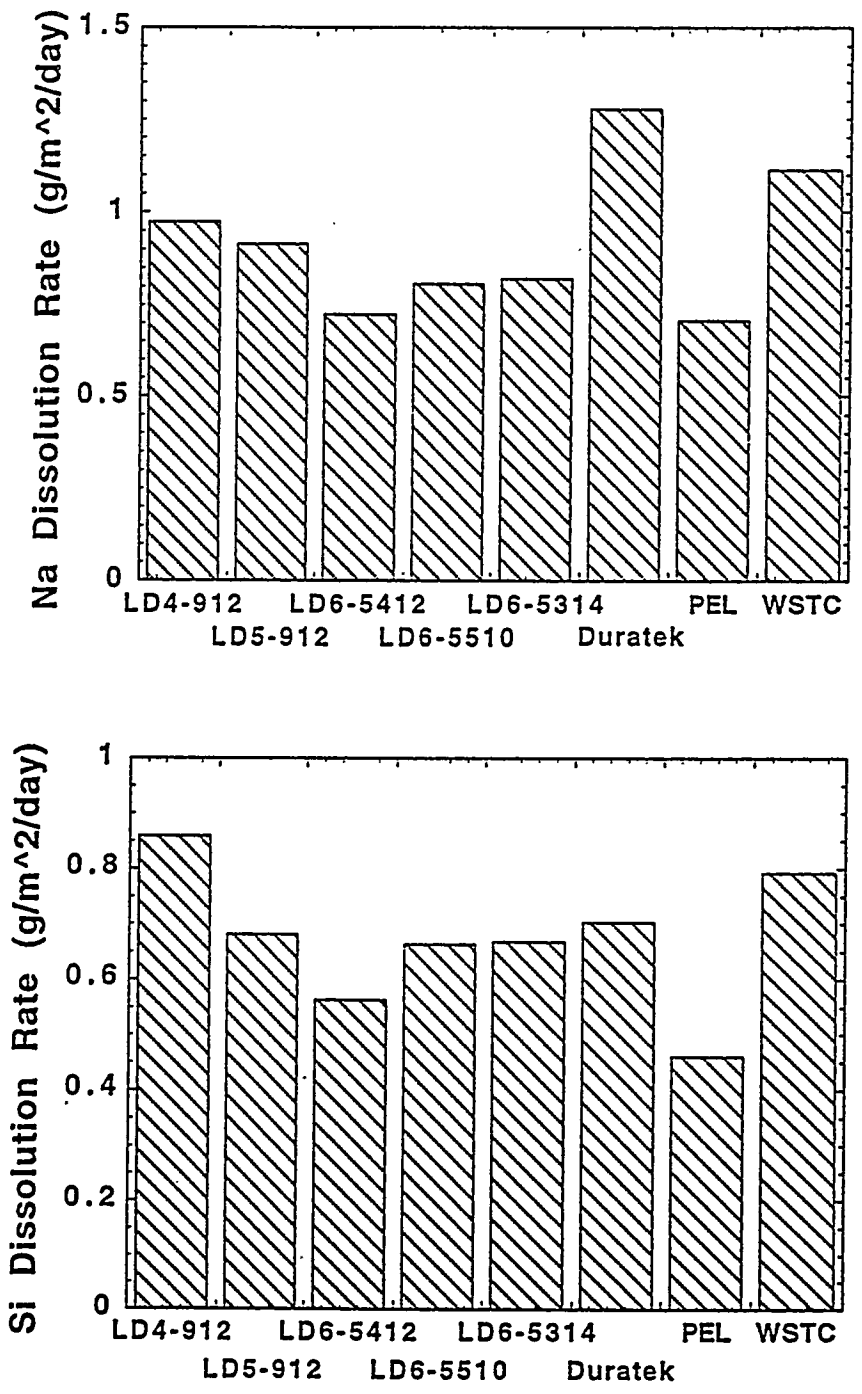

Figure 3.24. Single-Pass Flow-Through Results for Phase I Vendor Glasses Using DSSF Wastes

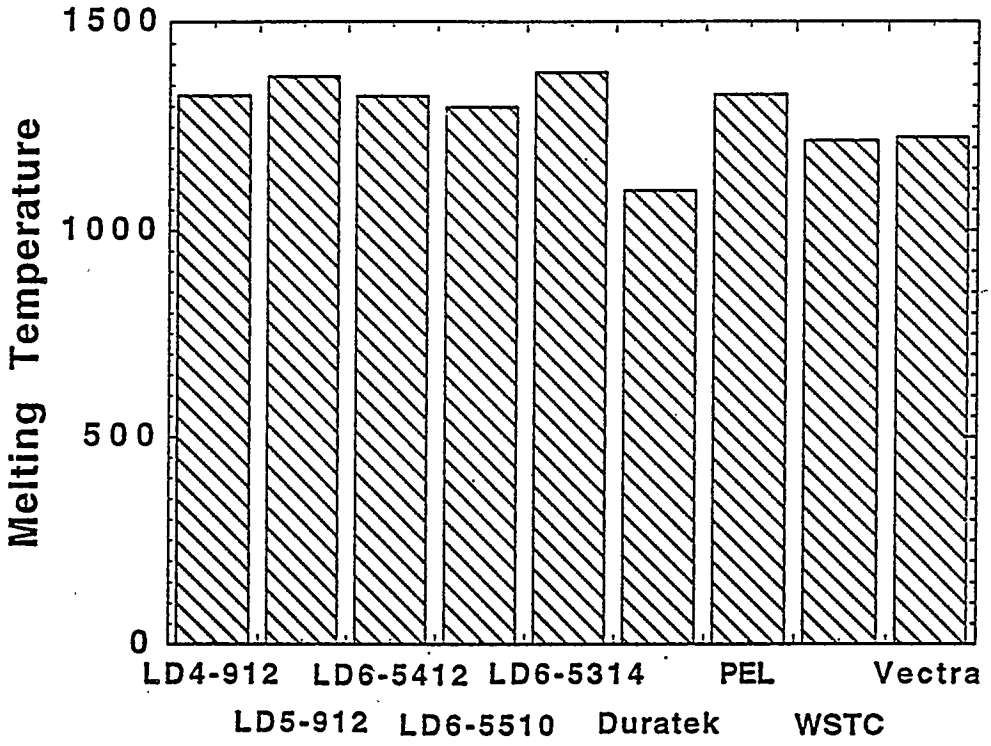

Figure 3.25. Melting Temperatures at 10 Pa•s for Phase I Vendor Glasses Using DSSF Wastes

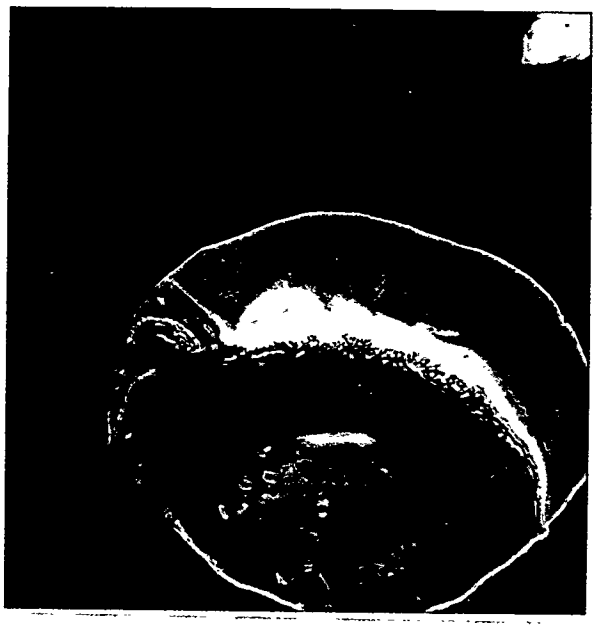

a

b

Figure 3.26. LRM-1 was Melted for (a) the First Hour at 1345°C and (b) for the Second Hour at 1345°C

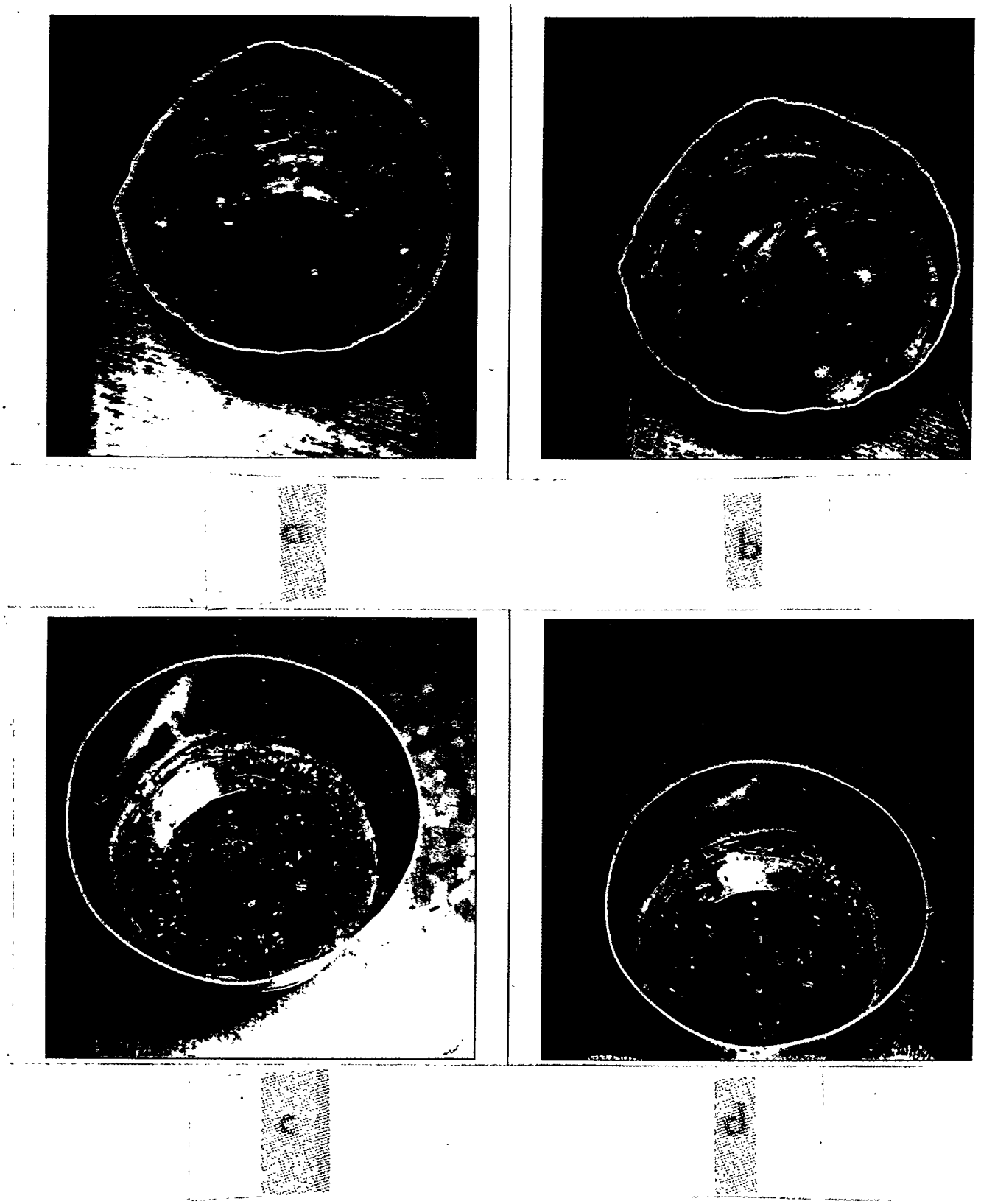

Figure 3.27. LRM-0912 was Melted at 1375°C: (a) for 30 min During the First Melting; (b) for 60 min During the First Melting; (c) for 60 min During the Second Melting, 15 min After Cooling; (d) for 60 min, During the Second Melting, Immediately out of Oven

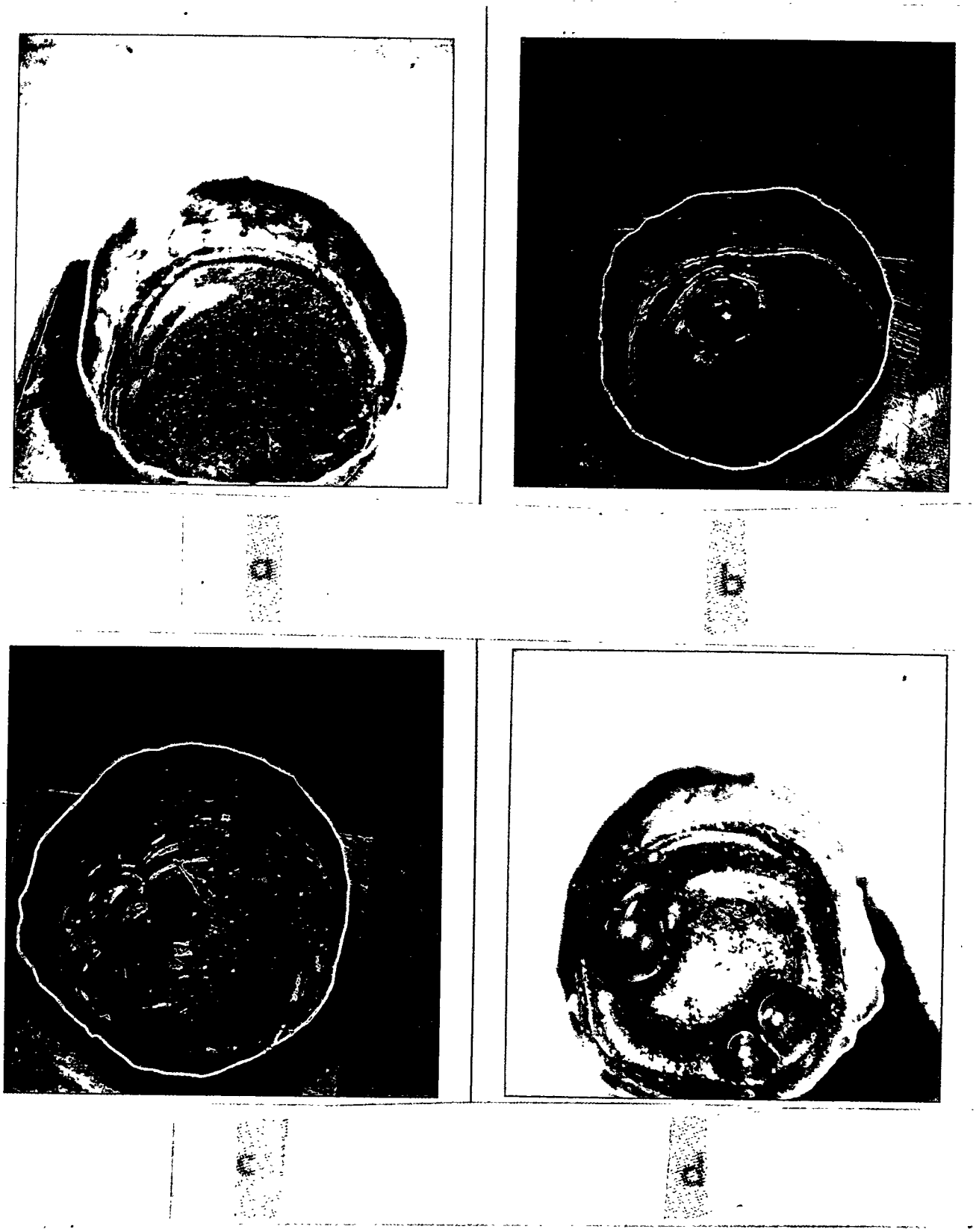

Figure 3.28. LRM-2 was Melted at 1360°C: (a) for 30 min During the First Melting; (b) for 60 min During the First Melting; (c) for 30 min During the Second Melting; and (d) for 60 min During the Second Melting

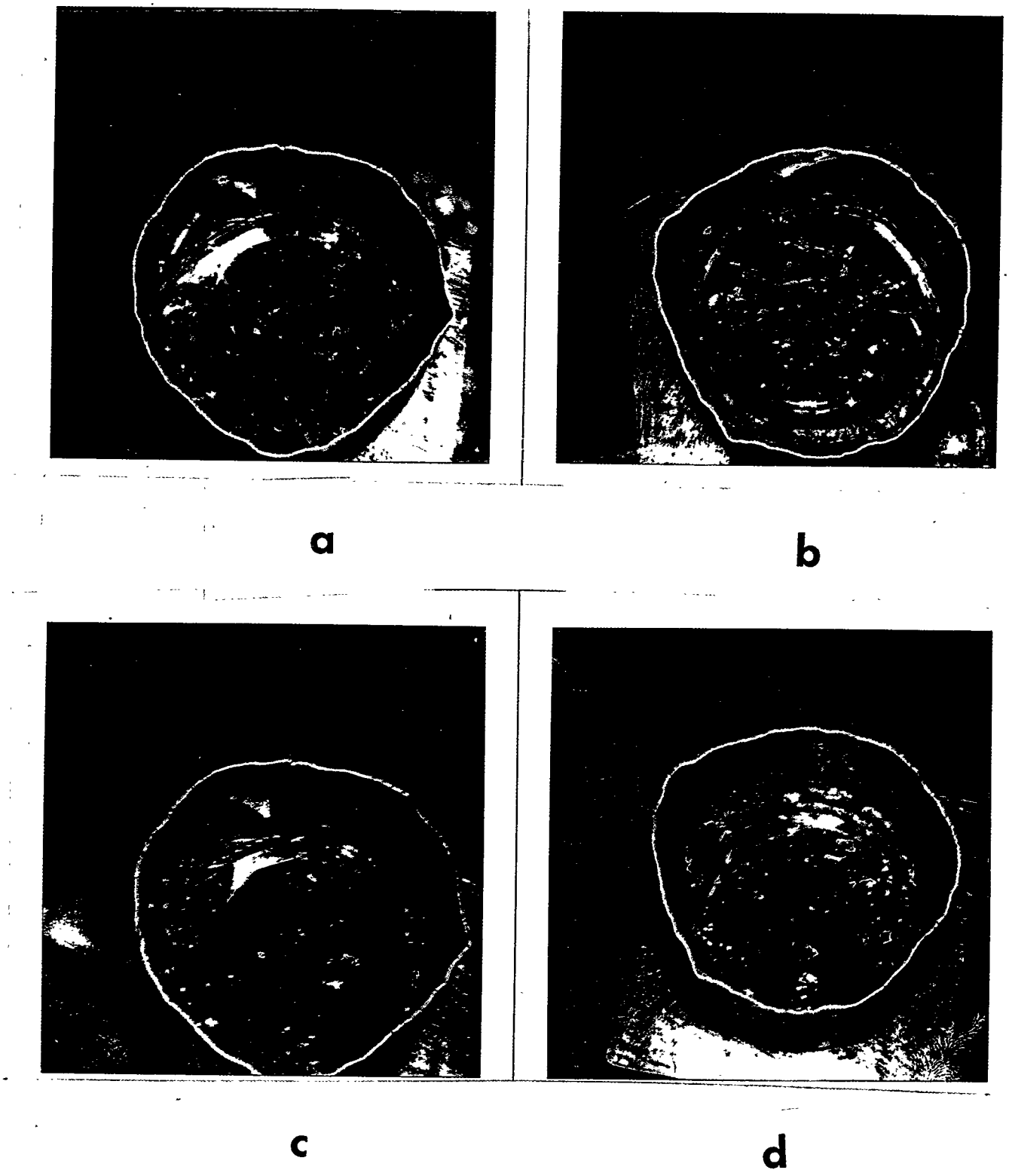

Figure 3.29. LRM-3 was melted at 1444°C: (a) for 30 min During the First Melting; (b) for 60 min During the First Melting; (c) for 30 min During the Second Melting; and (d) for 60 min During the Second Melting

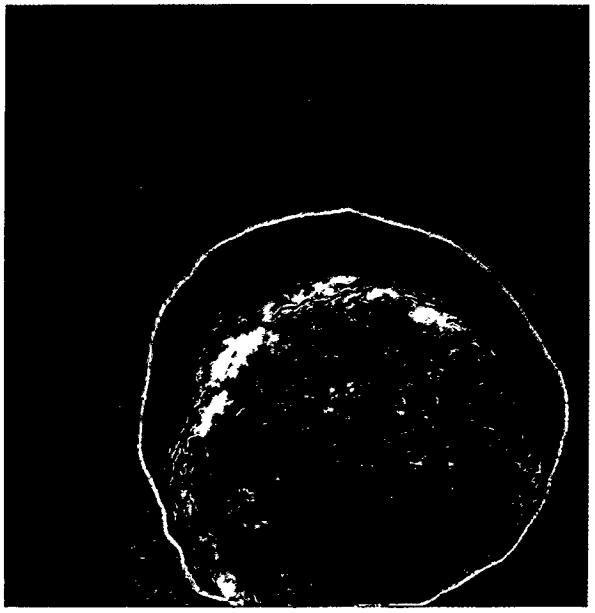

a

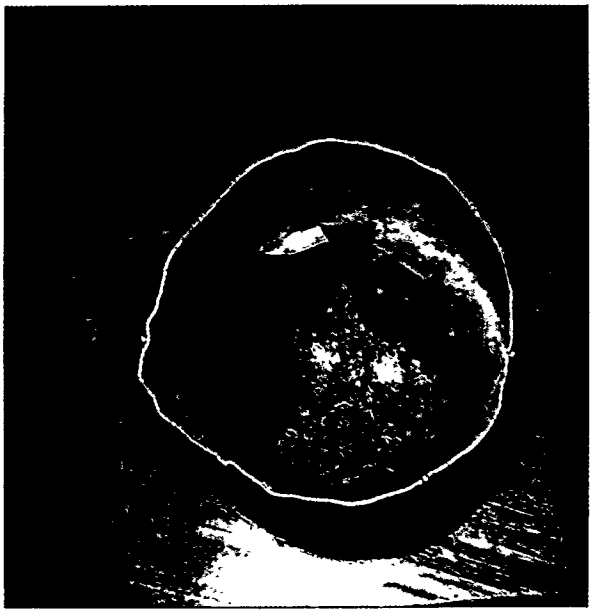

b

c

Figure 3.30. LRM-4 was melted at 1140°C: (a) for 30 min During the First Melting; (b) for 60 min During the First Melting; and for 60 min During the Second Melting

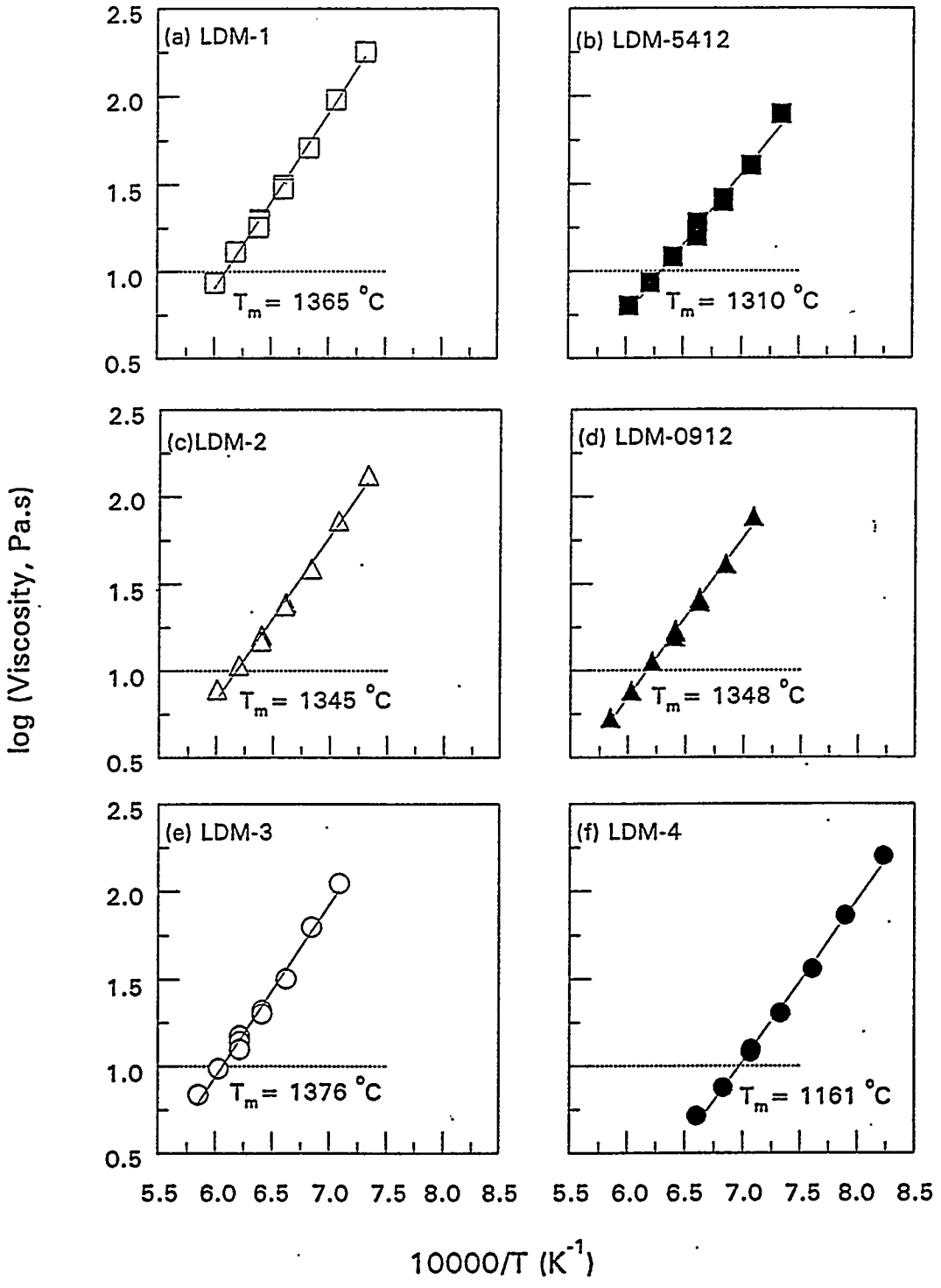

Figure 3.31. Viscosity Measurements and 10 Pa•s Temperature (T_m) for: (a) LDM-1; (b) LDM-5412; (c) LDM-2; (d) LDM-0912; (e) LDM-3; and (f) LDM-4

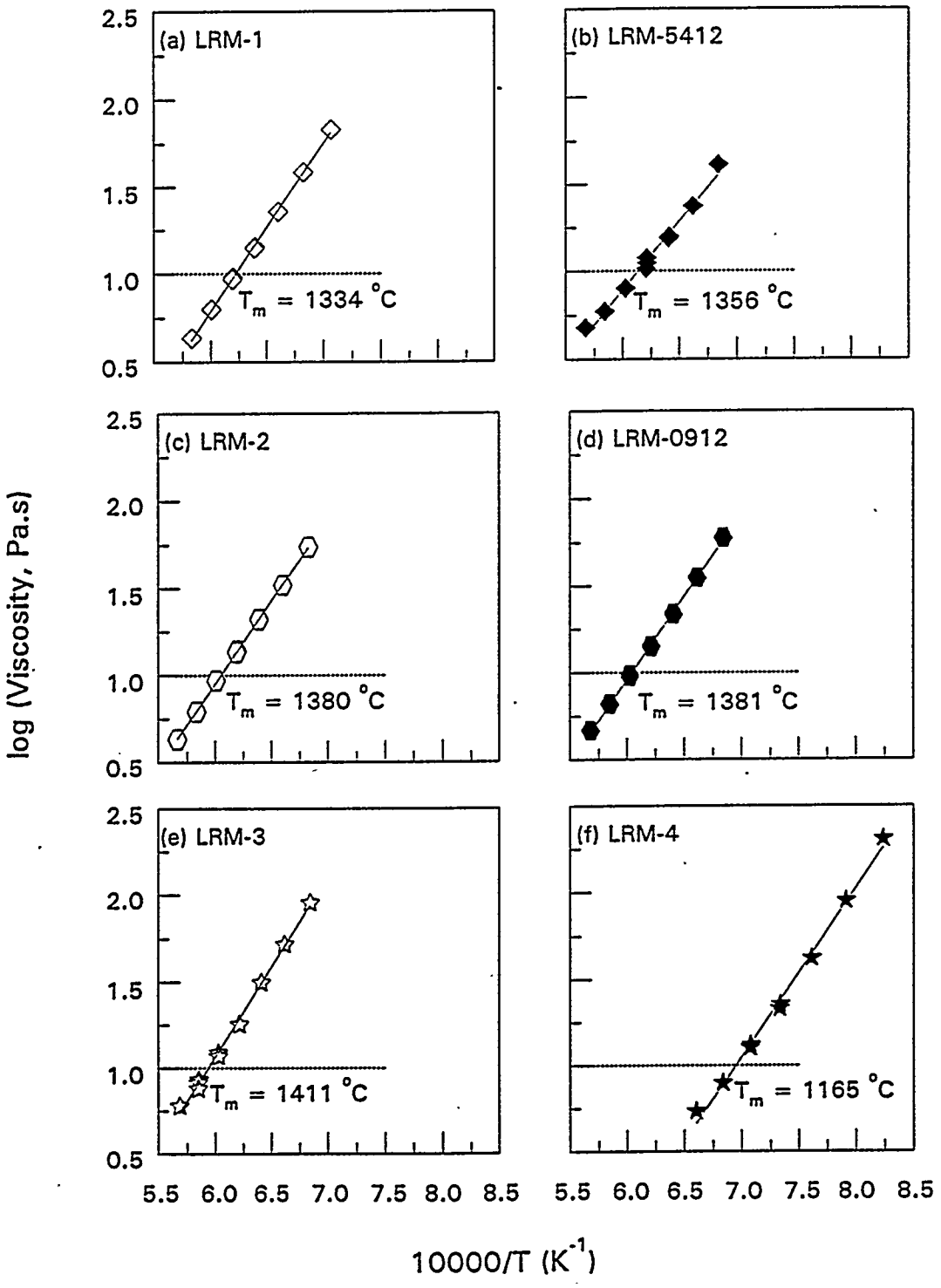

Figure 3.32. Viscosity Measurements and 10 Pa•s Temperature (T_m) for: (a) LRM-1; (b) LRM-5412; (c) LRM-2; (d) LRM-0912; (e) LRM-3; and (f) LRM-4

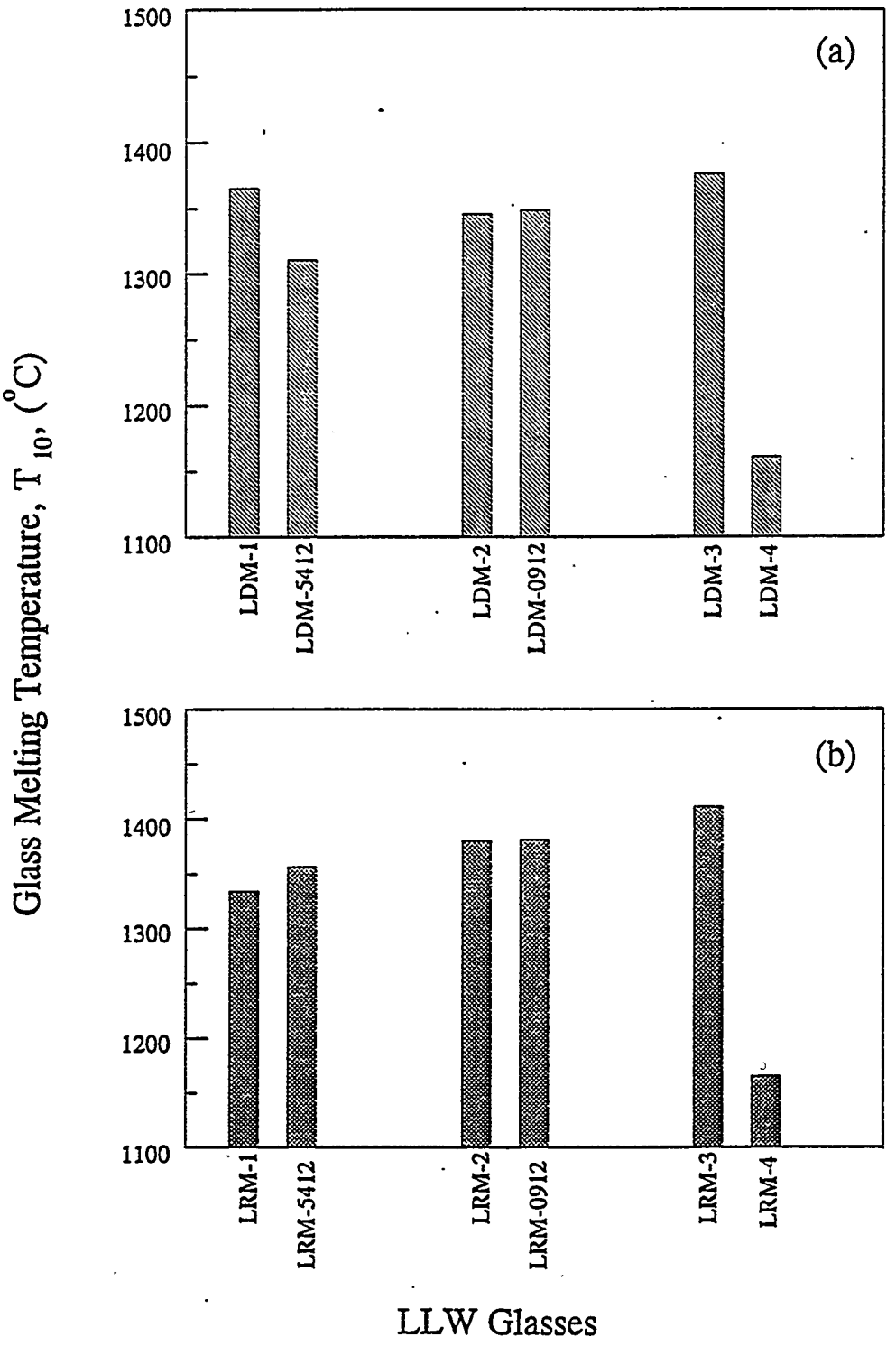

Figure 3.33. Comparison of Melting Temperature at 10 Pa•s Between (a) LDM Glasses and (b) LRM Glasses

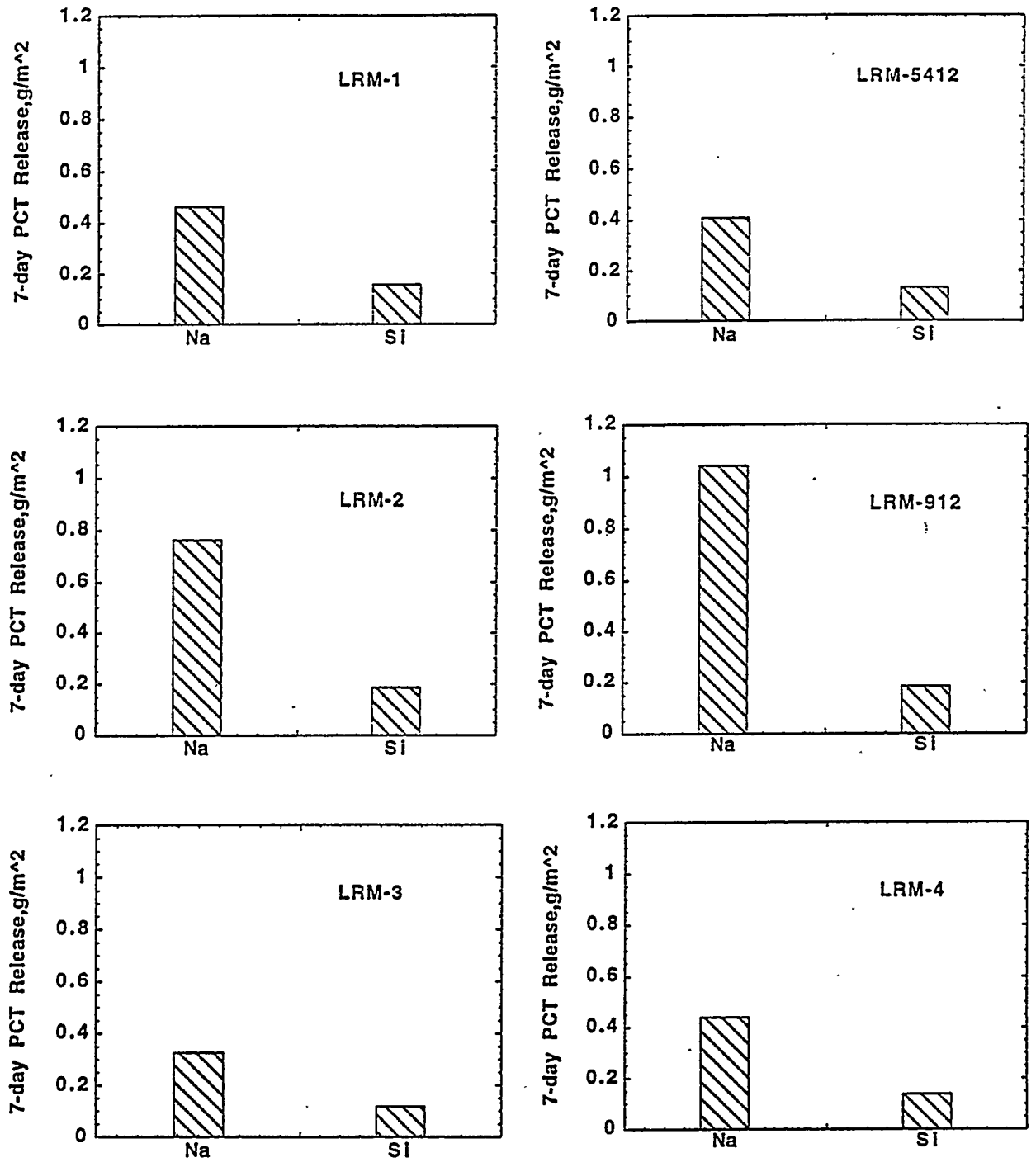

Figure 3.34. 7-Day PCT Results. Vendor glasses using M-DSSF wastes.

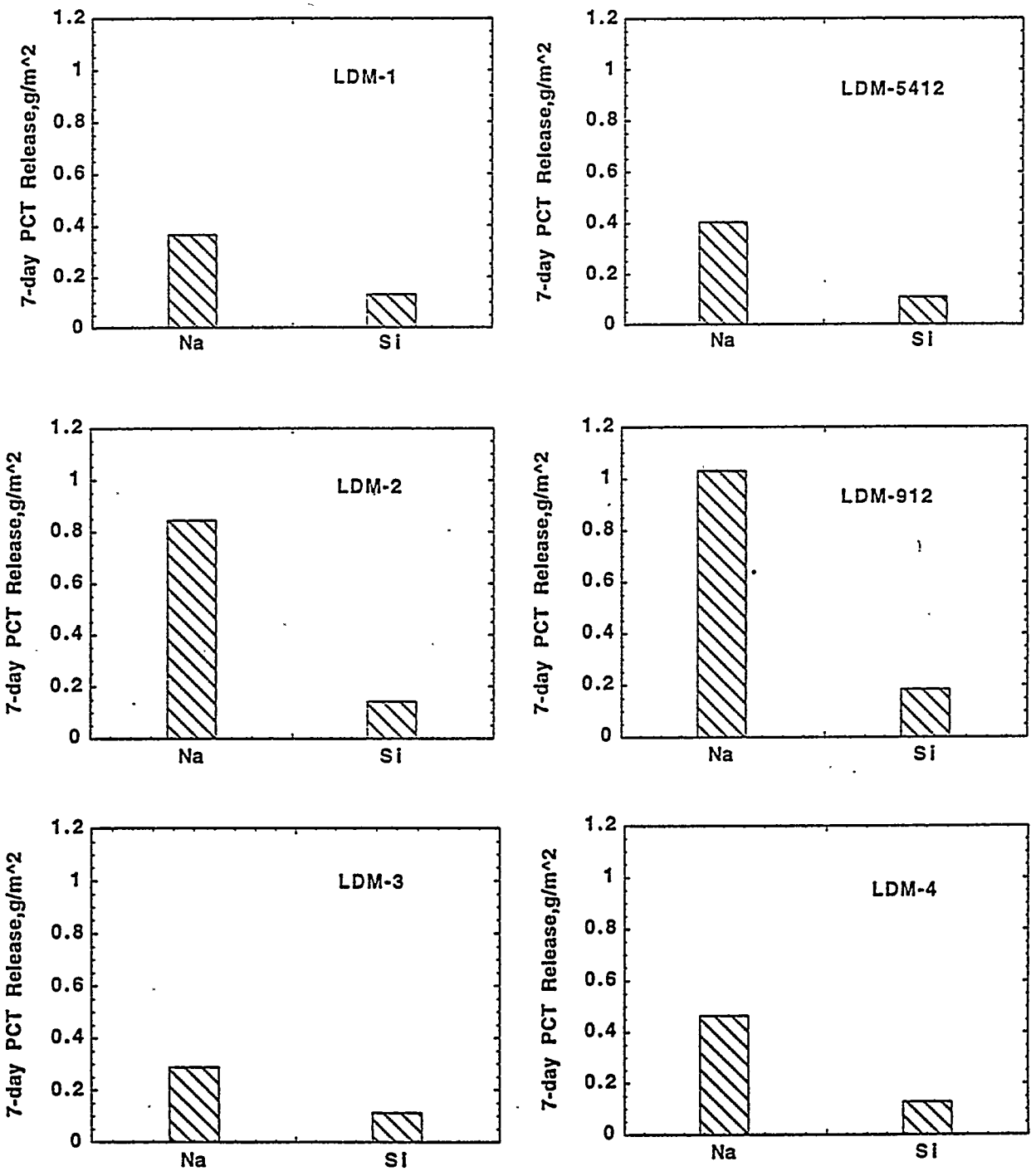

Figure 3.35. 7-Day PCT Results. Vendor glasses using M-RI wastes.

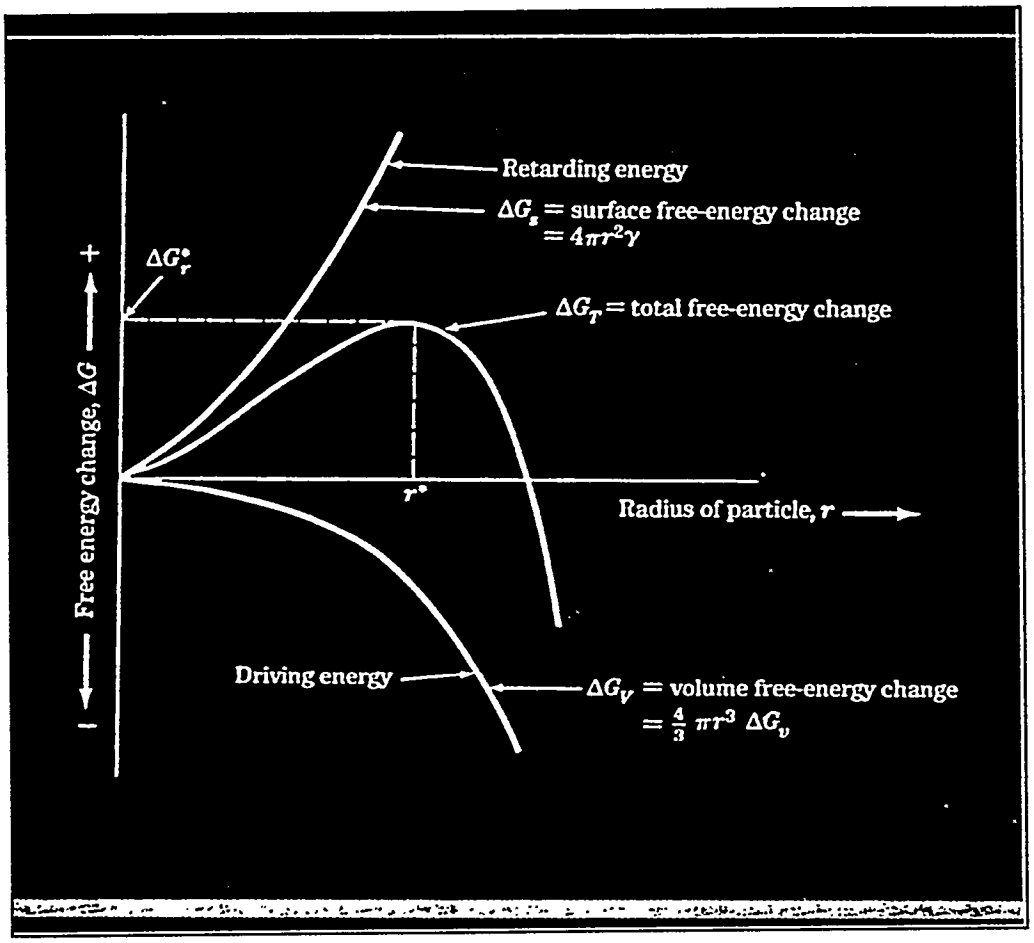

Figure 3.36. Schematic Representation of Energy Barrier for Homogeneous Nucleation

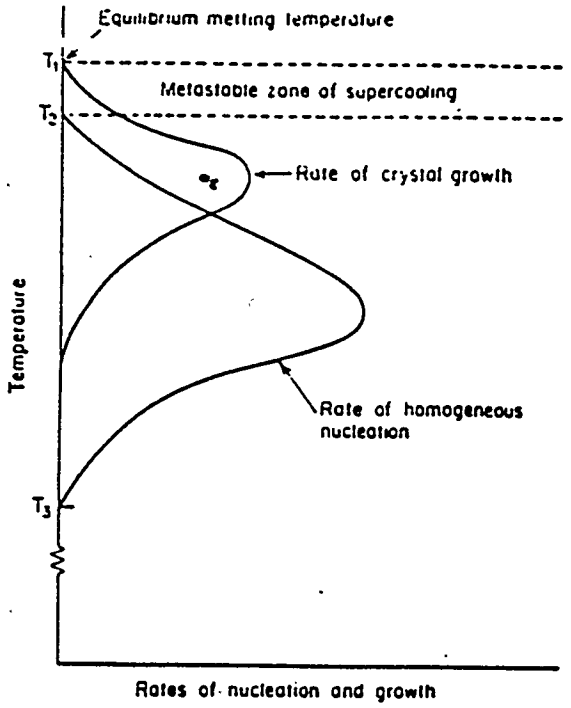

Figure 3.37. Temperature Dependence of Nucleation and Growth for a Simple (Homogeneously Nucleated) Glass System

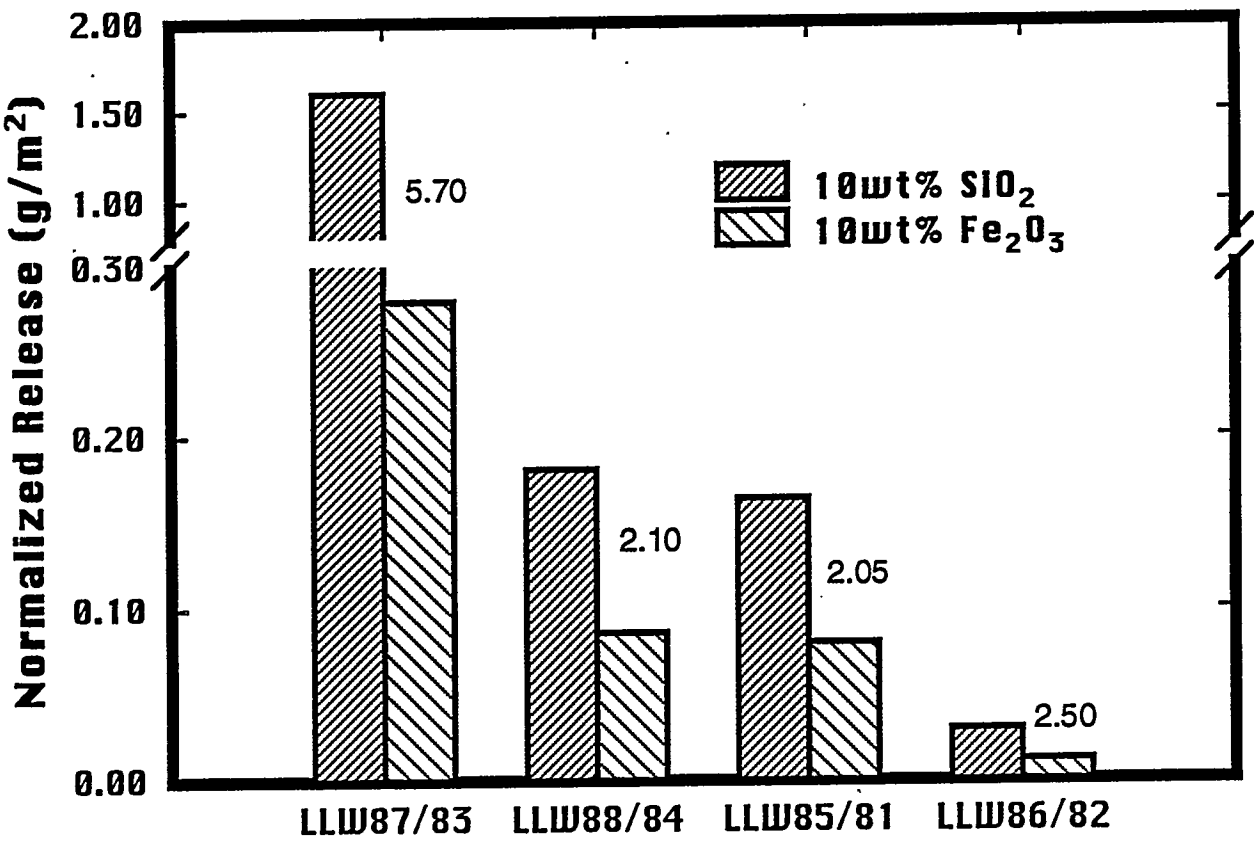

Figure 3.38. The Effect of Fe_2O_3 Replacing 10 wt% SiO_2 in Each Pair. Na_2O and Al_2O_3 are kept constant for the pairs compared. Numbers indicate leaching ratio.

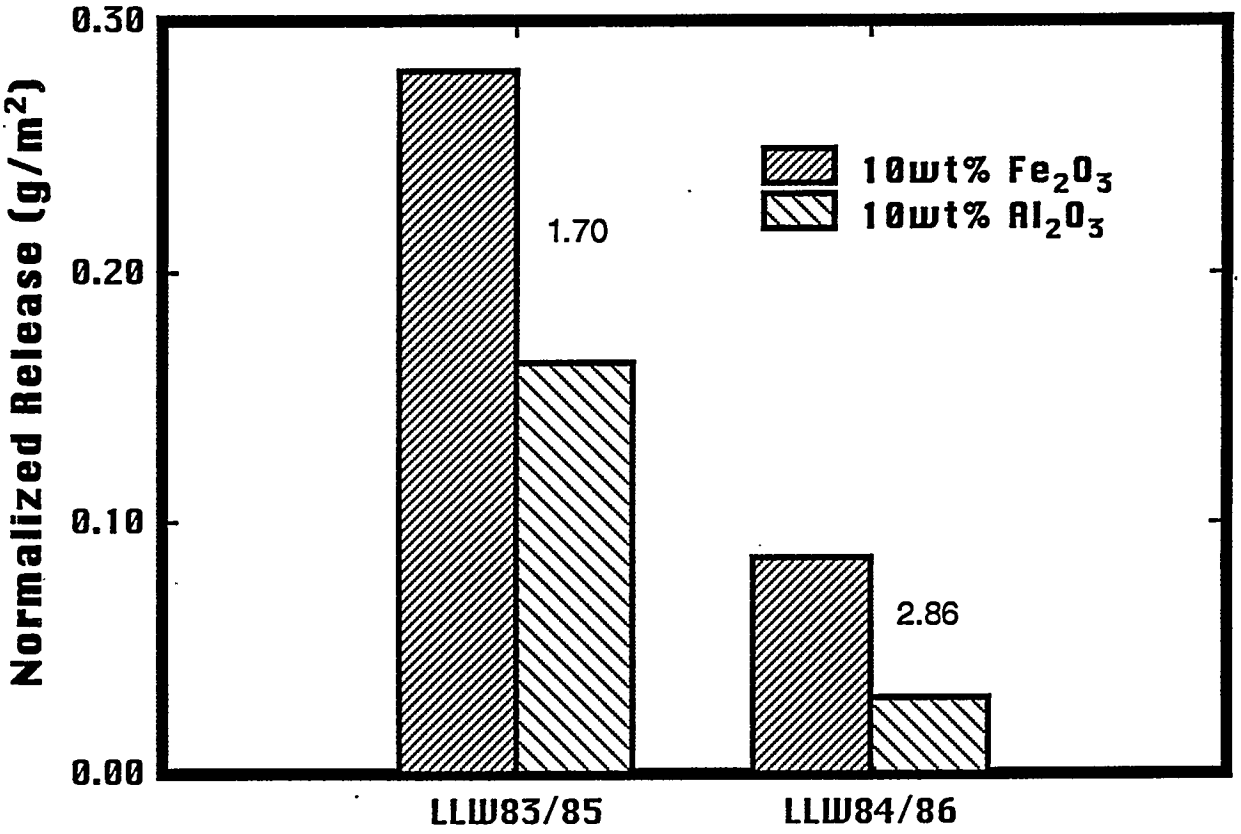

Figure 3.39. The Effect of Al_2O_3 Replacing 10 wt% Fe_2O_3 in Each Pair. Na_2O and SiO_2 are kept constant for the pairs compared. Numbers indicate leaching ratio.

4.0 Conclusions and Recommendations

The improvement on glass durability by the addition of similar amounts of oxides follows an order of $Al_2O_3 > ZrO_2 > SiO_2 > Fe_2O_3 > B_2O_3 > CaO$ for certain glasses. The composition effects on durability are composition-dependent, i.e., the effects of the added oxides depend on the concentrations of other components in the glass. The composition effects are nonlinear, i.e., the extent of improvement is not the same with equal amounts of addition. The effect is also inconsistent, i.e., the addition of an oxide can improve glass durability for one glass and can also decrease the durability of another glass. There is a need to understand these nonlinear and inconsistent composition effects on glass chemistry and glass structure. Boron-only glasses are more durable than calcium-only glasses, especially in terms of long-term durability such as vapor hydration test results. Zr-containing glasses are expected to have better long-term chemical durabilities in comparison with high-alumina formulations. Boron improves glass durability while the concentration is in the region of about 6 wt% or less in the LLW glasses investigated, but promotes volatility of the melts. Fe-containing glasses are expected to have good chemical durability while maintaining low melting temperatures; iron oxide can be considered as a good replacement for B_2O_3 without the volatility of boron. However, the benefit of iron oxide on chemical durability can only be realized under oxidizing conditions and with free alkalis to which Fe_2O_3 can bind. These results and structural chemistry considerations suggest that PCT and MCC-1 Na releases can be minimized by optimizing glass composition. However, LLW glass formulation must also comply with other requirements, such as the capability of glass to incorporate troublesome components (SO_3, P_2O_5, F, Cl, Cr_2O_3, etc.). Moreover, the effect of possible devitrification on durability must be taken into account. Finally, information from the long-term testing, vapor hydration studies, and flow-through dissolution data must be considered with respect to the relevance for the glass long-term performance.

The dependency of solubilities of minor components S, P, Cl, and F on temperature is negligible, but is significant on glass compositions. Volatilities of molten glass with the addition of F, Cl, S, and P can be significant once the minor components are in excess of their solubilities, which were in the order: $Cl > SO_3 \geq F$. Higher B_2O_3 content in glass further enhanced their volatilities.

Two types of phase segregation were observed among these minor components. For glasses oversaturated with Cl or SO_3, phase segregation initiated in the melt and then accumulated on the melt surface, which occurred at glass-processing temperature. For glasses oversaturated with F, P_2O_5 and Cr_2O_3, no phase segregation was observed on the melt surface, and crystallization occurred only in the melt. Chlorine and phosphate were found to increase glass melt viscosity, while fluorine had a pronounced opposite effect. SO_3, P_2O_5, and Cr_2O_3 decreased glass durability. F appeared to improve PCT durability by lowering solution pH, but decreased glass durability in the single-pass flow-through test.

Phase II glass formulations were developed that can accommodate 2.5 wt% P_2O_5 and 1.0 wt% SO_3, which are expected to be the highest possible concentrations of Hanford Site LLW streams, without significant processing problems under laboratory crucible conditions. These Phase II compositions are also a factor of 6 to 23 more durable than EA glasses. These glasses melted satisfactorily in high temperature ranges from 1160° to 1410°C to suit different melting technologies. The compositions included boron-free glasses for those melters that prefer low-volatility formulations; boron-containing glasses for those melters that can reduce volatility through cold-caps and other

operations; Zr-containing glasses for those vendors producing glasses with long-term durability; and Fe-containing glasses for those melters operated under oxidizing conditions.

5.0 References

Alexander,MN and PIK Onorato, CW Struck, JR Rozen, GW Tasker, and DR Uhlmann, "Structure of Alkali (Alumino)silicate Glasses. I. Tl+ Luminescence and the Nonbridging Oxygen Issue," J. Non-Cryst. Solids 79, 137-154 (1986).

Bakel, AJ and WL Ebert. 1994. "Long-Term and Accelerated Testing of Candidate Waste Forms for Low-Level Hanford Waste for FY94," in *FY 1994 Annual Report*. Argonne National Laboratory, Argonne, Illinois.

Bates, JK, LJ Jardine, and MJ Steindler. 1982. *The Hydration Process of Nuclear Waste Glasses: An Interim Report.* Argonne National Laboratory Report ANL-82-11, Argonne, Illinois.

Bates, JK and WL Ebert. 1994. *Investigation Plan for Long-Term and Accelerated Testing of Candidate Waste Forms for Low-Level Hanford Waste.* PVTD-C94-21.01F, Pacific Northwest Laboratory, Richland, Washington.

Bobkova, NM, OG Gorodetstkaya, SA Yankovskaya, and ZS Tizhovka. 1983. "Structural role of zirconium in zirconium borosilicates and aluminosilicate glasses." *Fizikai Khimiya Stekla* **9**:414-419.

Crichton, SN, MF Savage and M Tomozawa. 1995. "Volatilization Rates of Troublesome Components from a Simulated Low-Level Nuclear Waste Glass." *International Symposium on the Environmental Issues and Waste Management Technologies in Ceramic and Nuclear Industry*, Cincinnati, Ohio.

Crichton, SN and M Tomozawa. 1995. "*Effects of Minor Components on Phase Separation of Simulated Nuclear Waste Glasses*," Annual Report to Battelle, Pacific Northwest Laboratory, under contract number 191893-A-F1, August 15, 1995.

Cunnane, JC, Ed.; JK Bates, CR Bradley, EC Buck, JC Cunnane, WL Ebert, X Feng, JJ Mazer, DJ Wronkiewicz, J Sproull, WL Bourcier, BP McGrail, and MK Altenhofen. 1994 *High-Level Waste Borosilicate Glass: A Compendium of Corrosion Characteristics*. Vol. 1-3, DOE-EM-0177, U.S. Department of Energy, Office of Waste Management, Washington, DC.

Darab, JG, H Li, DW Matson and PA Smith, 1995. "Chemical and Structural Elucidation of Minor Components i n Simulated Hanford Low-Level Waste Glasses," (Invited paper) *Applications of Synchrotron Radiation in Chemistry and Related Fields Symposium*, 201th American Chemical Society National Meeting, Chicago, IL (in press).

Dell, WJ, PJ Bray, and SZ Xiao, "^{11}BNMR Studies and Structural Modeling of Na_2O-B_2O_3-SiO_2 Glasses of High Soda Content," J. Non-Cryst. Solids **58**: 1-16 (1983)

Dickenson, MP and PC Hess, "The Structural Role and Homogeneous Redox Equilibria of Iron in Peraluminous, Metaluminous and Peralkaline Silicate Melts," Contrib. Mineral. Petrol. **92** :, 207-217 (1986).

Ellison, AJG, JJ Mazer, and WL Ebert. 1994. *Effects of Glass Composition on Waste Form Durability: A Critical Review.* Argonne National Laboratory Report, ANL-94/28, Argonne, Illinois.

Feng, X. 1988. *Composition Effects on Chemical Durability and Viscosity of Nuclear Waste Glasses—Systematic Studies and Structural Thermodynamic Models.* Ph.D. Dissertation, The Catholic University of America, Washington, DC.

Feng, X, IL Pegg, A Barkatt, PB Macedo, SJ Cucinell, and S Lai. 1989. "Correlation between Composition Effects on Glass Durability and the Structural Role of Constituent Oxides," *Nuclear Technology*, Vol. 85(3), 334-345.

Feng, X, DJ Wronkiewicz, JK Bates, NR Brown, EC Buck, NL Dietz, M Gong, and JW Emery. 1994. *Vitreous Ceramic for Minimum Additive Waste Stabilization, Interim Program Report, May 1993-February 1994.* Argonne National Laboratory Report ANL-94/24, Argonne, Illinois.

Feng, X., et. al. 1995. Evaluation of Phase II Glass Formulations for Vitrification of Hanford Site Low-level Waste. PVTD-T3B-95-206, Pacific Northwest Laboratory, Richland, WA 99352.

"Hanford Federal Facility Agreement and Consent Order," Washington State Department of Ecology, US Environmental Protection Agency, and US Department of Energy, Olympia, Washington (1993, as amended).

Holmquist, S. 1966. "Oxygen Ion Activity and the Solubility of Sulfur Trioxide in Sodium Silicate Melts." *J.Am.Ceram.Soc.* **49**:467-473.

Jantzen, CM, NE Bibler, DC Beam, WR Ramsey, and BJ Waters. 1992. *Nuclear Waste Glass Product Consistency Test (PCT), Ver. 5.0*, WSRC-TR-90-539, Rev. 2, Westinghouse Savannah River Company, Aiken, South Carolina.

Kielpinski, AL "Evaluation of DWPF Viscosity PRocessing Algorithm for Mixed Wastes: I. Alkali and Alkaline Earth Effects (U)," WRSC-TR-94-0264, 1994.

Kim, D. 1994. *Evaluation and Recommendation of Candidate Glass Systems for LLW Vitrification.* PVTD-C94-21.01C, Pacific Northwest Laboratory, Richland, Washington.

Kim, D., PR Hrma, and JH Westsik, Jr. 1995. Glass Formulation Strategy for LLW Vitrification. PVTD-C95-02.01AD, Pacific Northwest Laboratory, Richland, Washington.

Li, H., JD Darab, PA Smith and PR Hrma. 1995. "Effect of Minor Components on Vitrification of Low-Level Simulated Radioactive Waste Glass." *Institute of Nuclear Materials Management 36th Annual Proceedings*, Palm Desert, California (in press).

Li, H, JD Darab, PA Smith, X Feng and DK Peeler. 1995. "Chemical Durability of Low-Level Simulated Radioactive Waste Glasses with High-Concentrations of Minor Components" *Institute of Nuclear Materials Management 36th Annual Proceedings*, Palm Desert, California (in press).

Li, H, MH Langowski, and PR Hrma. 1995. "Segregation of Sulfate and Phosphate in the

Vitrification of High-Level Wastes." *International Symposium on the Environmental Issues and Waste Management Technologies in Ceramic and Nuclear Industry*, Cincinnati, Ohio (in press).

Lokken, RO. 1995. *Makeup Procedures and Characterization Data For Modified DSSF and Modified Remaining Inventory Simulated Tank Wastes*. PVTD-T3B-95-211, Pacific Northwest Laboratory, Washington.

Marra, JC, "Glass Composition Development for Vitrification of Hanford High Sodium Content Low-Level Radioactive Liquid Waste, " Savannah River Technology Center, WRSC-TR-95-0034, Revision 0, 1995.

McGrail, BP and KM Olson. 1992. *Evaluating Long-term Performance of In-situ Vitrified Waste Forms: Methodology and Results*. PNL-8358, Pacific Northwest Laboratory, Richland, Washington.

Merrill, Richard A, et al 1995. "Development of Glasses for Low Level Waste from Hanford Tanks", DOE/MWFA, TTP No. RL332009, DRAFT, Pacific Northwest Laboratory, Richland, WA.

Papadopoulos, K. 1973. "The Solubility of SO_3 in Soda-Lime-Silica Melts." *Phys.Chem.Glasses* **14**:60-65.

Peters, R.D. et al 1993. "Vitrification Development Plan for U.S. Department of Energy Mixed Wastes," DOE/MWIP-11, Pacific Northwest Laboratory, Richland, WA.

Shade, JW, 1994. *Waste Simulant Development for Evaluation of LLW Melter System Technology*. WHC-SD-WM-TI-624. Westinghouse Hanford Company, Richland, Washington.

Singh, SP and GP Nath. 1981. "Thermodynamics of Cr^{3+} - Cr^{6+} Equilibrium in Borate Melts" *J.Mater.Sci.* **16**:2176-2180.

Sullivan, GK, MH Langowski and PR Hrma. 1995. "Sulfate Segregation in the Vitrification of Simulated Hanford Waste Glass." *International Symposium on the Environmental Issues and Waste Management Technologies in Ceramic and Nuclear Industry*, Cincinnati, Ohio.

Sun, KH and A Silverman. 1945. "Lewis Acid-Base Theory Applied to Glass." *J.Am.Ceram.Soc.* **28**:8-11.

Takusagawa, N. 1980. "Infrared Absorption Spectra and Structure of Fluorine-Containing Alkali Silicate Glasses." *J.Non-Cryst.Solids* **42**:35-40.

Tomozawa, M. 1972. "Effects of Oxide Nucleation Agents on Phase Separation of Simple Glass Systems." In *Advances in Nucleation and Crystallization in Glasses*, L.L. Hench and S.W. Freiman, eds., American Ceramics Society, Columbus, Ohio. pp. 41-50.

Wilson, CN, KC Burgard, ET Weber, and NR Brown. 1995. "Melter Technology Evaluation for Vitrification of Hanford Site Low-Level Waste." WHC-SA-2857-FP, *American Ceramic Society 97th Annual Meeting Proceedings*, April 30-May 3, Cincinnati, Ohio.

APPENDIX A

Glass Compositions for Glass Optimization Investigation

Appendix A1. Glass Compositions for Glass Optimization Investigatation

Vendor	Type	Glass ID	Al2O3	B2O3	CaO	Fe2O3	K2O	MgO	Na2O	SiO2	ZrO2
PNL	Nominal	L0-0	1.47			0.00	1.05	0.00	20.00	76.32	
PNL	Analyzed	L1-12	12.38	0.17	0.28		0.22		27.48	59.41	
PNL	Nominal	L1-12	12.00			0.00	1.05	0.00	20.00	65.78	
PNL	Analyzed	L1-15	15.29	2.30	0.27		0.20		26.35	55.55	
PNL	Nominal	L1-15	15.00			0.00	1.05	0.00	20.00	62.78	
PNL	Analyzed	L1-6	5.85	0.09	1.41			0.01	20.30	72.22	0.06
PNL	Nominal	L1-6	6.00			0.00	1.05	0.00	20.00	71.78	
PNL	Analyzed	L1-9	9.57	0.76	0.32		0.24		27.99	61.08	
PNL	Nominal	L1-9	9.00			0.00	1.05	0.00	20.00	68.78	
PNL	Analyzed	L4-1212	11.69	11.45	0.21		0.24		25.16	51.21	
PNL	Nominal	L4-1212	12.00	12.00		0.00	1.05	0.00	20.00	53.78	
PNL	Nominal	L4-1215	15.00	12.00		0.00	1.05	0.00	20.00	50.78	
PNL	Nominal	L4-129	9.00	12.00		0.00	1.05	0.00	20.00	56.78	
PNL	Analyzed	L4-612	12.16	6.54	0.23		0.26		25.08	55.69	
PNL	Nominal	L4-612	12.00	6.00		0.00	1.05	0.00	20.00	59.78	
PNL	Analyzed	L4-615	13.68	5.67	1.20			0.00	20.24	59.13	0.02
PNL	Nominal	L4-615	15.00	6.00		0.00	1.05	0.00	20.00	56.78	
PNL	Analyzed	L4-69	9.50	0.05	1.51			0.01	22.51	66.32	0.04
PNL	Nominal	L4-69	9.00	6.00		0.00	1.05	0.00	20.00	62.78	
PNL	Analyzed	L4-912	12.16	7.62	0.21		0.21		26.23	53.52	
PNL	Analyzed	L4-912	11.68	7.91	1.55			0.00	21.81	56.95	0.03
PNL	Nominal	L4-912	12.00	9.00		0.00	1.05	0.00	20.00	56.78	
PNL	Analyzed	L4-915	20.44	1.01	2.10			0.01	3.23	73.10	0.03
PNL	Nominal	L4-915	15.00	9.00		0.00	1.05	0.00	20.00	53.78	
PNL	Analyzed	L4-96	5.98	9.90	0.25		0.23		25.52	57.48	
PNL	Nominal	L4-96	6.00	9.00		0.00	1.05	0.00	20.00	62.78	
PNL	Analyzed	L4-99	8.82	8.39	0.28		0.23		25.67	56.56	
PNL	Nominal	L4-99	9.00	9.00		0.00	1.05	0.00	20.00	59.78	
PNL	Analyzed	L5-1212	11.31	0.12	11.21			0.09	21.44	55.76	0.02
PNL	Nominal	L5-1212	12.00		12.00	0.00	1.05	0.00	20.00	53.78	
PNL	Analyzed	L5-1215	14.17	0.07	10.48			0.08	19.51	55.61	0.02
PNL	Nominal	L5-1215	15.00		12.00	0.00	1.05	0.00	20.00	50.78	
PNL	Analyzed	L5-129	9.01	10.53	1.54			0.00	20.88	57.97	0.02
PNL	Nominal	L5-129	9.00		12.00	0.00	1.05	0.00	20.00	56.78	
PNL	Nominal	L5-612	12.00		6.00	0.00	1.05	0.00	20.00	59.78	
PNL	Nominal	L5-615	15.00		6.00	0.00	1.05	0.00	20.00	56.78	
PNL	Nominal	L5-69	9.00		6.00	0.00	1.05	0.00	20.00	62.78	
PNL	Analyzed	L5-912	12.48	2.80	8.06		0.24		22.63	53.75	
PNL	Nominal	L5-912	12.00		9.00	0.00	1.05	0.00	20.00	56.78	
PNL	Analyzed	L5-915	13.38	0.15	8.26			0.06	19.40	58.67	0.02
PNL	Nominal	L5-915	15.00		9.00	0.00	1.05	0.00	20.00	53.78	
PNL	Analyzed	L5-96	5.74	2.61	9.93		0.20		26.08	55.40	
PNL	Nominal	L5-96	6.00		9.00	0.00	1.05	0.00	20.00	62.78	
PNL	Analyzed	L5-99	8.94	0.38	9.12			0.06	21.63	59.78	0.02
PNL	Nominal	L5-99	9.00		9.00	0.00	1.05	0.00	20.00	59.78	

Appendix A1. Glass Compositions for Glass Optimization Investigatation (Cont.)

Vendor	Type	Glass ID	Al2O3	B2O3	CaO	Fe2O3	K2O	MgO	Na2O	SiO2	ZrO2
PNL	Nominal	L6-3312	12.00	3.00	3.00	0.00	1.04	0.00	20.00	59.78	
PNL	Analyzed	L6-5412	11.84	4.77	3.36		0.24		26.99	52.76	
PNL	Nominal	L6-5412	12.00	5.00	4.00	0.00	1.04	0.00	20.00	56.78	
PNL	Nominal	L6-5415	15.00	5.00	4.00	0.00	1.04	0.00	20.00	53.78	
PNL	Analyzed	L6-546	5.82	6.75	3.44		0.25		26.19	57.47	
PNL	Nominal	L6-546	6.00	5.00	4.00	0.00	1.04	0.00	20.00	62.78	
PNL	Analyzed	L6-549	8.72	5.55	3.48		0.21		27.02	54.98	
PNL	Nominal	L6-549	9.00	5.00	4.00	0.00	1.04	0.00	20.00	59.78	
PNL	Nominal	L6-6612	12.00	6.00	6.00	0.00	1.04	0.00	20.00	53.78	
PNL	Nominal	L6-669	9.00	6.00	6.00	0.00	1.04	0.00	20.00	56.78	
PNL	Analyzed	L7-15	12.59	6.92	3.86		0.15		20.14	56.30	
PNL	Nominal	L7-15	12.45	5.39	4.31	0.00	0.78	0.00	15.00	61.19	
PNL	Analyzed	L7-25	11.23	5.28	2.94		0.31		33.40	46.79	
PNL	Nominal	L7-25	11.55	4.61	3.69	0.00	1.31	0.00	25.00	52.38	
PNL	Analyzed	L7-3	10.84	4.87	2.83		0.35		30.04	50.98	
PNL	Nominal	L7-33	11.10	4.22	3.38	0.00	1.57	0.00	30.00	47.97	
PNL	Analyzed	L7-35	10.40	3.77	2.57		0.43		38.25	44.52	
PNL	Nominal	L7-35	10.65	3.84	3.07	0.00	1.83	0.00	35.00	43.57	
PNL	Nominal	L8-1	9.00	6.00		0.00	1.04	0.00	20.00	56.78	6.00
PNL	Nominal	L8-2	9.00		6.00	0.00	1.04	0.00	20.00	56.78	6.00
PNL	Nominal	L8-3	9.00	3.00	3.00	0.00	1.04	0.00	20.00	56.78	6.00
PNL	Nominal	L8-4	9.00	6.00		6.00	1.04	0.00	20.00	56.78	
PNL	Nominal	L8-5	9.00		6.00	6.00	1.04	0.00	20.00	56.78	
PNL	Nominal	L8-6	9.00	3.00	3.00	6.00	1.04	0.00	20.00	56.78	
PNL	Nominal	L8-7	9.00	6.00		3.00	1.04	0.00	20.00	56.78	3.00
PNL	Nominal	L8-8	9.00	5.00		0.00	1.04	4.00	20.00	59.80	

Appendix A1. Glass Compositions for Glass Optimization Investigatation (Cont.)

Vendor	Type	Glass ID	Cl	Cr2O3	Cs2O	F	I	MnO	MoO3	P2O5	SO3	SrO
PNL	Nominal	L0-0	0.25	0.03	0.11	0.21	0.09	0.00	0.11	0.14	0.15	0.08
PNL	Analyzed	L1-12		0.03				0.01				
PNL	Nominal	L1-12	0.25	0.03	0.11	0.21	0.09	0.00	0.11	0.14	0.15	0.08
PNL	Analyzed	L1-15		0.03				0.01				
PNL	Nominal	L1-15	0.25	0.03	0.11	0.21	0.09	0.00	0.11	0.14	0.15	0.08
PNL	Analyzed	L1-6		0.03	0.00			0.01				
PNL	Nominal	L1-6	0.25	0.03	0.11	0.21	0.09	0.00	0.11	0.14	0.15	0.08
PNL	Analyzed	L1-9		0.03				0.01				
PNL	Nominal	L1-9	0.25	0.03	0.11	0.21	0.09	0.00	0.11	0.14	0.15	0.08
PNL	Analyzed	L4-1212		0.03				0.01				
PNL	Nominal	L4-1212	0.25	0.03	0.11	0.21	0.09	0.00	0.11	0.14	0.15	0.08
PNL	Nominal	L4-1215	0.25	0.03	0.11	0.21	0.09	0.00	0.11	0.14	0.15	0.08
PNL	Nominal	L4-129	0.25	0.03	0.11	0.21	0.09	0.00	0.11	0.14	0.15	0.08
PNL	Analyzed	L4-612		0.03				0.01				
PNL	Nominal	L4-612	0.25	0.03	0.11	0.21	0.09	0.00	0.11	0.14	0.15	0.08
PNL	Analyzed	L4-615		0.03				0.01				
PNL	Nominal	L4-615	0.25	0.03	0.11	0.21	0.09	0.00	0.11	0.14	0.15	0.08
PNL	Analyzed	L4-69		0.04				0.01				
PNL	Nominal	L4-69	0.25	0.03	0.11	0.21	0.09	0.00	0.11	0.14	0.15	0.08
PNL	Analyzed	L4-912		0.03				0.01				
PNL	Analyzed	L4-912		0.04				0.01				
PNL	Nominal	L4-912	0.25	0.03	0.11	0.21	0.09	0.00	0.11	0.14	0.15	0.08
PNL	Analyzed	L4-915		0.05				0.01				
PNL	Nominal	L4-915	0.25	0.03	0.11	0.21	0.09	0.00	0.11	0.14	0.15	0.08
PNL	Analyzed	L4-96		0.03				0.01				
PNL	Nominal	L4-96	0.25	0.03	0.11	0.21	0.09	0.00	0.11	0.14	0.15	0.08
PNL	Analyzed	L4-99		0.03				0.01				
PNL	Nominal	L4-99	0.25	0.03	0.11	0.21	0.09	0.00	0.11	0.14	0.15	0.08
PNL	Analyzed	L5-1212		0.03				0.01				
PNL	Nominal	L5-1212	0.25	0.03	0.11	0.21	0.09	0.00	0.11	0.14	0.15	0.08
PNL	Analyzed	L5-1215		0.04				0.01				
PNL	Nominal	L5-1215	0.25	0.03	0.11	0.21	0.09	0.00	0.11	0.14	0.15	0.08
PNL	Analyzed	L5-129		0.03				0.01				
PNL	Nominal	L5-129	0.25	0.03	0.11	0.21	0.09	0.00	0.11	0.14	0.15	0.08
PNL	Nominal	L5-612	0.25	0.03	0.11	0.21	0.09	0.00	0.11	0.14	0.15	0.08
PNL	Nominal	L5-615	0.25	0.03	0.11	0.21	0.09	0.00	0.11	0.14	0.15	0.08
PNL	Nominal	L5-69	0.25	0.03	0.11	0.21	0.09	0.00	0.11	0.14	0.15	0.08
PNL	Analyzed	L5-912		0.03				0.01				
PNL	Nominal	L5-912	0.25	0.03	0.11	0.21	0.09	0.00	0.11	0.14	0.15	0.08
PNL	Analyzed	L5-915		0.03				0.01				
PNL	Nominal	L5-915	0.25	0.03	0.11	0.21	0.09	0.00	0.11	0.14	0.15	0.08
PNL	Analyzed	L5-96		0.03				0.01				
PNL	Nominal	L5-96	0.25	0.03	0.11	0.21	0.09	0.00	0.11	0.14	0.15	0.08
PNL	Analyzed	L5-99		0.03				0.01				
PNL	Nominal	L5-99	0.25	0.03	0.11	0.21	0.09	0.00	0.11	0.14	0.15	0.08

Appendix A1. Glass Compositions for Glass Optimization Investigatation (Cont.)

Vendor	Type	Glass ID	Cl	Cr2O3	Cs2O	F	I	MnO	MoO3	P2O5	SO3	SrO
PNL	Nominal	L6-3312	0.25	0.03	0.10	0.21	0.09	0.00	0.11	0.14	0.15	0.08
PNL	Analyzed	L6-5412		0.03				0.01				
PNL	Nominal	L6-5412	0.25	0.03	0.10	0.21	0.09	0.00	0.11	0.14	0.15	0.08
PNL	Nominal	L6-5415	0.25	0.03	0.10	0.21	0.09	0.00	0.11	0.14	0.15	0.08
PNL	Analyzed	L6-546		0.03				0.01				
PNL	Nominal	L6-546	0.25	0.03	0.10	0.21	0.09	0.00	0.11	0.14	0.15	0.08
PNL	Analyzed	L6-549		0.03				0.01				
PNL	Nominal	L6-549	0.25	0.03	0.10	0.21	0.09	0.00	0.11	0.14	0.15	0.08
PNL	Nominal	L6-6612	0.25	0.03	0.10	0.21	0.09	0.00	0.11	0.14	0.15	0.08
PNL	Nominal	L6-669	0.25	0.03	0.10	0.21	0.09	0.00	0.11	0.14	0.15	0.08
PNL	Analyzed	L7-15		0.02				0.01				
PNL	Nominal	L7-15	0.19	0.02	0.08	0.16	0.07	0.00	0.08	0.10	0.12	0.06
PNL	Analyzed	L7-25		0.04				0.01				
PNL	Nominal	L7-25	0.31	0.04	0.13	0.26	0.12	0.00	0.13	0.17	0.19	0.10
PNL	Analyzed	L7-3		0.05				0.01				
PNL	Nominal	L7-33	0.38	0.04	0.16	0.32	0.14	0.00	0.16	0.20	0.23	0.11
PNL	Analyzed	L7-35		0.05				0.01				
PNL	Nominal	L7-35	0.44	0.05	0.18	0.37	0.16	0.00	0.19	0.24	0.27	0.13
PNL	Nominal	L8-1	0.25	0.03	0.10	0.21	0.09	0.00	0.11	0.14	0.15	0.08
PNL	Nominal	L8-2	0.25	0.03	0.10	0.21	0.09	0.00	0.11	0.14	0.15	0.08
PNL	Nominal	L8-3	0.25	0.03	0.10	0.21	0.09	0.00	0.11	0.14	0.15	0.08
PNL	Nominal	L8-4	0.25	0.03	0.10	0.21	0.09	0.00	0.11	0.14	0.15	0.08
PNL	Nominal	L8-5	0.25	0.03	0.10	0.21	0.09	0.00	0.11	0.14	0.15	0.08
PNL	Nominal	L8-6	0.25	0.03	0.10	0.21	0.09	0.00	0.11	0.14	0.15	0.08
PNL	Nominal	L8-7	0.25	0.03	0.10	0.21	0.09	0.00	0.11	0.14	0.15	0.08
PNL	Nominal	L8-8	0.25	0.03	0.10	0.21	0.09	0.00	0.11	0.14	0.15	0.08

Appendix A2. Phase I Vendor Glass Compositions

Vendor	Type	Glass ID	Al2O3	B2O3	CaO	Fe2O3	K2O	MgO	Na2O	SiO2	ZrO2
BCW	Analyzed	B1G9-011C4	12.15	1.41	5.16	0.44	3.71	0.25	12.05	63.87	0.08
BCW	Analyzed	B1G9-014C	12.60	1.62	5.22	0.58	2.84	0.24	13.37	62.56	0.06
BCW	Analyzed	B1G9-13C5	12.94	1.39	5.14	0.66	3.15	0.23	12.50	63.00	0.06
GDI	Analyzed	D1G4-002P	4.85	18.91	7.10	4.73	4.51	4.03	11.92	40.42	1.47
GDI	Analyzed	D1G4-009P	5.26	12.04	7.97	6.54	6.20	2.03	15.79	40.73	1.32
GDI	Analyzed	D1G4-017P	6.29	7.76	8.27	7.31	6.43	0.82	17.50	40.35	3.02
GDI	Analyzed	D1G4-022P2	6.70	7.36	8.69	7.77	2.46	0.61	18.00	42.47	3.62
GDI	Analyzed	D1G4-023P3	6.41	7.10	8.57	7.76	3.02	0.53	18.24	42.27	3.82
GDI	Analyzed	D1G4-026P4	6.49	6.66	8.50	7.82	3.83	0.42	18.22	41.83	4.01
GDI	Norminal	Duratek	6.14	6.15	7.80	7.50	3.68		18.82	42.23	5.09
PEI	Norminal	PEI	6.00		9.73	1.00	1.50	0.13	18.82	59.22	2.00
PNL	Norminal	LD4-912	12.00	9.00			1.46		20.00	55.91	
PNL	Norminal	LD5-912	12.00		9.00		1.46		20.00	55.91	
PNL	Norminal	LD6-5314	14.00	5.00	3.00		1.46		20.00	54.91	
PNL	Norminal	LD6-5412	12.00	5.00	4.00		1.46		20.00	55.91	
PNL	Analyzed	LD6-5412	12.17	5.05	4.12	0.11	1.66		20.41	55.44	0.08
PNL	Analyzed	SSHTM-3	11.63	6.09	4.14	0.02	1.04		22.55	52.81	0.34
PNL	Norminal	LD6-5510	10.00	5.00	5.00		1.46		20.00	56.91	
UBM	Analyzed	M1G1-008P	14.98	1.81	9.50	1.06		0.39	13.21	47.82	
UBM	Analyzed	M1G1-011P	13.35	2.53	6.75	1.16		0.30	15.24	50.53	
VTI	Analyzed	V1M2 6 32 011 P1	10.28	7.01	2.99	1.04	1.23	2.14	16.22	58.09	0.06
VTI	Analyzed	V1M2 6 32 040 P2	10.42	7.18	3.06	1.02	2.26	2.21	15.53	57.35	0.04
VTI	Analyzed	V1M2 6 34 015 P	10.76	7.24	3.03	1.04	1.36	2.21	16.29	57.22	0.05
VTI	Analyzed	V1M3 6 32 059 P1	10.62	7.29	3.33	1.04	2.00	2.21	15.97	56.69	0.05
VTI	Analyzed	V1M3 6 32 075 P2	10.98	7.61	3.51	1.14	1.81	2.28	12.67	59.08	0.03
VTI	Analyzed	V1M3 6 34 071 P	16.92	6.84	3.02	0.96	1.71	2.08	14.85	52.98	0.04
VTI	Analyzed	V1M4 6 32 088 P1	10.59	7.33	3.35	1.20	2.02	2.13	16.80	55.63	0.04
VTI	Analyzed	V1M4 6 32 096 P2	10.87	7.52	2.99	0.99	2.12	2.15	16.54	55.97	0.04
VTI	Norminal	Vectra	10.00	8.00	2.90	1.00	1.46	2.10	20.00	52.90	
VTI	Analyzed	Vectra	9.45	8.20	2.90	1.10	0.91	1.87	20.82	53.31	0.02
VTI	Analyzed	Vectra I	10.11	8.11	2.93	1.08	1.48	1.85	21.37	51.81	
WSTC	Norminal	WSTC	18.22	9.45	4.65		1.44		18.82	42.90	2.10

Appendix A2. Phase I Vendor Glass Compositions (Continued)

Vendor	Type	Glass ID	BaO	CeO2	Cr2O3	Li2O	MnO	MoO3	Nd2O3	NiO	P2O5	SO3	SrO	TiO2	ZnO
BCW	Analyzed	B1G9-011C4	0.01		0.05	0.00	0.02	0.06	0.08	0.04			0.10	0.19	0.14
BCW	Analyzed	B1G9-014C	0.01		0.05		0.02	0.07	0.13	0.04			0.10	0.17	0.19
BCW	Analyzed	B1G9-13C5	0.01		0.05	0.00	0.02	0.06	0.11	0.04			0.10	0.17	0.12
GDI	Analyzed	D1G4-002P	0.32	0.04	0.31	0.04	0.06	0.03	0.10	0.19		0.21	0.03	0.21	0.31
GDI	Analyzed	D1G4-009P	0.15	0.05	0.25	0.02	0.03	0.10	0.11	0.13		0.23	0.07	0.62	0.17
GDI	Analyzed	D1G4-017P	0.06	0.07	0.18		0.02	0.14	0.11	0.08		0.22	0.09	0.81	0.18
GDI	Analyzed	D1G4-022P2	0.04	0.07	0.21		0.02	0.15	0.05	0.06	0.06	0.21	0.10	0.89	0.21
GDI	Analyzed	D1G4-023P3	0.04	0.04	0.19		0.02	0.15	0.03	0.07	0.04	0.21	0.10	0.91	0.27
GDI	Analyzed	D1G4-026P4	0.03	0.12	0.15		0.02	0.15	0.09	0.04	0.05	0.23	0.10	0.90	0.17
GDI	Norminal	Duratek			0.04			0.15			0.19	0.21	0.10	1.00	
PEI	Norminal	PEI			0.04			0.15			0.19	0.21	0.10		
PNL	Norminal	LD4-912													
PNL	Norminal	LD5-912													
PNL	Norminal	LD6-5314													
PNL	Norminal	LD6-5412													
PNL	Analyzed	LD6-5412			0.05072	0.01	0.01	0.13	0.06	0.03	0.22	0.18	0.09	0.02	0.14
PNL	Analyzed	SSHTM-3			0.16387	0.02	0.01	0.14	0.02	0.03	0.31	0.29	0.07	0.07	0.26
PNL	Norminal	LD6-5510													
UBM	Analyzed	M1G1-008P						0.07						0.68	
UBM	Analyzed	M1G1-011P						0.09						0.35	
VTI	Analyzed	V1M2 6 32 011 P1			0.31		0.01	0.22	0.02	0.04			0.06	0.01	0.08
VTI	Analyzed	V1M2 6 32 040 P2		0.01	0.29		0.01	0.19	0.04	0.04			0.06	0.01	0.06
VTI	Analyzed	V1M2 6 34 015 P		0.01	0.31		0.01	0.21	0.07	0.04			0.06	0.02	
VTI	Analyzed	V1M3 6 32 059 P1		0.06	0.27		0.01	0.16	0.10	0.04			0.08	0.01	0.07
VTI	Analyzed	V1M3 6 32 075 P2	0.01	0.06	0.29	0.01	0.02	0.16	0.09	0.04			0.08	0.02	0.08
VTI	Analyzed	V1M3 6 34 071 P			0.25		0.01	0.15	0.06	0.03			0.06	0.03	
VTI	Analyzed	V1M4 6 32 088 P1	0.01	0.05	0.31	0.03	0.03	0.13	0.09	0.04			0.09	0.02	0.08
VTI	Analyzed	V1M4 6 32 096 P2			0.30		0.01	0.13	0.06	0.03			0.08	0.01	
VTI	Norminal	Vectra													
VTI	Analyzed	Vectra			0.04			0.15	0.03	0.03	0.40	0.22	0.11		0.28
VTI	Analyzed	Vectra I			0.04			0.15	0.01		0.64		0.11	0.01	0.28
WSTC	Norminal	WSTC				0.83									

Appendix A3. Phase II Vendor Glass Compositions(Continued)

Vendor	Type	Glass ID	CeO2	Cl	Cr2O3	Cs2O	F	I	Li2O	MnO	MoO3	Nd2O3	NiO	P2O5	SO3	SrO	TiO2	ZnO	Other
PNL	Norminal	LDM-912		0.64	0.04	0.14	0.82	0.13		0.00	0.15			0.19	0.21	0.10			
PNL	Analyzed	LDM-912	0.06								0.16			0.24	0.26	0.12			
PNL	Norminal	LDM-1		0.64	0.04	0.14	0.82	0.13		0.00	0.15			0.19	0.21	0.10			
PNL	Analyzed	LDM-1	0.05		0.05					0.01	0.15	0.05		0.46	0.22	0.10	0.01	0.11	
PNL	Norminal	LDM-2		0.64	0.04	0.14	0.82	0.13		0.00	0.15			0.19	0.21	0.10			
PNL	Analyzed	LDM-2			0.05						0.15	0.06		0.28	0.23	0.11		0.06	
PNL	Norminal	LDM-3		0.64	0.04	0.14	0.82	0.13		0.00	0.15			0.19	0.21	0.10			
PNL	Analyzed	LDM-3	0.08		0.05						0.16	0.07	0.05	0.28	0.21	0.12	0.01	0.08	
PNL	Norminal	LDM-4		0.64	0.04	0.14	0.82	0.13		0.00	0.15			0.19	0.21	0.10			
PNL	Analyzed	LDM-4			0.05					0.01	0.15	0.08	0.03	0.27	0.26	0.12		0.14	
PNL	Norminal	LDM-5412		0.64	0.04	0.14	0.82	0.13		0.00	0.15			0.19	0.21	0.10			
PNL	Analyzed	LDM-5412			0.05						0.16	0.06		0.62	0.69	0.11	0.01	0.16	
PNL	Norminal	LDMS-1		0.64	0.04	0.14	0.82	0.13		0.00	0.14			0.19	0.21	0.10			
PNL	Analyzed	LDMS-1	0.05		0.03				0.01	0.01	0.13	0.08	0.02	0.28	0.26	0.09	0.02	0.06	
PNL	Norminal	LDMSM-1		0.62	0.26	0.14	0.79	0.12		0.20	0.69		0.46	0.18	0.21	0.10		0.45	1.87*
PNL	Analyzed	LDMSM-1	0.05		0.17				0.01	0.23	0.30	0.10	0.48	0.30	0.27	0.10	0.02	0.49	
PNL	Norminal	LRM-912		0.04	0.04	0.15	0.26	0.14		0.01	0.15			2.52	1.01	0.11			
PNL	Analyzed	LRM-912	0.05		0.04					0.01	0.16	0.09		2.67	1.01	0.13		0.10	
PNL	Norminal	LRM-1		0.04	0.04	0.15	0.26	0.14	1.00	0.01	0.15			2.52	1.01	0.11			
PNL	Analyzed	LRM-1			0.04				1.02	0.02	0.15			2.72	0.76	0.12	0.02	0.21	
PNL	Norminal	LRM-2		0.04	0.04	0.15	0.26	0.14		0.01	0.15			2.52	1.01	0.11			
PNL	Analyzed	LRM-2			0.04					0.02	0.16	0.03		2.52	0.74	0.12	0.01	0.18	
PNL	Norminal	LRM-3		0.04	0.04	0.15	0.26	0.14		0.01	0.15			2.52	1.01	0.11			
PNL	Analyzed	LRM-3			0.04					0.01	0.17	0.04		2.82	0.59	0.13	0.01	0.24	
PNL	Norminal	LRM-4		0.04	0.04	0.15	0.26	0.14	0.50	0.01	0.15			2.52	1.01	0.11			
PNL	Analyzed	LRM-4	0.06		0.04				0.49	0.02	0.15	0.09	0.02	2.62	0.93	0.12	0.01	0.09	
PNL	Norminal	LRM-5412		0.04	0.04	0.15	0.26	0.14		0.01	0.15			2.52	1.01	0.11			
PNL	Analyzed	LRM-5412	0.05		0.04					0.01	0.16	0.08	0.03	2.67	0.87	0.13		0.11	
PNL	Norminal	LRMS-1		0.04	0.04	0.15	0.26	0.14	1.00	0.01	0.15			2.52	1.01	0.11			
PNL	Analyzed	LRMS-1	0.05		0.03				1.01	0.01	0.15	0.10	0.02	2.57	1.01	0.11	0.02	0.06	
PNL	Norminal	LRMSM-1		0.03	0.25	0.15	0.25	0.13	0.96	0.20	0.69		0.46	2.43	0.97	0.11		0.45	1.87*
PNL	Analyzed	LRMSM-1	0.07		0.21				0.95	0.24	0.43	0.12	0.49	2.57	0.76	0.11	0.02	0.49	

* Others in clude Bi2O3, CdO, PbO, Sb2O3, CuO, SnO, As2O3

Appendix A3. Phase II Vendor Glass Compositions

Vendor	Type	Glass ID	Al2O3	B2O3	CaO	Fe2O3	K2O	MgO	Na2O	SiO2	ZrO2
PNL	Norminal	LDM-912	12.00		9.00	0.00	1.43	0.00	20.00	55.14	
PNL	Analyzed	LDM-912	12.22		9.60	0.06	1.67	0.10	19.92	55.30	
PNL	Norminal	LDM-1	12.00	2.00	2.00	6.00	1.43	0.00	20.00	50.14	4.00
PNL	Analyzed	LDM-1	12.17	2.01	1.78	6.21	1.46		21.05	50.06	4.02
PNL	Norminal	LDM-2	12.00		6.00	6.00	1.43	0.00	20.00	52.14	
PNL	Analyzed	LDM-2	12.08		6.24	6.19	1.79		20.30	51.87	0.01
PNL	Norminal	LDM-3	12.00	6.00	0.00	0.00	1.43	0.00	20.00	52.14	6.00
PNL	Analyzed	LDM-3	12.44	6.31	0.12	0.05	2.30		18.85	53.50	5.27
PNL	Norminal	LDM-4	10.00	6.00	6.00	6.00	1.43	0.00	20.00	44.14	4.00
PNL	Analyzed	LDM-4	10.06	6.25	6.48	6.14	2.02		20.36	43.70	3.82
PNL	Norminal	LDM-5412	12.00	5.00	4.00	0.00	1.43	0.00	20.00	55.14	
PNL	Analyzed	LDM-5412	12.05	5.01	3.94	0.06	2.13	0.15	21.22	53.56	
PNL	Norminal	LDMS-1	12.00	2.00	2.00	6.00	1.43	0.00	20.00	50.14	4.00
PNL	Analyzed	LDMS-1	12.13	2.03	2.05	6.07	2.50	0.11	20.83	48.03	4.05
PNL	Norminal	LDMSM-1	11.55	1.93	1.93	5.78	1.38		19.25	48.26	3.85
PNL	Analyzed	LDMSM-1	11.77	1.93	2.12	5.76	2.71	0.11		46.91	
PNL	Norminal	LRM-912	12.00		9.00	0.00	0.03		20.00	54.54	
PNL	Analyzed	LRM-912	11.79	0.03	9.41	0.05	0.70	0.12	20.42	53.19	
PNL	Norminal	LRM-1	12.00	2.00	2.00	6.00	0.03		20.00	48.54	4.00
PNL	Analyzed	LRM-1	12.19	2.02	1.82	6.24			21.23	47.42	3.99
PNL	Norminal	LRM-2	12.00		6.00	6.00	0.03		20.00	51.54	
PNL	Analyzed	LRM-2	11.41		6.13	5.87		0.11	22.13	48.20	
PNL	Norminal	LRM-3	12.00	6.00	0.00	0.00	0.03		20.00	51.54	6.00
PNL	Analyzed	LRM-3	12.62	6.38	0.19	0.05	0.44		18.11	55.29	5.07
PNL	Norminal	LRM-4	10.00	6.00	6.00	6.00	0.03		20.00	43.04	4.00
PNL	Analyzed	LRM-4	9.77	6.01	6.19	5.98	1.46	0.11	20.22	41.74	3.82
PNL	Norminal	LRM-5412	12.00	5.00	4.00	0.00	0.03		20.00	54.54	
PNL	Analyzed	LRM-5412	11.86	5.09	4.23	0.05	0.92		20.27	53.41	
PNL	Norminal	LRMS-1	12.00	2.00	2.00	6.00	0.03		20.00	48.54	4.00
PNL	Analyzed	LRMS-1	11.91	2.01	2.20	5.98	1.76	0.11		47.17	
PNL	Norminal	LRMSM-1	11.55	1.93	1.93	5.78	0.03		19.25	46.72	3.85
PNL	Analyzed	LRMSM-1	11.44	1.90	2.12	5.73	2.44	0.13		44.99	

APPENDIX B

7-Day PCT Elemental Release Data

Appendix B1. 7-Day PCT Elemental Release (g/m²) of LLW Glasses

Vendor	Glass ID	Comp. Used	pH	Al2O3	B2O3	CaO	Fe2O3	K2O	Na2O	SiO2	SO3	MnO	MoO3
PNL	L1-12C	Nominal	12.33	0.39			6.24		2.57	0.40		1.91	
PNL	L1-12C	Nominal	12.33	0.39					2.65	0.40			
PNL	L1-12D	Nominal	12.35	0.39			6.41		2.64	0.40		1.96	
PNL	L1-9C	Nominal	12.72	0.39	0.00		11.15		5.99	0.93	1.08	3.33	
PNL	L1-9D	Nominal	12.75	0.39	0.00		12.19		6.18	0.94	1.13	3.39	
PNL	L4-1212R	Nominal	10.41	0.13	1.15		3.54	0.03	0.75	0.13	0.25		
PNL	L4-912CR	Nominal	10.52	0.13	0.28		3.77		0.30	0.13	0.40		
PNL	L4-912DR	Nominal	10.54	0.13	0.28		3.60	0.04	0.30	0.13	0.26		
PNL	L5-1215R	Nominal	11.75	0.09		0.06			0.61	0.09	0.22		
PNL	L6-3312C	Nominal	11.63	0.15	0.16	0.02	1.03		0.56	0.15	0.27		
PNL	L6-3312D	Nominal	11.64	0.15	0.17	0.02	0.67		0.59	0.16	0.26		
PNL	L6-5412C	Nominal	11.39	0.11	0.13	0.02	0.26		0.39	0.12	0.19		
PNL	L6-5412D	Nominal	11.41	0.11	0.13	0.02			0.40	0.12	0.19		
PNL	L6-5415C	Nominal	11.22	0.10	0.11	0.02	0.27		0.31	0.10	0.16		
PNL	L6-5415D	Nominal	11.26	0.10	0.11	0.02	0.32		0.30	0.10	0.15		
PNL	L6-546C	Nominal	11.89	0.18	0.23	0.04		0.04	0.91	0.22	0.39		
PNL	L6-546D	Nominal	11.91	0.19	0.24	0.04			0.97	0.22	0.39		
PNL	L6-549C	Nominal	11.64	0.14	0.17	0.03	0.20	0.03	0.58	0.15	0.28		
PNL	L6-549D	Nominal	11.66	0.15	0.17	0.03			0.61	0.16	0.26		
PNL	L6-6612C	Nominal	11.47	0.10	0.12	0.04			0.39	0.11	0.18		
PNL	L6-6612D	Nominal	11.46	0.10	0.11	0.04			0.37	0.10	0.19		
PNL	L6-669C	Nominal	11.36	0.12	0.14	0.04		0.07	0.49	0.13	0.31		
PNL	L6-669D	Nominal	11.37	0.12	0.14	0.04		0.04	0.49	0.13	0.30		
PNL	L7-35C	Nominal	13.33	0.25	52.60		13.82	10.35	41.93	19.62	92.05		0.31
PNL	L7-35D	Nominal	13.38	0.15	36.17		16.31	9.20	29.11	13.59	64.05		0.26
PNL	L8-4C	Nominal	10.70		1.28		0.01	0.08	1.00	0.43	2.52	0.50	0.01
PNL	L8-4D	Nominal	10.71		1.30		0.01	0.05	1.03	0.43	2.47	0.18	0.01
PNL	L8-5C	Nominal	11.93	0.22		0.01	0.01	0.04	1.17	0.21	0.53		
PNL	L8-5D	Nominal	11.94	0.20		0.01	0.01	0.03	1.15	0.22	0.59		
PNL	L8-6C	Nominal	11.46	0.17	0.24	0.02	0.04		0.62	0.19	0.41		
PNL	L8-6D	Nominal	11.48	0.17	0.24	0.02	0.04		0.61	0.19	0.44		
PNL	L8-7C	Nominal	10.99	0.14	0.19		0.13		0.35	0.14	0.30	0.30	
PNL	L8-7D	Nominal	10.98	0.15	0.18		0.17		0.35	0.14	0.25	0.40	
PNL	L8-8C	Nominal	11.30	0.09	1.43		3.08	0.08	1.36	0.38	2.31	0.23	0.01
PNL	L8-8D	Nominal	11.27	0.05	1.44		1.36	0.05	1.21	0.42	2.67		0.01

Note: R stands for repeated measurement.

Appendix B2. 7-Day PCT Elemental Release (g/m²) of Phase I Vendor Glasses

Vendor	Glass ID	Comp. Used	pH	Al2O3	B2O3	CaO	Fe2O3	K2O	MgO	Na2O	SiO2
BCW	B1G9-005 C	Anal. B1G9-014C	10.52	0.051	0.065	0.035	0.002			0.142	0.048
BCW	B1G9-005 D	Anal. B1G9-014C	10.56	0.051	0.066	0.034	0.002			0.146	0.048
BCW	B1G9-006 C	Anal. B1G9-014C	10.61	0.057	0.065	0.035	0.002			0.153	0.047
BCW	B1G9-006 D	Anal. B1G9-014C	10.57	0.056	0.065	0.035	0.002			0.153	0.047
BCW	B1G9-008 C	Anal. B1G9-014C	10.21	0.055	0.031	0.027	0.004			0.095	0.040
BCW	B1G9-008 D	Anal. B1G9-014C	10.23	0.055	0.031	0.026	0.004			0.097	0.040
BCW	B1G9-011 C	Anal. B1G9-014C	10.37	0.040	0.049	0.034	0.001			0.124	0.050
BCW	B1G9-011 D	Anal. B1G9-014C	10.36	0.040	0.049	0.034	0.001			0.126	0.050
BCW	B1G9-013 C	Anal. B1G9-014C	10.6	0.047	0.065	0.036	0.002			0.160	0.052
BCW	B1G9-013 D	Anal. B1G9-014C	10.64	0.046	0.064	0.035	0.004			0.155	0.051
BCW	B1G9-014 C	Anal. B1G9-014C	10.44	0.043	0.045	0.033	0.002			0.125	0.049
BCW	B1G9-014 D	Anal. B1G9-014C	10.45	0.043	0.045	0.033	0.004	0.007		0.123	0.049
GDI	D1G4-022P2 C	Norminal	11.46	0.080	0.534	0.006	0.000	0.353		0.619	0.167
GDI	D1G4-022P2 D	Norminal	11.45	0.080	0.542	0.006	0.000	0.368		0.621	0.168
GDI	D1G4-023P3 C	Norminal	11.46	0.086	0.502	0.005	0.000	0.345		0.610	0.167
GDI	D1G4-023P3 D	Norminal	11.45	0.085	0.500	0.005	0.000	0.339		0.606	0.166
PEI	PEI-(A) C	Norminal	12.12	0.193		0.016	0.004	0.555	0.070	1.684	0.250
PEI	PEI-(B) D	Norminal	12.16	0.201		0.018	0.004	0.685	0.147	1.708	0.265
PNL	LD4-912 C	Norminal	10.56	0.126	0.352			0.165		0.314	0.127
PNL	LD4-912 D	Norminal	10.53	0.124	0.351			0.083		0.317	0.127
PNL	LD5-912 C	Norminal	12.02	0.216		0.013		0.330		1.240	0.224
PNL	LD5-912 D	Norminal	12.04	0.217		0.013		0.289		1.217	0.224
PNL	LD6-5314 C	Norminal	11.05	0.086	0.099	0.028		0.083		0.253	0.090
PNL	LD6-5314 D	Norminal	11.05	0.086	0.098	0.028		0.083		0.260	0.090
PNL	LD6-5412 C	Norminal	11.37	0.097	0.111	0.050		0.083		0.371	0.104
PNL	LD6-5412 D	Norminal	11.4	0.098	0.113	0.050		0.083		0.381	0.105
PNL	LD6-5510 C	Norminal	11.62	0.111	0.130	0.066		0.083		0.529	0.120
PNL	LD6-5510 D	Norminal	11.33	0.110	0.136	0.063		0.413		0.505	0.118
PNL	LD6-5510 D	Norminal		0.112	0.131	0.068		0.206		0.519	0.121
PNL	SSHTM-3 C	Norm. LD6-5412	11.36	0.110	0.174	0.028		0.106		0.444	0.119
PNL	SSHTM-3 D	Norm. LD6-5413	11.29	0.109	0.173	0.028		0.114		0.433	0.118

Appendix B2. 7-Day PCT Elemental Release (g/m²) of Phase I Vendor Glasses (Continued)

Vendor	Glass ID	Comp. Used	pH	Cr2O3	Li2O	MnO	MoO3	Nd2O3	P2O5	SO3	SrO	ZrO2
BCW	B1G9-005 C	Anal. B1G9-014C	10.52				0.057				0.018	
BCW	B1G9-005 D	Anal. B1G9-014C	10.56				0.057				0.018	
BCW	B1G9-006 C	Anal. B1G9-014C	10.61				0.057				0.018	
BCW	B1G9-006 D	Anal. B1G9-014C	10.57				0.057				0.018	
BCW	B1G9-008 C	Anal. B1G9-014C	10.21				0.034				0.012	
BCW	B1G9-008 D	Anal. B1G9-014C	10.23				0.023				0.012	
BCW	B1G9-011 C	Anal. B1G9-014C	10.37				0.034				0.018	
BCW	B1G9-011 D	Anal. B1G9-014C	10.36				0.045				0.018	
BCW	B1G9-013 C	Anal. B1G9-014C	10.6				0.057				0.018	
BCW	B1G9-013 D	Anal. B1G9-014C	10.64				0.057				0.018	
BCW	B1G9-014 C	Anal. B1G9-014C	10.44				0.045				0.018	
BCW	B1G9-014 D	Anal. B1G9-014C	10.45				0.045				0.018	
GDI	D1G4-022P2 C	Norminal	11.46	0.110			0.360		0.199	0.363		
GDI	D1G4-022P2 D	Norminal	11.45	0.110			0.365		0.199	0.369		
GDI	D1G4-023P3 C	Norminal	11.46	0.110			0.360		0.283	0.345		
GDI	D1G4-023P3 D	Norminal	11.45	0.110			0.360		0.289	0.339		
PEI	PEI-(A) C	Norminal	12.12	0.073			0.355		0.103	0.297	0.024	
PEI	PEI-(B) D	Norminal	12.16	0.110			0.390		0.133	0.339	0.030	0.001
PNL	LD4-912 C	Norminal	10.56									
PNL	LD4-912 D	Norminal	10.53									
PNL	LD5-912 C	Norminal	12.02									
PNL	LD5-912 D	Norminal	12.04									
PNL	LD6-5314 C	Norminal	11.05									
PNL	LD6-5314 D	Norminal	11.05									
PNL	LD6-5412 C	Norminal	11.37									
PNL	LD6-5412 D	Norminal	11.4									
PNL	LD6-5510 C	Norminal	11.62									
PNL	LD6-5510 D	Norminal	11.33									
PNL	LD6-5510 D	Norminal										
PNL	SSHTM-3 C	Norm. LD6-5412	11.36									
PNL	SSHTM-3 D	Norm. LD6-5413	11.29									

Appendix B2. 7-Day PCT Elemental Release (g/m²) of Phase I Vendor Glasses (Continued)

Vendor	Glass ID	Comp. Used	pH	Al2O3	B2O3	CaO	Fe2O3	K2O	MgO	Na2O	SiO2
UBM	M1G1-008P C	Analyzed	10.27	0.05	0.08	0.05				0.22	0.06
UBM	M1G1-008P D	Analyzed	10.8	0.05	0.08	0.05				0.22	0.06
UBM	M1G1-011P C	Analyzed	11.06	0.06	0.10	0.05				0.32	0.08
UBM	M1G1-011P D	Analyzed	11.06	0.06	0.10	0.05				0.32	0.08
VTI	V1M2 6 32 011 P1C	Analyzed	10.27	0.060	0.134	0.011	0.003	0.084	0.005	0.214	0.094
VTI	V1M2 6 32 011 P1D	Analyzed	10.32	0.060	0.133	0.011	0.003	0.087	0.004	0.212	0.094
VTI	V1M2 6 32 040 P2C	Analyzed	10.23	0.054	0.129	0.013	0.002	0.057	0.004	0.190	0.087
VTI	V1M2 6 32 040 P2D	Analyzed	10.2	0.054	0.129	0.013	0.002	0.056	0.004	0.189	0.087
VTI	V1M3 6 32 059 P1C	Analyzed	10.33	0.059	0.144	0.010	0.003	0.077	0.004	0.219	0.095
VTI	V1M3 6 32 059 P1D	Analyzed	10.35	0.061	0.149	0.011	0.003	0.058	0.004	0.227	0.097
VTI	V1M3 6 32 075 P2C	Analyzed	10.32	0.056	0.131	0.011	0.003	0.068	0.005	0.264	0.088
VTI	V1M3 6 32 075 P2D	Analyzed	10.31	0.056	0.129	0.011	0.003	0.071	0.004	0.260	0.087
VTI	V1M4 6 32 088 P1C	Analyzed	10.38	0.059	0.142	0.012	0.001	0.073	0.003	0.213	0.094
VTI	V1M4 6 32 088 P1D	Analyzed	10.37	0.059	0.141	0.012	0.002	0.084	0.004	0.210	0.093
VTI	V1M4 6 32 096 P2C	Analyzed	10.37	0.059	0.148	0.011	0.002	0.063	0.003	0.219	0.096
VTI	V1M4 6 32 096 P2D	Analyzed	10.37	0.059	0.148	0.012	0.002	0.069	0.004	0.218	0.096
VTI	Vectra C	Analyzed	11.11	0.130	0.451	0.012	0.036	0.199	0.040	0.540	0.182
VTI	Vectra D	Analyzed	11.12	0.133	0.470	0.012	0.039	0.235	0.045	0.557	0.187
WSTC	WSTC C	Norminal		0.085	0.149	0.003				0.240	0.082
WSTC	WSTC C	Norminal	10.82	0.088	0.152	0.006		0.114		0.246	0.086
WSTC	WSTC D	Norminal	10.81	0.088	0.153	0.006		0.110		0.246	0.086

Appendix B2. 7-Day PCT Elemental Release (g/m²) of Phase I Vendor Glasses (Continued)

Vendor	Glass ID	Comp. Used	pH	Cr2O3	Li2O	MnO	MoO3	Nd2O3	P2O5	SO3	SrO	ZrO2
UBM	M1G1-008P C	Analyzed	10.27				1.07					
UBM	M1G1-008P D	Analyzed	10.8				1.07					
UBM	M1G1-011P C	Analyzed	11.06				1.11					
UBM	M1G1-011P D	Analyzed	11.06				1.14					
VTI	V1M2 6 32 011 P1C	Analyzed	10.27	0.009			0.125	0.074			0.008	
VTI	V1M2 6 32 011 P1D	Analyzed	10.32	0.009			0.126	0.083			0.008	
VTI	V1M2 6 32 040 P2C	Analyzed	10.23	0.009			0.122	0.065			0.008	
VTI	V1M2 6 32 040 P2D	Analyzed	10.2	0.009			0.122	0.067			0.008	
VTI	V1M3 6 32 059 P1C	Analyzed	10.33	0.011			0.159	0.027			0.007	
VTI	V1M3 6 32 059 P1D	Analyzed	10.35	0.011			0.164	0.015			0.007	
VTI	V1M3 6 32 075 P2C	Analyzed	10.32	0.011			0.211	0.019			0.007	
VTI	V1M3 6 32 075 P2D	Analyzed	10.31	0.011			0.210	0.022			0.008	
VTI	V1M4 6 32 088 P1C	Analyzed	10.38	0.015			0.347	0.024			0.008	
VTI	V1M4 6 32 088 P1D	Analyzed	10.37	0.016			0.358	0.032			0.008	
VTI	V1M4 6 32 096 P2C	Analyzed	10.37	0.012			0.216	0.026			0.007	
VTI	V1M4 6 32 096 P2D	Analyzed	10.37	0.013			0.216	0.035			0.007	
VTI	Vectra C	Analyzed	11.11									
VTI	Vectra D	Analyzed	11.12									
WSTC	WSTC C	Norminal			0.079							
WSTC	WSTC C	Norminal	10.82		0.080							0.001
WSTC	WSTC D	Norminal	10.81		0.079							0.001

Appendix B3. 7-Day PCT Elemental Release (g/m²) of Phase II Vendor Glasses

Vendor	Glass ID	Comp. Used	pH	Al2O3	B2O3	CaO	Fe2O3	K2O	MgO	Na2O	SiO2
PNL	LDM-0912C	Norminal	11.81	0.212		0.015		0.361		1.204	0.220
PNL	LDM-0912D	Norminal	11.82	0.209		0.014		0.375		1.190	0.217
PNL	LDM-1C	Norminal	11.12	0.138	0.173		0.020	0.147		0.365	0.131
PNL	LDM-1D	Norminal	11.12	0.136	0.172		0.020	0.141		0.365	0.131
PNL	LDM-2C	Norminal	10.66	0.137		0.013	0.005	0.215		0.772	0.143
PNL	LDM-2D	Norminal	10.67	0.170		0.017	0.006	0.266		0.917	0.142
PNL	LDM-3C	Norminal	10.66	0.115	0.162		1.227	0.058		0.282	0.110
PNL	LDM-3D	Norminal	10.67	0.117	0.169		1.346	0.087		0.293	0.112
PNL	LDM-4C	Norminal	10.93	0.116	0.281		0.005	0.240		0.464	0.130
PNL	LDM-4D	Norminal	10.96	0.113	0.282		0.006	0.230		0.462	0.128
PNL	LDM-5412C	Norminal	10.93	0.101	0.125	0.039		0.158		0.388	0.109
PNL	LDM-5412D	Norminal	10.96	0.109	0.127	0.041		0.121		0.421	0.109
PNL	LDMS-1C	Analyzed	10.89	0.129	0.153	0.011	0.019	0.056		0.305	0.125
PNL	LDMS-1D	Analyzed	10.92	0.131	0.155	0.010	0.020	0.053		0.306	0.126
PNL	LDMSM-1C	Analyzed	11.09	0.153	0.192	0.007	0.013	0.062		0.386	0.145
PNL	LDMSM-1D	Analyzed	11.11	0.153	0.193	0.005	0.013	0.063		0.389	0.146
PNL	LRM-0912C	Norminal	11.71	0.162		0.026		2.385		1.020	0.182
PNL	LRM-0912D	Norminal	11.75	0.168		0.024		2.835		1.039	0.187
PNL	LRM-1C	Norminal	11.22	0.163	0.206		0.024	2.087		0.466	0.155
PNL	LRM-1D	Norminal	11.23	0.160	0.203		0.024	2.592		0.458	0.153
PNL	LRM-2C	Norminal	11.50	0.179		0.006	0.015	3.011		0.716	0.184
PNL	LRM-2D	Norminal	11.49	0.206		0.007	0.016	3.649		0.807	0.186
PNL	LRM-3C	Norminal	10.85	0.122	0.163		0.758	1.659		0.325	0.118
PNL	LRM-3D	Norminal	10.86	0.149	0.164		0.758	1.586		0.392	0.118
PNL	LRM-4C	Norminal	11.19	0.135	0.283		0.006	2.195		0.468	0.148
PNL	LRM-4D	Norminal	11.19	0.134	0.290		0.006	2.542		0.472	0.149
PNL	LRM-5412C	Norminal	10.97	0.146	0.152	0.008				0.409	0.132
PNL	LRM-5412D	Norminal	10.98	0.130	0.155	0.006		0.908		0.372	0.135
PNL	LRMS-1C	Analyzed	11.23	0.165	0.205	0.009	0.015	0.000		0.444	0.159
PNL	LRMS-1D	Analyzed	11.23	0.165	0.205	0.008	0.015	0.000		0.445	0.159
PNL	LRMSM-1C	Analyzed	11.30	0.187	0.248	0.006	0.010	0.000		0.512	0.180
PNL	LRMSM-1D	Analyzed	11.30	0.186	0.247	0.006	0.010	0.000		0.509	0.180

Appendix B3. 7-Day PCT Elemental Release (g/m²) of Phase II Vendor Glasse (Continued)

Vendor	Glass ID	Comp. Used	pH	Cr2O3	Li2O	MnO	MoO3	Nd2O3	P2O5	SO3	SrO	ZrO2	CuO	SO4	CdO	NiO	ZnO
PNL	LDM-0912C	Norminal	11.81	0.091			0.298		1.524	0.272	0.040						
PNL	LDM-0912D	Norminal	11.82	0.092			0.294		1.742	0.272	0.038						
PNL	LDM-1C	Norminal	11.12				0.162		0.529	0.148	0.005	0.009					
PNL	LDM-1D	Norminal	11.12				0.163		0.514	0.148	0.005	0.009					
PNL	LDM-2C	Norminal	10.66				0.180		0.652	0.154	0.010						
PNL	LDM-2D	Norminal	10.67				0.192		0.851	0.119	0.012						
PNL	LDM-3C	Norminal	10.66	0.098		0.112	0.123		0.911	0.067	0.016	0.073					
PNL	LDM-3D	Norminal	10.67	0.104		0.123	0.128		0.888	0.070	0.016	0.074					
PNL	LDM-4C	Norminal	10.93				0.243		1.477	0.273							
PNL	LDM-4D	Norminal	10.96				0.241		1.484	0.266	0.002	0.000					
PNL	LDM-5412C	Norminal	10.93				0.121		0.901	0.079	0.024						
PNL	LDM-5412D	Norminal	10.96				0.123		1.056	0.067	0.026						
PNL	LDMS-1C	Analyzed	10.89				0.138		0.174			0.009					
PNL	LDMS-1D	Analyzed	10.92				0.138		0.110			0.009					
PNL	LDMSM-1C	Analyzed	11.09	0.014	0.000	0.006	0.153		0.115			0.005	0.013	0.070	0.005	0.007	0.012
PNL	LDMSM-1D	Analyzed	11.11	0.014	0.000	0.009	0.155		0.102			0.005	0.013	0.064	0.005	0.007	0.014
PNL	LRM-0912C	Norminal	11.71	0.070			0.214		0.046	0.203	0.038						
PNL	LRM-0912D	Norminal	11.75	0.073			0.221		0.054	0.209	0.038						
PNL	LRM-1C	Norminal	11.22		0.106	0.026	0.230		0.194	0.179	0.007	0.006					
PNL	LRM-1D	Norminal	11.23		0.104	0.028	0.226		0.191	0.175	0.007	0.004					
PNL	LRM-2C	Norminal	11.50	0.049			0.256		0.113	0.185	0.007						
PNL	LRM-2D	Norminal	11.49	0.055		0.022	0.275		0.095	0.174	0.008						
PNL	LRM-3C	Norminal	10.85	0.105		0.061	0.205		0.075	0.120	0.017	0.005					
PNL	LRM-3D	Norminal	10.86	0.105		0.061	0.255		0.065	0.115	0.017	0.009					
PNL	LRM-4C	Norminal	11.19		0.133		0.250		0.206	0.249							
PNL	LRM-4D	Norminal	11.19		0.135		0.256		0.229	0.257							
PNL	LRM-5412C	Norminal	10.97				0.148		0.107	0.098	0.008						
PNL	LRM-5412D	Norminal	10.98				0.145		0.088	0.114	0.007						
PNL	LRMS-1C	Analyzed	11.23		0.095		0.166		0.186			0.001					
PNL	LRMS-1D	Analyzed	11.23		0.097		0.166		0.187			0.002					
PNL	LRMSM-1C	Analyzed	11.30	0.019	0.000	0.003	0.193		0.230			0.000	0.008	0.184	0.005	0.004	0.006
PNL	LRMSM-1D	Analyzed	11.30	0.019	0.000	0.003	0.193		0.229			0.001	0.008	0.184	0.005	0.004	0.006

APPENDIX C

Glass Compositions

Table C.1. Glass Compositions: Glasses 1 - 5

Oxide	Comp. 1	Comp. 2	Comp. 3	Comp. 4	Comp. 5
SiO_2	42.84	44.65	46.87	43.07	42.16
Na_2O	19.06	19.06	19.07	19.06	19.06
Al_2O_3	13.09	13.47	14.00	18.29	17.99
B_2O_3	9.43	9.80	4.23	9.50	3.77
CaO	3.02	4.91	5.14	4.76	4.61
ZrO_2	6.86	2.26	7.47	2.19	6.71
Li_2O	3.39	3.55	0.91	0.83	3.39
K_2O	1.45	1.45	1.45	1.45	1.45
SO_3	0.21	0.21	0.21	0.21	0.21
P_2O_5	0.19	0.19	0.19	0.19	0.19
MoO_3	0.15	0.15	0.15	0.15	0.15
Cs_2O	0.15	0.15	0.15	0.15	0.15
SrO	0.11	0.11	0.11	0.11	0.11
Cr_2O_3	0.04	0.04	0.04	0.04	0.04
Fe_2O_3	0.004	0.004	0.004	0.004	0.004
MgO	0.002	0.002	0.002	0.002	0.002
MnO_2	0.002	0.002	0.002	0.002	0.002
Total	99.998	100.008	99.998	100.008	99.998

Table C.2. Glass Compositions: Glasses 6 - 10

Oxide	Comp. 6	Comp. 7	Comp. 8	Comp. 9	Comp. 10
SiO_2	44.09	40.16	43.40	49.63	51.63
Na_2O	19.04	19.07	19.07	19.06	19.04
Al_2O_3	18.65	17.25	13.17	14.60	15.11
B_2O_3	9.72	8.83	9.51	4.45	4.67
CaO	3.09	2.80	4.76	3.47	3.62
ZrO_2	2.19	6.42	6.95	2.49	2.56
Li_2O	0.91	3.17	0.83	4.00	1.06
K_2O	1.45	1.45	1.45	1.45	1.45
SO_3	0.21	0.21	0.21	0.21	0.21
P_2O_5	0.19	0.19	0.19	0.19	0.19
MoO_3	0.15	0.15	0.15	0.15	0.15
Cs_2O	0.15	0.15	0.15	0.15	0.15
SrO	0.11	0.11	0.11	0.11	0.11
Cr_2O_3	0.04	0.04	0.04	0.04	0.04
Fe_2O_3	0.004	0.004	0.004	0.004	0.004
MgO	0.002	0.002	0.002	0.002	0.002
MnO_2	0.002	0.002	0.002	0.002	0.002
Total	99.998	100.008	99.998	100.008	99.998

Table C.3. Glass Compositions: Glasses 11 - 15

Oxide	Comp. 11	Comp. 12	Comp. 13	Comp. 14	Comp. 15
SiO_2	44.65	44.88	52.87	46.61	49.70
Na_2O	19.06	19.06	19.06	19.06	19.06
Al_2O_3	18.82	18.90	13.77	18.14	13.16
B_2O_3	4.00	4.07	4.75	4.22	10.94
CaO	3.10	4.91	5.81	3.25	3.47
ZrO_2	7.16	2.26	1.21	6.18	1.13
Li_2O	0.91	3.62	0.23	0.23	0.23
K_2O	1.45	1.45	1.45	1.45	1.45
SO_3	0.21	0.21	0.21	0.21	0.21
P_2O_5	0.19	0.19	0.19	0.19	0.19
MoO_3	0.15	0.15	0.15	0.15	0.15
Cs_2O	0.15	0.15	0.15	0.15	0.15
SrO	0.11	0.11	0.11	0.11	0.11
Cr_2O_3	0.04	0.04	0.04	0.04	0.04
Fe_2O_3	0.004	0.004	0.004	0.004	0.004
MgO	0.002	0.002	0.002	0.002	0.002
MnO_2	0.002	0.002	0.002	0.002	0.002
Total	100.008	100.008	100.008	99.998	99.998

Table C.4. Glass Compositions: Glasses 16 - 20

Oxide	Comp. 16	Comp. 17	Comp. 18	Comp. 19	Comp. 20
SiO_2	47.82	48.65	43.07	50.31	47.14
Na_2O	19.06	19.06	19.06	19.06	19.06
Al_2O_3	12.78	10.52	14.82	16.78	11.65
B_2O_3	10.56	12.14	10.79	6.03	11.77
CaO	3.32	3.40	4.76	5.51	5.21
ZrO_2	1.06	3.92	3.47	0.00	0.00
Li_2O	3.09	0.00	1.73	0.00	2.87
K_2O	1.45	1.45	1.45	1.45	1.45
SO_3	0.21	0.21	0.21	0.21	0.21
P_2O_5	0.19	0.19	0.19	0.19	0.19
MoO_3	0.15	0.15	0.15	0.15	0.15
Cs_2O	0.15	0.15	0.15	0.15	0.15
SrO	0.11	0.11	0.11	0.11	0.11
Cr_2O_3	0.04	0.04	0.04	0.04	0.04
Fe_2O_3	0.004	0.004	0.004	0.004	0.004
MgO	0.002	0.002	0.002	0.002	0.002
MnO_2	0.002	0.002	0.002	0.002	0.002
Total	99.998	99.998	100.008	99.998	100.008

Table C.5. Glass Compositions: Glasses 21 - 24

Oxide	Comp. 21	Comp. 22	Comp. 23	Comp. 24
SiO_2	45.10	44.65	43.07	45.48
Na_2O	19.06	19.06	19.06	19.06
Al_2O_3	15.42	16.63	13.16	17.76
B_2O_3	13.58	7.54	11.62	6.34
CaO	3.17	4.91	3.02	3.17
ZrO_2	0.00	4.90	5.58	5.88
Li_2O	1.36	0.00	2.19	0.00
K_2O	1.45	1.45	1.45	1.45
SO_3	0.21	0.21	0.21	0.21
P_2O_5	0.19	0.19	0.19	0.19
MoO_3	0.15	0.15	0.15	0.15
Cs_2O	0.15	0.15	0.15	0.15
SrO	0.11	0.11	0.11	0.11
Cr_2O_3	0.04	0.04	0.04	0.04
Fe_2O_3	0.004	0.004	0.004	0.004
MgO	0.002	0.002	0.002	0.002
MnO_2	0.002	0.002	0.002	0.002
Total	99.998	99.998	100.008	99.998

APPENDIX D

Ratings and Ranking After Each Round

Table D.1. Ratings and Ranking After Round 1.

Composition	Durability	Viscosity	Homogeneity	Volatility	Total
4	35	25	25	15	100
6	35	25	25	15	100
8	35	24.5	25	15	99.5
9	31.2	25	25	15	96.2
3	35	25	12.5	15	87.5
12	35	25	12.5	15	87.5
10	35	12	25	15	87
1	35	6.5	25	15	81.5
7	35	13.5	12.5	15	76
2	27.3	4.5	25	15	71.8
5	-*	25	0	15	-
11	-*	2.4	0	15	-

* Durability (PCT) not measured since composition did not form a glass.

Table D.2. Ratings and Ranking After Round 2.

Composition	Durability	Viscosity	Homogeneity	Volatility	Total
4	35	25	25	15	100
6	35	25	25	15	100
15	35	25	25	15	100
8	35	24.5	25	15	99.5
9	31.2	25	25	15	96.2
13	35	16.8	25	15	91.8
3	35	25	12.5	15	87.5
16	30.8	15.5	25	15	86.3
12	35	25	12.5	15	87.5
10	35	12.5	25	15	87
1	35	6.5	25	15	81.5
14	-*	0	0	15	-

* Durability (PCT) not measured since composition did not form a glass.

Table D.3. Ratings and Ranking After Round 3.

Composition	Durability	Viscosity	Homogeneity	Volatility	Total
4	35	25	25	15	100
6	35	25	25	15	100
15	35	25	25	15	100
8	35	24.5	25	15	99.5
9	31.2	25	25	15	96.2
13	35	16.8	25	15	91.8
18	35	16.2	25	15	91.2
17	35	25	12.5	15	87.5
3	35	25	12.5	15	87.5
16	30.8	15.5	25	15	86.3
20	-*	6.5	25	15	-
19	-*	6.5	12.5	15	-

* Durability (PCT) not measured since composition did not form a glass.

APPENDIX E

Viscosities of LLW Glasses

Appendix E1. Viscosities of LLW Glasses

Vendor	Glass ID												
PNL	L4-1215	Temp (°C)	1140	1189	1239	1288	1337	1338	1387	1388	1388	1437	1488
		Viscosity (Pa*S)	43.9	27.6	18.4	10.5	7.3	7.6	5.2	5.8	6.6	4.4	3.5
PNL	L4-129	Temp (°C)	1089	1139	1189	1238	1287	1287	1336	1337	1338	1387	1437
		Viscosity (Pa*S)	41.6	24.9	15.8	9.5	6.6	6.7	4.7	4.9	5.3	3.7	2.9
PNL	L4-615	Temp (°C)	1214	1264	1314	1363	1412	1413	1462	1462	1464	1516	
		Viscosity (Pa*S)	79.1	50.1	32.9	18.9	13.9	13.5	9.5	10.1	11.1	9.7	
PNL	L4-912	Temp (°C)	1140	1189	1239	1289	1338	1338	1388	1388	1388	1438	1489
		Viscosity (Pa*S)	66.5	40.6	26.4	14.3	10.2	10.4	7.2	7.6	8.9	6.0	5.0
PNL	L4-96	Temp (°C)	1139	1189	1239	1288	1337	1337	1387	1387	1388	1437	1488
		Viscosity (Pa*S)	40.8	25.5	16.4	9.5	6.8	6.9	4.8	5.0	5.6	3.7	2.9
PNL	L5-1215	Temp (°C)	1139	1189	1238	1287	1287	1336	1337	1338	1387	1437	1487
		Viscosity (Pa*S)	85.2	46.6	27.1	16.5	16.5	10.8	10.8	10.8	7.3	4.9	3.3
PNL	L5-129	Temp (°C)	1089	1139	1189	1238	1238	1287	1287	1288	1337	1387	1438
		Viscosity (Pa*S)	108.8	58.0	32.0	19.5	19.7	12.8	12.9	12.9	8.4	5.8	4.0
PNL	L5-96	Temp (°C)	1139	1189	1238	1287	1287	1336	1337	1338	1387	1437	1487
		Viscosity (Pa*S)	74.5	43.0	26.0	16.5	16.6	11.2	11.2	11.4	7.6	5.5	3.9
PNL	L6-3312	Temp (°C)	1188	1238	1287	1336	1336	1386	1386	1388	1436	1487	1538
		Viscosity (Pa*S)	86.9	53.2	29.8	19.9	20.3	13.6	14.4	15.5	10.1	7.4	5.6
PNL	L6-5412	Temp (°C)	1139	1188	1238	1287	1287	1337	1337	1337	1387	1437	
		Viscosity (Pa*S)	71.3	43.1	24.6	16.0	16.5	10.9	11.7	12.6	8.4	6.2	
PNL	L6-5415	Temp (°C)	1138	1188	1237	1287	1287	1336	1336	1337	1386	1437	
		Viscosity (Pa*S)	89.4	53.2	31.7	20.5	21.0	13.6	14.5	15.0	10.0	7.3	
PNL	L6-546	Temp (°C)	1089	1138	1188	1237	1238	1286	1287	1287	1337	1387	1437
		Viscosity (Pa*S)	78.6	45.1	25.6	16.7	16.4	11.5	11.0	12.2	8.0	5.9	4.3
PNL	L6-549	Temp (°C)	1089	1138	1187	1236	1237	1286	1286	1287	1336	1386	1436
		Viscosity (Pa*S)	95.2	55.0	29.5	19.6	19.0	12.8	13.6	14.8	9.4	6.9	5.1
PNL	L6-6612	Temp (°C)	1089	1138	1188	1238	1238	1287	1287	1287	1337	1387	
		Viscosity (Pa*S)	62.8	36.2	21.3	14.2	14.3	9.4	9.7	9.9	6.9	4.9	
PNL	L6-669	Temp (°C)	1090	1140	1189	1239	1239	1288	1288	1289	1338	1388	
		Viscosity (Pa*S)	50.7	29.4	17.2	11.5	11.6	7.7	8.0	8.3	5.6	4.1	
PNL	L7-15	Temp (°C)	1188	1237	1287	1336	1386	1386	1436	1436	1436		
		Viscosity (Pa*S)	154.5	91.3	56.3	35.8	23.6	25.0	15.7	17.7	16.7		
PNL	L7-25	Temp (°C)	1089	1138	1188	1237	1237	1286	1286	1287	1336	1387	
		Viscosity (Pa*S)	36.4	22.6	13.8	9.4	9.5	6.4	6.6	6.7	4.6	3.3	
PNL	L7-30	Temp (°C)	990	1040	1090	1139	1188	1189	1238	1238	1239	1288	
		Viscosity (Pa*S)	43.7	25.4	15.4	9.7	6.5	6.5	4.4	4.4	4.5	3.1	
PNL	L7-35	Temp (°C)	891	941	991	1040	1089	1089	1139	1139	1140	1189	
		Viscosity (Pa*S)	63.7	32.4	18.3	11.0	6.8	6.8	4.4	4.4	4.4	3.0	

Appendix E1. Viscosities of LLW Glasses (Continued)

Vendor	Glass ID												
PNL	L8-1	Temp (°C)	1189	1239	1288	1338	1388	1389	1438	1438	1438	1488	
		Viscosity (Pa*S)	72.5	42.1	26.1	14.4	10.0	9.7	6.9	7.5	7.7	5.7	
PNL	L8-2	Temp (°C)	1186	1236	1286	1336	1336	1386	1386	1386	1436	1486	1536
		Viscosity (Pa*S)	108.9	60.1	32.6	19.8	20.0	12.9	12.9	13.1	8.4	5.7	4.0
PNL	L8-3	Temp (°C)	1189	1239	1288	1338	1338	1388	1388	1388	1438	1488	
		Viscosity (Pa*S)	83.1	47.7	26.7	16.5	17.0	10.5	11.3	11.9	7.8	5.5	
PNL	L8-4	Temp (°C)	1094	1145	1194	1244	1244	1294	1294	1294	1344	1344	
		Viscosity (Pa*S)	77.3	39.7	21.8	13.3	13.4	8.1	8.4	8.5	5.4	5.7	
PNL	L8-5	Temp (°C)	1091	1141	1191	1241	1291	1341	1391				
		Viscosity (Pa*S)	143.3	78.6	45.6	28.2	17.8	12.0	8.2				
PNL	L8-6	Temp (°C)	1142	1192	1242	1292	1292	1342	1342	1343	1392	1443	
		Viscosity (Pa*S)	60.0	35.8	21.9	14.9	14.6	10.0	10.4	10.7	7.3	5.5	
PNL	L8-7	Temp (°C)	1141	1191	1240	1290	1290	1340	1340	1341	1390	1442	
		Viscosity (Pa*S)	76.3	45.3	24.1	15.7	15.9	10.6	11.2	12.4	7.9	6.0	
PNL	L8-8	Temp (°C)	1190	1239	1289	1339	1339	1388	1389	1390	1439	1489	
		Viscosity (Pa*S)	54.5	33.1	19.6	13.3	13.4	9.3	9.0	10.2	7.1	5.4	
PNL	LD4-912	Temp (°C)	1045	1144	1243	1342	1343	1392	1442	1492			
		Viscosity (Pa*S)	153.4	48.5	19.4	7.4	9.2	5.8	4.4	3.7			
PNL	LD5-912	Temp (°C)	1095	1145	1244	1343	1343	1393	1443				
		Viscosity (Pa*S)	179.9	94.6	32.2	12.3	12.6	8.2	5.8				
PNL	LD6-5314	Temp (°C)	1070	1119	1220	1318	1319	1368	1418				
		Viscosity (Pa*S)	198.3	109.4	39.6	14.4	16.9	10.6	8.1				
PNL	LD6-5412	Temp (°C)	1046	1145	1244	1342							
		Viscosity (Pa*S)	161.0	49.7	19.1	8.7							
PNL	LD6-5510	Temp (°C)	997	1096	1195	1294	1294	1344					
		Viscosity (Pa*S)	244.2	69.4	23.7	9.6	10.3	7.1					
PNL	LDM-0912	Temp (°C)	1138	1186	1236	1236	1285	1285	1286	1336	1385	1436	
		Viscosity (Pa*S)	76.8	40.9	24.8	25.9	15.6	16.5	17.1	11.2	7.6	5.3	
PNL	LDM-1	Temp (°C)	1092	1142	1191	1241	1241	1290	1290	1292	1343	1392	
		Viscosity (Pa*S)	179.3	96.1	50.8	29.8	31.1	17.9	19.3	19.8	13.0	8.6	
PNL	LDM-2	Temp (°C)	1091	1141	1190	1239	1240	1289	1290	1290	1340	1392	
		Viscosity (Pa*S)	133.5	72.7	38.6	24.7	23.7	15.7	14.9	16.1	10.8	7.8	
PNL	LDM-3	Temp (°C)	1138	1187	1236	1286	1286	1336	1336	1336	1386	1436	
		Viscosity (Pa*S)	111.1	62.8	31.8	20.0	20.8	12.5	13.9	15.0	9.7	6.9	
PNL	LDM-4	Temp (°C)	941	992	1041	1090	1091	1140	1141	1141	1190	1240	
		Viscosity (Pa*S)	158.7	72.6	35.9	20.1	20.1	12.2	11.9	12.4	7.5	5.2	
PNL	LDM-5412	Temp (°C)	1088	1138	1187	1187	1236	1237	1237	1286	1336	1386	
		Viscosity (Pa*S)	78.7	40.0	24.9	25.9	15.8	17.0	18.8	12.0	8.6	6.3	
PNL	LDMS-1	Temp (°C)	1143	1193	1243	1292	1293	1342	1342	1344	1393	1444	
		Viscosity (Pa*S)	108.1	60.3	30.1	19.9	18.8	12.2	13.4	14.4	8.8	6.3	
PNL	LDMSM-1	Temp (°C)	1143	1194	1244	1294	1295	1344	1344	1344	1395	1445	
		Viscosity (Pa*S)	64.3	36.0	18.9	12.5	12.0	7.4	8.1	9.0	5.7	4.0	

Appendix E1. Viscosities of LLW Glasses (Continued)

Vendor	Glass ID												
PNL	LRM-091	Temp (°C)	1187	1237	1286	1336	1336	1386	1386	1386	1436	1487	
		Viscosity (Pa*S)	59.9	35.3	21.8	14.0	14.2	9.6	9.7	9.7	6.6	4.7	
PNL	LRM-1	Temp (°C)	1142	1192	1242	1291	1292	1341	1341	1342	1392	1442	
		Viscosity (Pa*S)	67.3	38.3	22.6	14.2	14.0	9.2	9.5	9.5	6.3	4.3	
PNL	LRM-2	Temp (°C)	1191	1241	1291	1291	1340	1340	1342	1392	1441	1492	
		Viscosity (Pa*S)	54.9	33.0	20.9	21.0	13.7	13.9	13.6	9.4	6.2	4.3	
PNL	LRM-3	Temp (°C)	1187	1237	1286	1336	1386	1386	1435	1436	1436	1485	
		Viscosity (Pa*S)	90.3	51.9	31.3	17.9	11.7	12.2	7.6	8.2	8.5	6.0	
PNL	LRM-4	Temp (°C)	940	990	1040	1089	1090	1139	1140	1140	1189	1240	
		Viscosity (Pa*S)	203.9	89.4	41.9	22.4	21.3	12.7	12.8	13.1	7.9	5.4	
PNL	LRM-541	Temp (°C)	1188	1237	1286	1287	1336	1336	1337	1386	1437	1488	
		Viscosity (Pa*S)	40.8	23.6	15.8	15.3	10.3	11.1	11.9	8.0	5.9	4.8	
PNL	LRMS-1	Temp (°C)	1142	1192	1243	1292	1293	1341	1342	1343	1392	1443	
		Viscosity (Pa*S)	67.3	38.5	22.5	14.1	14.0	9.4	9.6	9.8	6.6	4.6	
PNL	LRMSM-	Temp (°C)	1092	1143	1193	1245	1294	1295	1344	1344	1344	1394	
		Viscosity (Pa*S)	84.5	45.7	26.7	15.1	9.9	9.8	6.6	6.8	7.0	4.6	
PNL	SSHTM-1	Temp (°C)	1195	1245	1294	1295	1344	1345	1345	1395	1446		
		Viscosity (Pa*S)	46.9	22.4	14.2	13.7	8.6	9.1	9.0	5.8	3.9		
GDI	Duratek	Temp (°C)	941	992	1041	1091	1091	1140	1141	1141	1190	1241	
		Viscosity (Pa*S)	76.5	35.0	17.3	9.8	9.9	6.0	5.9	6.2	3.9	2.9	
PEI	PEI	Temp (°C)	1090	1140	1188	1238	1238	1287	1287	1288	1337	1387	1438
		Viscosity (Pa*S)	116.8	64.7	35.0	21.3	21.4	13.6	13.7	13.9	9.1	6.3	4.4
VTI	VECTRA	Temp (°C)	1090	1140	1190	1240	1240	1289	1290	1291	1340	1390	
		Viscosity (Pa*S)	33.4	20.6	12.6	8.4	8.4	5.9	6.0	6.4	4.4	3.2	
WSTC	WSTC	Temp (°C)	1040	1090	1090	1139	1139	1140	1188	1237	1238	1287	1337
		Viscosity (Pa*S)	54.7	30.8	31.3	18.6	18.8	20.1	12.1	8.2	8.6	5.8	4.1

Distribution

No. of Copies

Offsite

12 DOE/Office of Scientific and Technical Information

Oak Ridge National Laboratory
P.O. Box 2008
Oak Ridge, TN 37831
Attn: J. B. Berry
A. Bleier
C. W. Forsberg

J. Baker
U.S. Department of Energy
Trevion II Bldg., Rm. 334
12800 Middlebrooke Road
Germantown, MD 20874

F. E. Woolley
Corning Inc.
HP-ME-2-38
Corning, NY 14831

Argonne National Laboratory
Bldg. 205
9700 S. Cass Avenue
Argonne, IL 60439-4837
Attn: A. J. Bakel
J. Bates
W. L. Ebert
J. J. Laidler

D. Fillmore
LITCO, MS 3423
P.O. Box 1625
Idaho Falls, ID 83415

No. of Copies

T. H. Pigford
University of California, Berkeley
Department of Nuclear Engineering
Berkeley, CA 94720

L. W. Gray
Lawrence Livermore National Laboratory
L-592
P.O. Box 5508, 7000 E. Ave.
Livermore, CA 94550

Westinghouse Savannah River Co.
Savannah River Technology Center
Bldg 707-C
P.O. Box 616
Aiken, SC 29808
Attn: D. F. Bickford
C. M. Jantzen
J. R. Murphy
D. Peeler
G. Wicks
N. E. Bibler
J. Sproull
S. L. Marra

P. Hart
U.S. Department of Energy
MS-E06
P.O. Box 880
Morgantown, WV 26507-0880

W. Lutze
University of New Mexico
Department of Chemical and Nuclear Engineering, Farris Engineering Center
Room 209
Albuquerque, NM 87131-1341

No. of Copies

The Catholic University of America
Vitreous State Laboratory
620 Michigan Avenue, N.E.
Washington, DC 20064
Attn: I. L. Pegg
P. B. Macedo

M. J. Plodinec
Westinghouse Savannah River Co.
Savannah River Site
P.O. Box 616
Aiken, SC 29802

W. G. Ramsey
Westinghouse Savannah River Co.
Savannah River Technology Center
773-A, Room B104
P.O. Box 616
Aiken, SC 29808

D. M. Strachan
Argonne National Laboratory
Chemical Technology Division
Bldg. 205
9700 S. Cass Avenue
Argonne, IL 60439-4837

J. Tseng
U.S. Department of Energy
Office of Environmental Restoration
and Waste Management
Trevion II Bldg.
1000 Independence Avenue, S.E.
Washington, DC 20585

J. Allison
U.S. Department of Energy
Office of Waste Operations
Germantown, MD

S. Bates
Idaho National Engineering Laboratory
Idaho Falls, ID 83415

No. of Copies

W. Bourcier
Lawrence Livermore National Laboratory
Livermore, CA

R. C. Ewing
University of New Mexico
Department of Geology
Albuquerque, NM 87131-1341

U.S. Department of Energy
Office of Technology Development
Germantown, MD
Attn: G.C.S. Ordaz
W. C. Schutte

M. Tomozawa
Rensselaer Polytechnic Institute
Troy, NY

B. W. Bowan
GTS Duratck, 8955
Guilford Road
Suite 200
Columbia, MD 31046

D. Clark
University of Flordia
Advanced Material Research
One Progress Blvd., #14
Alachua, FL 32615

R. A. Palmer
West Valley Nuclear Services
P.O. Box 191
West Valley, NY 14171

J. L. Resce
Environmental Systems Eng.
Rich Environmental Research Laboratory
Clemson Research Park
Clemson, SC 29634-0919

No. of Copies

D. E. Day
University of Missouri-Rolla
Materials Research Center
Rolla, MO 65401

R. H. Doremus
Rensselaer Polytechnic Inst.
Materials Engineering Department
Troy, NY 12180-3950

Foreign

B. Grambow
Kernforschungszentrum Karlsruhe
GmbH
GERMANY

P. Van Isegham
Boerecamp
BELGIUM

E. Vernaz
Centre d'Etudes Nucleares
de la Valle du Rhone
Marcoule,
FRANCE

L. Werme
Svensk Karnbranslehantering AB
Stockholm
SWEDEN

Onsite

1 **DOE Richland Operations Office**

N. R. Brown, K6-51

No. of Copies

71 **Pacific Northwest Laboratory**

A. L. Boldt, H5-49
K. D. Boomer, H5-61
B. C. Bunker, K2-45
G. Chen, K5-12
R. P. Colburn, H5-27
M. L. Elliott, P7-41
X. Feng, P8-44 (34)
A. Fillion, P7-72
C. J. Freeman, P7-41
J. S. Garfield, H5-49
R. L. Gibby, H5-27
W. K. Hahn, P8-37
B. A. Higley, H5-27
P. R. Hrma, P8-37
S. L. Lambert, H5-27
D. A. Lamar, P7-41
H. Li, P9-44
J. Luey, P7-41
C. M. McConville, H5-49
B. P. McGrail, K2-44
R. M. Orme, H5-27
Y. Peng, P8-37
J. Perez, P7-41
G. F. Piepel, K5-12
M. J. Schewiger, P8-37
J. W. Shade, H5-27
D. E. Smith, P8-37
J. E. Surma, P7-43
J. D. Vienna, P8-44
D. Washenfelder, H5-27
J. H. Westsik, Jr., K9-80
C. N. Wilson, H5-27
Publishing Coordination
Technical Report Files (5)